In vitro generation of human innate lymphoid cells from CD34$^+$ hematopoietic progenitors recapitulates phenotype and function of *ex vivo* counterparts

D I S S E R T A T I O N

zur Erlangung des akademischen Grades

DOCTOR RERUM NATURALIUM

(Dr. rer. nat.)

eingereicht an der

Lebenswissenschaftlichen Fakultät der Humboldt-Universität zu Berlin

von

Daniela Carolina Hernández Torres, M. Sc.

Kommissarischer Präsident der Humboldt-Universität zu Berlin

Präsident (komm.) Prof. Dr. Peter Frensch

Dekan der Lebenswissenschaftlichen Fakultät

der Humboldt-Universität zu Berlin

Prof. Dr. Dr. Christian Ulrichs

Gutachter/innen

1. Prof. Chiara Romagnani
2. Prof. Arturo Zychlinsky
3. Prof. Hyun-Dong Chang

Tag der mündlichen Prüfung: 05.07.2022

Zusammenfassung

Angeborene lymphatische Zellen (ILC) sind wichtige Effektorzellen der angeborenen Immunantwort, deren Entwicklung und Aktivierungswege attraktive therapeutische Ziele darstellen. Sie bestehen aus ILC der Gruppe 1 (Natürliche Killerzellen (NK) und ILC1), ILC2 und ILC3. Neben T-Zellen leisten ILCs einen entscheidenen Beitrag zu den Typ-1-, Typ-2- und Typ-3-Immunantworten. Die Entwicklung von ILCs beim Menschen wurde jedoch noch nicht systematisch untersucht, und frühere *in vitro* Untersuchungen stützten sich auf die Analyse einiger weniger Marker oder Zytokine, die für die Bestimmung der Identität der verschiedenen ILC-Linien suboptimal sind. Um diese Mängel zu beheben, stellen wir hier eine Plattform vor, die zuverlässig alle menschlichen ILC-Linien aus $CD34^+$ $CD45RA^+$ hämatopoetischen Vorläuferzellen, gewonnen aus Nabelschnurblut und Knochenmark, erzeugt. Mit einem systematischen Ansatz zeigt diese Arbeit, dass eine einzige Kulturbedingung nicht ausreicht, um alle ILC-Untergruppen zu generieren, sondern stattdessen bestimmte Kombinationen von Zytokinen und Notch-Signalen für die Entscheidung über das Schicksal der Linien wesentlich ist. Eine umfangreiche Analyse des Transkriptoms ergab, dass der Erwerb von CD161 robust eine globale ILC-Signatur identifiziert und *in vitro* ILCs von T-Zell-Signaturen trennt. Die Identität spezifischer *in vitro* generierter ILC-Linien (NK-Zellen und ILC1, ILC2 und ILC3) wurde durch Proteinexpression, funktionelle Assays und Transkriptomanalysen auf globaler sowie auf Einzelzellebene umfassend validiert. Diese *in vitro* erzeugten ILC-Linien rekapitulieren die Signaturen und Funktionen ihrer *ex vivo* isolierten ILC-Pendants. Des Weiteren, behandeln diese Daten die Einschränkungen der Unterscheidung von menschlichen NK Zellen und ILC1 sowohl in vitro als auch ex vivo an. Darüber hinaus löst diese Plattform gängige Probleme bei der Untersuchung menschlicher ILCs, wie z. B. unzureichende Zellzahlen oder die mangelnde Verfügbarkeit von Gewebeproben. Insgesamt stellt diese Arbeit eine Ressource dar, die nicht nur zur Klärung der Biologie und Differenzierung menschlicher ILCs beiträgt, sondern auch als wichtiges Instrument zur Untersuchung der Dysregulation von ILC-Funktionen dient, die bei verschiedenen entzündlichen Erkrankungen des Menschen eine Rolle spielen.

Summary

Innate lymphoid cells (ILCs) are critical effectors of innate immunity and inflammation that consist of Group 1 ILCs (natural killer (NK) cells and ILC1), ILC2, and ILC3. As tissue resident lymphocytes, they play a crucial role type 1, type 2 and type 3 immune responses, respectively. Importantly, dysregulated ILC populations have been linked to the pathogenesis of a variety of chronic inflammatory diseases and thus represent attractive therapeutic targets with a potential for autologous cell therapies. However, human ILC generation has not been systematically explored, and previous *in vitro* investigations have relied on the analysis of few markers or cytokines, which are suboptimal to assign lineage identity and full functional capacity. To address these faults, we present here an effective *in vitro* platform, which reliably generates the core human ILC lineages from $CD34^+$ $CD45RA^+$ hematopoietic progenitors derived from cord blood and bone marrow. With a systematic approach, this work shows that a single culture condition is insufficient to generate all ILC subsets, and instead, distinct combinations of cytokines and Notch signaling are essential for lineage fate making decisions. In depth transcriptomic analysis revealed that acquisition of CD161 robustly identifies a global ILC signature and separates them from T cell signatures *in vitro*. The identity of specific ILC subsets, (NK cells and ILC1, ILC2, and ILC3) generated *in vitro* was validated extensively by protein expression, functional assays, and both global and single-cell transcriptome analysis. These *in vitro* generated ILC subsets recapitulate the signatures and functions of their *ex vivo* ILC counterparts. Finally, these data shed light on the limitations in untying the identity of human NK cells and ILC1 *in vitro*, similarly correlating to lineage identification difficulties *ex vivo*. Additionally, this platform tackles common problems in human ILC studies such as insufficient cell numbers and scarce availability of tissue samples. Altogether, this work presents a resource not only to aid in clarifying human ILC biology and differentiation, but also to serve as an important tool to study dysregulation of ILC functions, which have been implied in various inflammatory diseases in humans.

Hernández DC, Juelke K, Müller NC, Durek P, Ugursu B, Mashreghi MF, Rückert T, Romagnani C. *An in vitro platform supports generation of human innate lymphoid cells from CD34$^+$ hematopoietic progenitors that recapitulate ex vivo identity*. Immunity. 2021 Oct 12;54(10):2417-2432.e5. doi: 10.1016/j.immuni.2021.07.019. Epub 2021 Aug 27. PMID: 34453879.

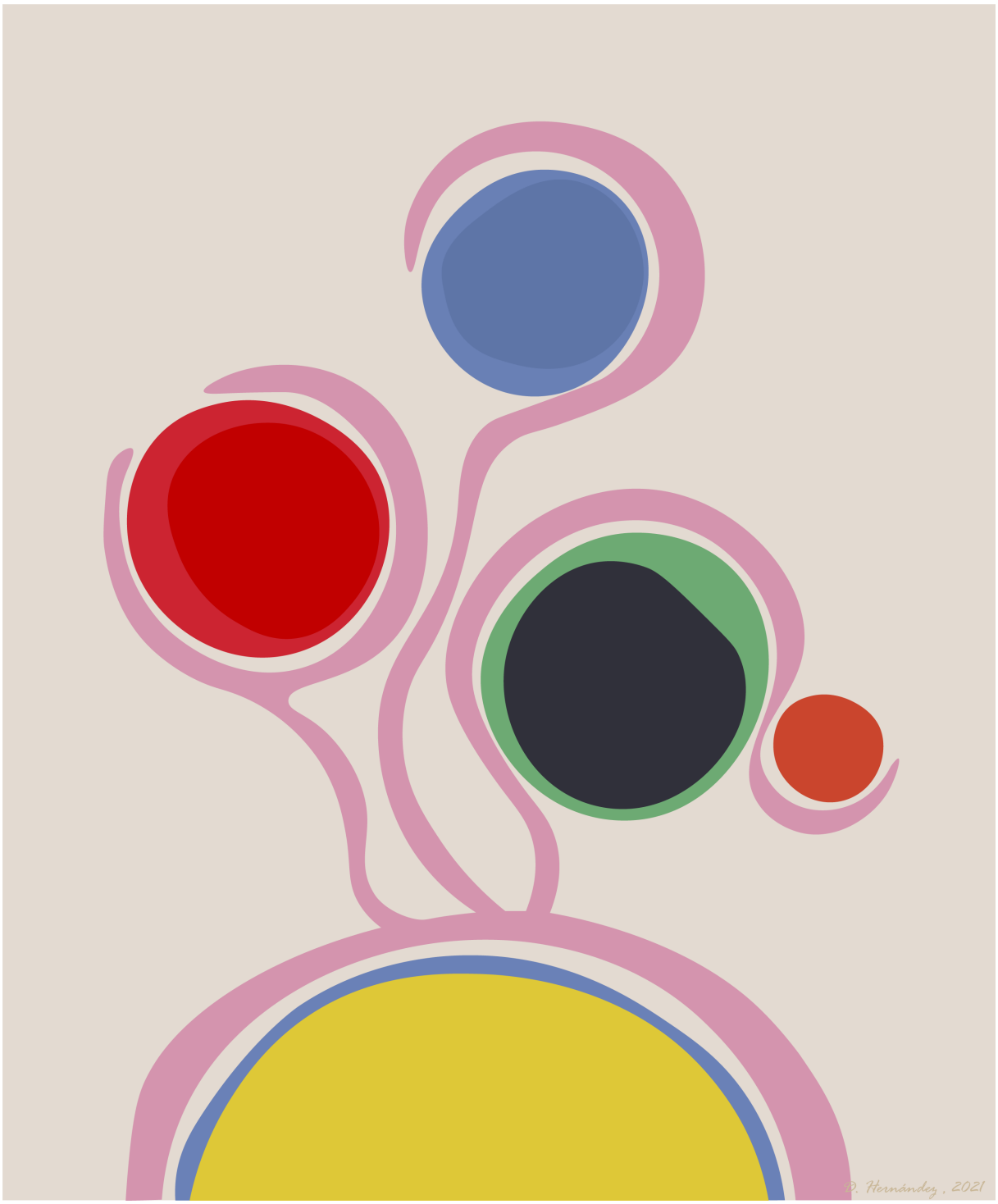

ILC development as seen through Sonia Delaunay. Depicted here, in the style of French contemporary artist Sonia Delaunay, is an artistic rendering of ILC development and the work presented in this thesis. At center stage, a $CD34^{+}$ mother cell (yellow) gives rise to all core ILC subsets (blue, red, brown) as well as a non-ILC subset (orange) through discrete, yet connected, developmental pathways (pink). Inspiration: *Costume pour Carnaval de Rio, by Sonia Delaunay, pochoir,* 1928.

CONTENTS

1 Introduction

1.1 The immune system

The immune system as a whole is an intricate network of cells and tissues whose tendrils lay deep in most systems of the body, and which react to changes and challenges in order to maintain the host in a state of homeostasis. Its cellular armies consist of T lymphocytes, B lymphocytes, and a plethora of innate immune cells including antigen-presenting cells, macrophages, granulocytes and innate lymphoid cells. In vertebrates, the immune system has been conventionally classified into two arms: adaptive and innate. The adaptive immune system consists of T and B cells, both of which have the capacity for genetic rearrangement of germline encoded antigen receptors, providing their distinctive specificity and thus, endowing them with the ability to respond powerfully and specifically to pathogens under subsequent challenge – a concept termed immunological memory. Its ancient and more promiscuous sibling, the innate immune system, is an evolutionarily conserved foundation of immunity which reacts swiftly and indiscriminately to each pathogen encounter, as well as to non-pathogenic stress and environmental signals through a wide array of germline encoded innate immune receptors[1].

1.2 The family of innate lymphoid cells

Innate lymphoid cells (ILCs) are a family of lymphocytes whose characterization and unification has expanded in the past decade. They consist of group 1 ILCs (Natural Killer (NK) cells and ILC1) ILC2, and ILC3 subsets, which are able to respond promptly to cytokines, stress signals, nutrients and other environmental triggers, modulating inflammation and homeostasis in the host (reviewed in Vivier *et al.*, 2018[2]). Although unified by their lymphocyte morphology and shared effector functions, a lack of rearranged antigen receptors separates them from T lymphocytes, placing them in the innate arm of immunological cells. A hallmark, and also a curse, of ILC biology lies in their difficult identification strategy – they are identified primarily as $CD45^+$ lymphocytes which lack surface T cell receptors (TCR), B cell receptors (BCR), and

associated molecules CD3, CD19 and CD20. In the absence of these lineage identifying markers (also known as negative identification), ILCs can be positively identified through surface expression of the interleukin (IL-)7 receptor (also known as CD127) in both mice and humans, a critical cytokine for their development and maintenance (refer to section **1.3.4**), as well as receptor CD161 in humans[2,4]. Studies and categorization of innate lymphocytes have classically borrowed from the T cell characterization paradigm, categorizing ILC effector functions and transcriptional requirements as parallels of those of T lymphocytes. In this regard, NK cells mirror $CD8^+$ T cells due to their interferon-γ (IFNγ) secretion, cytotoxic abilities and transcription factor (TF) Eomesodermin (Eomes) as well as T-box expressed in T cells (T-bet) expression. ILC1 reflect $CD4^+$ T_H1 cells with their type 1 effector functions, IFNγ secretion and transcriptional requirements for T-bet. NK cells and ILC1 are collectively categorized into Group 1 ILCs and are at the helm of the type 1 effector response of the innate immune system, geared towards protection against intracellular bacteria and viruses, as well as tumours (**Figure 1**). ILC2 are the type 2 responders from the ILC family, which secrete IL-4, IL-5, and IL-13, and are regulated through expression of TF GATA Binding Protein 3 (GATA3), similar to $CD4^+$ T_H2 cells (**Figure 1**). ILC2 are important players in the response against parasites as well as allergic inflammation. Finally, ILC3 are type 3 responders, regulated by RAR-related orphan receptor-γ (RORγt), secrete IL-22 and IL-17, and are involved in the defense against extracellular pathogens, particularly at mucosal surfaces, reflecting T_H17 and T_H22 cells[2] (**Figure 1**). Studies into the steady state nature of ILC1, ILC2 and ILC3 subsets have posited that they seed tissues during embryogenesis, and remain resident within those tissues into adult life, unlike NK cells which largely circulate[5–7]. Not only are these cells present within tissues, but they have the ability to expand therein, and in certain cases migrate to other organs during inflammation where they can rapidly secrete remarkable amounts of cytokines, highlighting their important role as innate sentinels of mucosal sites and regulators of homeostasis[5,6,8]. The fast moving pace of the ILC field is both advantageous and unfavourable, as it leaves the scientific community with little room to consolidate information and reach a consensus regarding identification, characterization and even nomenclature in the field.

Indeed, uniform ILC nomenclature was only agreed on in recent years, and frequently undergoes revisions[2,9]. Nevertheless, as dysregulation of ILC responses have been associated with impaired clearance of helminths, susceptibility to bacterial and fungal infection, as well as a multitude of inflammatory diseases such as asthma, atopic dermatitis, psoriasis, and inflammatory bowel disease, they make an attractive research topic for potential therapeutic intervention[10,11].

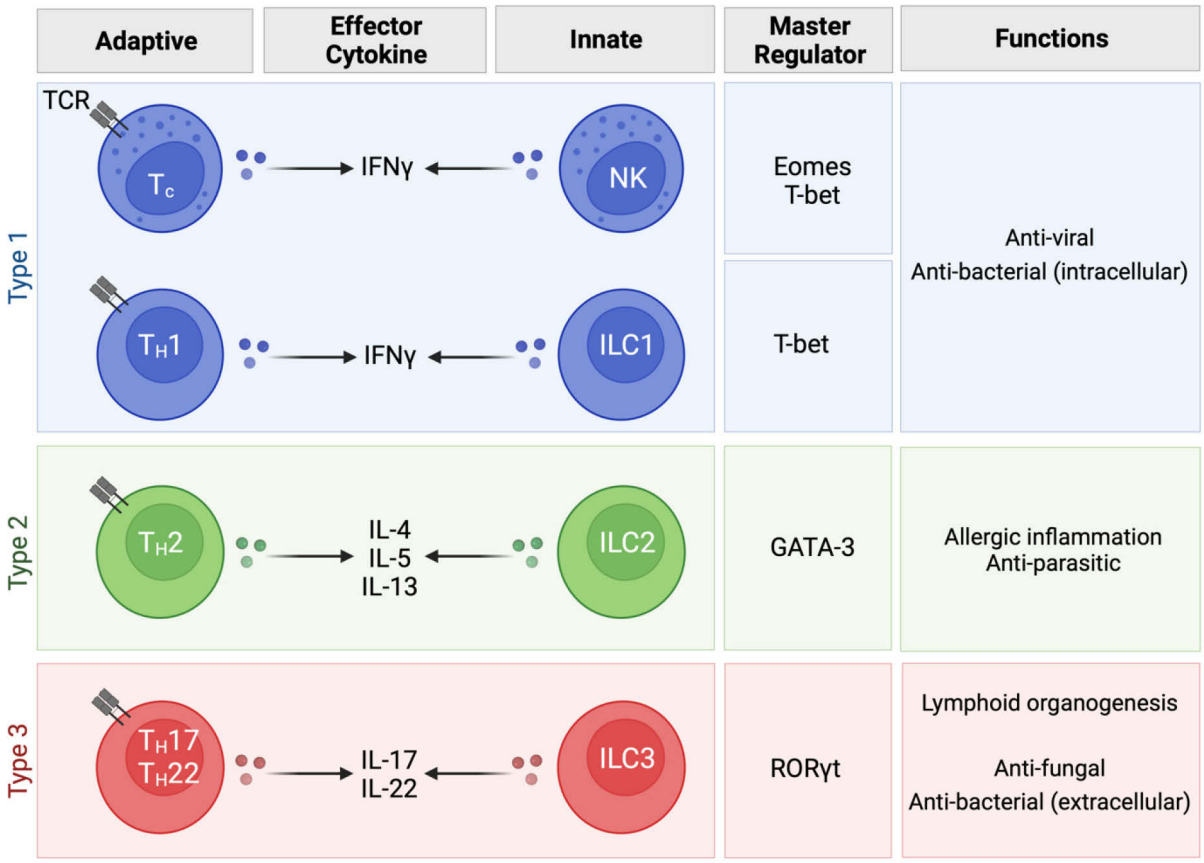

Figure 1: The innate lymphoid cell family and their effector functions. An overview of T cell and ILC family categorization and main hallmarks. Type 1 responders of the innate immune system, NK cells and ILC1, are both regulated by transcription factor (TF) T-bet, in addition to Eomes for NK cells. NK cells and ILC1 (also known as Group 1 ILCs) are involved in responses against intracellular pathogens such as viruses and bacteria, similar to T_H1 and cytotoxic T cells. ILC2 are the type 2 responders of the ILC family, secrete interleukin (IL)-4, IL-5, and IL-13, and are regulated by TF GATA3, similar to T_H2 cells. ILC2 are involved in allergic inflammation and anti-parasitic responses. ILC3 are the type 3 responders of the innate immune system and secrete IL-17 and IL-22, and are regulated by TF RORγt, akin to $T_H17/22$ cells. ILC3 are involved in protection against extracellular pathogens such as fungi and bacteria, and include a subset termed lymphoid tissue inducer (LTi) cells (not depicted) which play a role in lymphoid organogenesis.

1.2.1 Group 1 ILCs

Natural killer cells

Natural killer cells, the founding members of the ILC family, were discovered in the early 1970's in a series of *in vitro* experiments where lymphocytes of unrelated individuals were found to display "natural" cytotoxicity against cells bearing tumor antigen[12], in direct contrast to T lymphocytes which require several days to exert cytotoxic functions. Since then, the field of NK cell studies has progressed immensely, showing that these cells are ubiquitously present in almost every organ in both human and mouse, in which they comprise the majority of all ILC subsets and share conserved functions across species[13]. NK cells share a host of features with other members of the ILC family, but are demarcated by their high expression of TF Eomes and their cell lysis ability mediated by granule-stored cytolytic machinery such as perforins and granzymes. Upon degranulation, marked by upregulation of CD107a, perforin molecules oligomerize and form a pore in the target cell membrane through which granzymes diffuse and induce cellular caspase-dependent and independent cell death[14]. In human peripheral blood, where NK cells circulate and constitute a significant portion of all lymphocytes, a distinction in phenotype and effector functions of conventional NK cells is delineated by CD56 expression (as reviewed in Vivier *et al.*, 2008[3]). $CD56^{bright}$ NK cells are potent type 1 cytokine (IFNγ, tumor necrosis factor α (TNFα)) producers, lack expression of type III Fcγ receptor (CD16) and cytotoxic ability, and are enriched within tissues and secondary lymphoid organs[15,16]. $CD56^{dim}$ NK cells are thought to mature from the $CD56^{bright}$ subset and acquire CD16 expression and the ability for antibody dependent cellular cytotoxicity[3,17,18]. Resembling the maturation steps of human NK cells, mouse NK cell maturation stages can be identified through surface marker expression of CD27 and CD11b. $CD27^{+}$ $CD11b^{-}$ NK cells populate the bone marrow, lymph nodes and liver and are potent proliferators. Gain of CD11b marks an intermediate stage, and finally, loss of CD27 marks the terminal differentiation of NK cells which then gain cytotoxic activity and populate peripheral sites[19]. NK cells are crucial tools of the innate immune system in the response against viral

and intracellular pathogens, as well as altered states of self as found in tumor tissue. They recognize and regulate effector functions in response to ligand interaction with a host of both activating and inhibiting NK cell receptors termed natural cytotoxicity receptors (NCRs), such as NKp80 and NKp46, the latter of which is conserved across a multitude of species ranging from mice to humans, and with which NK cells can be identified[20]. A hallmark of NK cells is their recognition of transformed or infected host cells through altered or absent expression of major histocompatibility complex class I (MHC-I), a trait termed recognition of "missing self", and mediated through Killer-cell immunoglobulin-like receptors (KIRs), CD94/NKG2A heterodimers in humans, and lectin-like Ly49 dimers in mice[20–22]. Apart from NCRs and KIRs, NK cells respond to cytokine signals such as IL-12, IL-15 and IL-18, produced by myeloid cells in response to stress or infection. It is through a careful consolidation of these various signals that NK cells exert their anti-viral and anti-tumor effector functions or abstain therefrom.

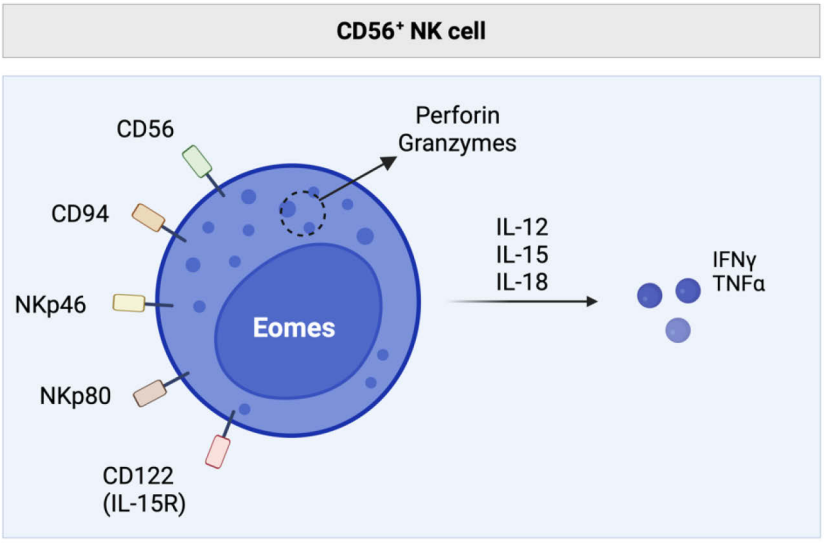

Figure 2: Human natural killer cells. Human natural killer (NK) cells express a myriad of proteins on their surface including natural cytotoxicity receptors (NCRs) and cytokine receptors, as well as intracellular cytotoxic proteins such as perforin and granzymes. Cytokine stimulation with IL-12, IL-15 and IL-18 induce IFNγ and TNFα production.

ILC1

As Group 1 ILC members, ILC1 and NK cells share a multitude of features. Chief among them the secretion of type 1 cytokine IFNγ in response to cytokine stimuli from IL-12, IL-15 and IL-18, and the requirement of TF T-bet for these functions. The first descriptions of ILC1 were based on mouse studies of the small intestine lamina propria, where a group of cells were described as CD127^{low} T-bet expressing type 1 ILCs with a potent ability for IFNγ secretion[23,24].

Unlike NK cells, mouse ILC1 lack Ly49 receptors, responsible for self-recognition of viral infected or tumor transformed cells through MHC-I, as well as the cytolytic machinery (perforin, granzymes) necessary for cell killing. Distinct populations of murine ILC1 with variable expression of CD127, as well as tissue resident NK cells, have been described in many organs as well as solid tumors[25]. Interestingly, T-bet deficient mice lack ILC1 but retain NK cell populations, suggesting T-bet is not necessary for mouse NK cell development, and cementing Eomes as a central identifier of NK cells[26]. As ILC2 and ILC3, ILC1 also have a requirement of GATA3 for their development, further separating them from conventional NK cell lineages[27].

In humans, two subsets of non-NK cell type 1 innate responders have been identified. One of these ILC1 subsets was first described in human tonsil and intestine as IFNγ-producing innate cells which differ from conventional NK cells based on their lack of cytotoxicity, low to no expression of CD56 and CD94, and high expression of CD127 and CD161, both markers of ILCs (**Figure 3**)[28]. Akin to mouse ILC1, these cells were described to express T-bet, lack Eomes, and dwell in the intestinal lamina propria and other mucosal tissues. These ILC1 were proposed to contribute to inflammation, due to the observation that they accumulate within inflamed intestinal lamina propria of patients with inflammatory bowel disease, at the expense of ILC3[28–30]. The second human ILC1 subset described was an intraepithelial (ie) $CD103^+$ subset in the tonsil and intestine which, in contrast to other ILC subsets, lacks CD127[31]. These ieILC1 share many features with canonical NK cells and express NK-associated markers and cytotoxic molecules such as CD56, CD94, perforin and granzymes A and B.

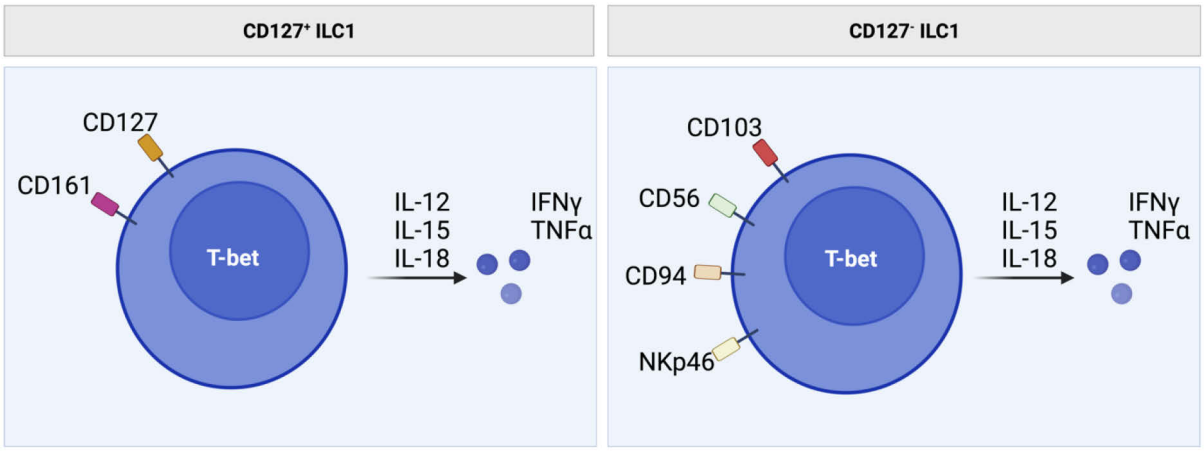

Figure 3: Human ILC1 subsets. Two subsets of human ILC1 have been described, which can be identified by their differential expression of CD127. CD127$^+$ ILC1 lack expression of markers normally associated to type 1 responders. In contrast, CD127$^-$ CD103$^+$ intraepithelial ILC1 share a range of protein expression with NK cells, including CD56, CD94 and NKp46. Both ILC1 subsets are regulated by the master transcription factor T-bet, and secrete IFNγ and TNFα in response to cytokine stimulation from IL-12, IL-15 and IL-18.

1.2.2 Group 2 ILCs

Originally termed “Nuocytes” or “natural helper cells”, ILC2 were the earliest member of the ILC family apart from NK cells to obtain their own classification[32–34]. As critical producers of type 2 cytokines, ILC2 are at the helm of type 2 innate immune responses, and are of particular importance in defence against parasitic infection and induction of eosinophilic inflammation, hence playing a role in allergic reactions[13,35–37]. Mouse ILC2 encompass a significant fraction of the ILC pool at barrier sites, such as the lung, skin, the gastrointestinal tract, and most recently the central nervous system (CNS)[38–43]. Contrary to their murine counterpart, human ILC2 have relatively low frequencies in peripheral blood, lung and gut, but similarly are main players in the skin[13,44,45]. Human ILC2 express CD127 and CD161, and can be positively identified by expression of the activating prostaglandin D_2 receptor 2 (CRTH2), a receptor for prostaglandin D_2 (PGD2), which correlates to high GATA3 expression[4,46]. Apart from high GATA3 expression, ILC2 are regulated by TF RAR Related Orphan Receptor α (RORα), and are rich in prostaglandin signaling not only through CRTH2 but also through prostaglandin synthesis and breakdown, as seen by high expression of hydroxyprostaglandin dehydrogenase-15 (HPGD) and hematopoietic prostaglandin D synthase (HPGDS)[47,48]. Assessment of ILC2 from human peripheral blood, lung, and fetal gut show expression of

chemokine receptors CCR2 and CCR4, highlighting that they can be recruited by other cell types in response to stress or infection[4,49]. Activation of ILC2 within tissue can be mediated by cytokine signaling, in particular through IL-33 and IL-25. Interestingly, a recent single-cell RNA sequencing study cross-examined mouse ILC2 phenotypes across tissue niches and revealed that, besides a core gene set of *Gata3* and *Il7r* transcripts, mouse ILC2 signatures vary in a tissue-dependent manner, not only in the adult but also in the neonate[50,51]. The IL-33 receptor is preferentially expressed in ILC2 from the lung, adipose tissue, bone marrow and CNS, while IL-17RB (the IL-25 receptor) is highly expressed in small intestine ILC2 instead[42,43,50]. In humans, circulating peripheral blood ILC2 express both receptors at only very low levels, although they can be upregulated in response to their respective cytokine[52,53]. The varied cytokine receptor expression on mouse ILC2 suggests that tissue-specific signals play a role in the surface phenotype and functionality of these cells, an aspect of human ILC2 which remains to be thoroughly evaluated.

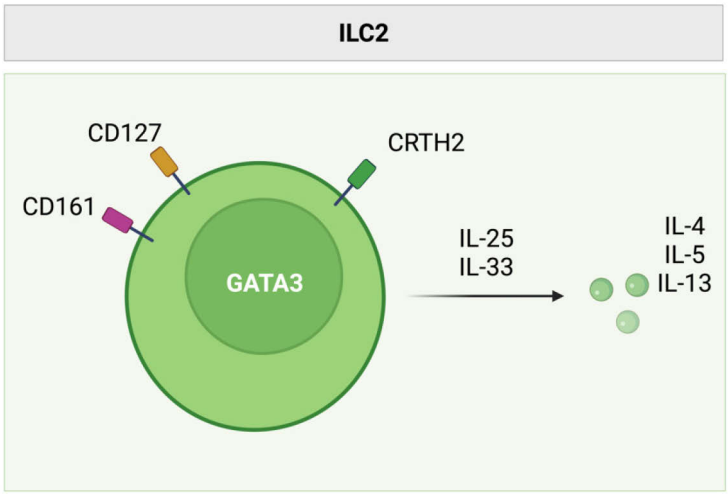

Figure 4: Human ILC2. Human ILC2 are chiefly recognized by their expression of prostaglandin D2 receptor 2 (CRTH2) together with high levels of master regulating transcription factor GATA binding protein 3 (GATA3). ILC2 secrete type 2 effector cytokines interleukin (IL)-4, IL-5 and IL-13 in response to stimulation with cytokines IL-25 and IL-33.

1.2.3 Group 3 ILCs

Group 3 ILCs comprise of ILC3 and lymphoid tissue inducer (LTi) cells, both of which require RORγt for their development and function.

Lymphoid tissue inducer (LTi) cells

LTi cells were described early on in the mouse, where they appear during embryogenesis and play a role in orchestrating the development of lymphoid structures. Murine CD127^{+} RORγt^{+}

LTi cells can be discerned from other ILC3 subsets by their expression of CD4 and additionally chemokine receptor CCR6[54]. Chemokine receptors CXCR5 and CCR7 on LTi cells during embryogenesis allow for homing to future lymph node anlagen, where the accumulation of LTi cells and their expression of lymphotoxin (LT)$\alpha_1\beta_2$ triggers the organization of specialized stromal cells into lymph nodes and Peyer's Patches (PP), and promotes the retention of LTi cells and other lymphocytes. The ability of LTi cells to generate lymph nodes is not only dependent on TF RORγt, as lymph nodes and other lymphoid associated tissues are missing in *Rorc* deficient mice[55,56], but also on a network of TFs including RORα, which antagonize TF T-bet[57].

In the human fetus, LTi cells are detected in the mesentery during the first trimester and within developing lymph nodes in the second trimester as $CD127^+$ $CD161^+$ $ROR\gamma t^+$ cells expressing Receptor activator of nuclear factor kappa-B ligand (RANKL) and chemokine receptor CCR7, allowing for homing to the lymph nodes[58]. Although a population of LTi-like cells expressing CCR6 and CD4 can be identified in the adult mouse, various single-cell RNA sequencing studies from *ex vivo* isolated ILC3 in adult humans from various compartments such as tonsil, lung, and gut, have thus far failed to identify an LTi signature as a separate identity from the rest of ILC3[47,48,59,60]. Nevertheless, individuals with a deficiency in *RORC* (encoding RORγt) fail to develop palpable cervical and axillary lymph nodes and have a decreased thymus size, suggesting that *RORC* contributes to lymphoid structure organogenesis in humans as well[61]. It remains an open question whether LTi cells in humans are present chiefly during embryogenesis to guide lymph node development, or whether an LTi-like population remains post-birth.

ILC3

In both mice and humans, ILC3 can be separated into NCR^+ and NCR^- subsets. NCR^+ ILC3 in mouse express NKp46 and require T-bet for development and maintenance[71,72]. Human NCR^+ ILC3 express NKp46 at low levels (in comparison to the high levels expressed by NK cells) as well as high levels of NKp44. They dominate in tonsils, where all ILC subsets have been well

described, and the gastrointestinal tract, increasing in frequency from the duodenum to the colon[44,45,73] (**Figure 6**). In adult tonsil, ILC3 were originally identified as CD127$^+$ cells expressing surface NCRs NKp46 and NKp44 with the capacity for IL-22 production, and were termed NK-22[58,62]. Though ILC3 and NK cells share expression of several activating receptors, ILC3 represent a distinct lineage based on their requirements for TF RORγt and lack of dependency on Eomes or T-bet[58,62–68]. Interestingly, NKp44$^+$ ILC3 are associated with higher IL-22 expression[74,75], a cytokine involved in epithelial repair and regeneration, and are decreased in chronic inflammatory diseases involving epithelial damage such as Crohn's disease or ulcerative colitis[28,30,75]. Unlike in mice, T-bet expression or dependence in human NCR$^+$ ILC3 *ex vivo* has yet to be described.

Heavily involved in defense against extracellular bacteria and fungi, as well as regulation of the microbiota, ILC3 lead the innate type 3 response and are major producers of type 3 cytokines such as IL-22 and IL-17 at steady state, particularly at mucosal surfaces such as the tonsil and intestine[58,62]. ILC3 respond to cytokine stimulation from IL-23 and IL-1β, and express both cytokine receptors across tissues, together with surface expression of stem cell factor receptor (CD117, also known as c-kit) and RANKL (**Figure 5**)[47,48]. Apart from canonical cytokines IL-22 and IL-17, ILC3 can secrete IL-26, a cytokine involved in epithelial cell activation[69], as well as LTA, LTB, granulocyte macrophage-colony stimulating factor (GM-CSF), and chemokines IL-8 and CCL20[48,58,60,62]. Despite their hallmark tissue residency, the microenvironment and precise localization of ILC3 within tissue is as of now largely unknown. A recent study on adult tonsil samples has shown through multi-epitope ligand cartography (MELC) the precise microanatomical location of human ILC3, and revealed them to cluster together (in groups of 2-4 cells) in the vicinity of plasma cells[70]. The functional relevance of this finding remains to be investigated.

In addition to production of cytokines at mucosal surfaces, recent studies have brought the ability of ILC3 to regulate adaptive responses to the forefront. Expression of MHC-II in ILC3

was first described in the small intestine and colon in mice, and was found to be restricted to NCR$^-$ ILC3[76], later confirmed by single-cell transcriptomics[77]. This, and a subsequent report by von Burg *et al*., revealed that ILC3 from the mesenteric lymph nodes, small intestine, or colon fail to express costimulatory molecules such as CD40, CD80 and CD86 either at steady state or after innate inflammatory signals, such as those provided by IL-1β. Instead, splenic ILC3 respond robustly to IL-1β to upregulate MHC-II and associated costimulatory proteins, thus having a higher efficiency in activating CD4$^+$ T cells than their small intestine counterpart[76,78–80]. In humans, MHC-II expression (*HLA-DR*, *-DP, -DQ*) on ILC3 has also been reported by single-cell transcriptomics in the tonsil, lung and non-inflamed colon, and at protein levels in the colon of individuals with inflammatory bowel disease, or non-inflamed controls[47,48,80,81]. These cells, which in the tonsil comprise of NCR$^-$ ILC3, may represent the equivalent to MHC-II expressing intestinal mouse ILC3, which tune T cell responses.

Overall, Group 3 ILCs encompass a largely heterogeneous family of RORγt dependent cells, which exert potent lymphoid organogenesis as well as anti-bacterial functions and regulate adaptive responses.

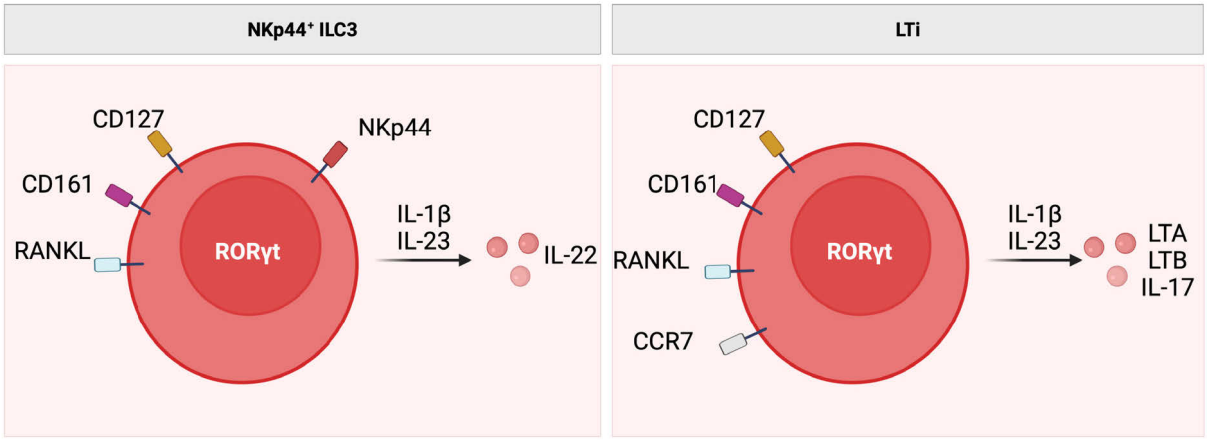

Figure 5: Human Group 3 ILCs. Human Group 3 ILCs comprise of ILC3 which exert anti-bacterial and anti-fungal functions, and lymphoid tissue inducer (LTi) cells which play a role in orchestrating lymphoid organogenesis. The former can be identified in mucosal tissue as RORγt expressing ILCs, and further enriched for through RANKL and NKp44 expression. Cytokine stimulation with interleukin (IL)-1β and IL-23 leads to IL-22 production from NKp44$^+$ ILC3. LTi cells, particularly in the fetus, are RORγt$^+$ ILC3 which express RANKL and chemokine receptor CCR7, and produce lymphotoxins A and B (LTA, LTB) as well as IL-17.

1.2 Identification of human ILCs

A standardized identification strategy based on flow cytometric assessment of surface proteins has been proposed to identify all human ILC subsets, in an effort to aid the consistency of investigations[9] **(Figure 6; own data)**. This strategy is based on data mainly from tonsil and peripheral blood, tissues which are relatively readily accessible, and where all ILC subsets have been described[82]. As human ILCs are present in most tissues at low frequencies, depletion of $CD3^+$ T cells and/or $CD19^+$ B cells through magnetic- or fluorescence- based sorting can aid in the enrichment of ILCs for identification and isolation. In the absence of lineage-identifying markers (denoting macrophages and dendritic cells, as well as T and B cells), NK cells can be positively identified by their surface expression of CD56 and CD94 (**Figure 6a**). These markers correlate to high TF levels of both Eomes and T-bet (**Figure 6b**). From the population of non-lineage, non-NK cells present in these tissues, ILCs are identified as $CD127^+$ cells with or without the addition of CD161. $CD127^+$ ILCs comprise of ILC1, ILC2, and ILC3 subsets, whose frequencies vary in a tissue- and inflammation-dependent manner. Unlike the mouse, staining of TFs such as RORγt in primary human tissue can lack resolution and vibrancy, necessitating the combination of TF factor staining with surrogate surface markers[9]. From $CD127^+$ ILCs, the dual usage of CD117 and CRTH2 can facilitate identification of ILC3 as $CD117^+$ $CRTH2^-$ cells which encompass both $NKp44^+$ ILC3 and $NKp44^-$ ILCs, in which RORγt expression can be appreciated (**Figure 6a,b**). ILC2 are denoted as $CRTH2^+$ cells with high GATA3 expression, however, CRTH2 can be downregulated in inflammatory tissue environments, as observed in chronic obstructive pulmonary disease in the lung[47,83] (**Figure 6a,b**). Thus far, a reliable substitute for CRTH2 has yet to be identified, although usage of ST2 (IL-33R) or very high expression of CD161 alone has been suggested[82]. Finally, $CD117^-$ $CRTH2^-$ cells comprise of a population of $CD127^+$ ILC1, which can lack NKp44 and CD56 expression. Unlike the mouse, human $CD127^+$ ILC1 express low amounts of T-bet, making identification through TF staining difficult (**Figure 6b**). The second subset of human ILC1, $CD103^+$ ieILC1, can be found in the $CD127^-$ compartment. All in all, this strategy is well regarded and utilized across studies to identify human ILC subsets *ex vivo*.

1.2.2 Untangling human NK cells and ILC1

Despite this clear strategy, the lines between NK cell and ILC1 identity in human are confounded by the fact that overlaps in phenotype and function can be observed in various organs and inflammatory conditions. Recent attempts to shed light on this issue using complex single-cell technologies such as RNA sequencing of NK cells and ILC1 throughout various healthy adult tissues has done little to clarify the matter. One of these recent studies showed that the classical CD127^{+} ILC1 found in organs such as lung and intestine share a large genetic signature with NK cells, and indeed, can also express CD56, CD94, Eomes and other NK cell markers unlike originally described[59]. In accordance, another independent single-cell RNA sequencing investigation described Eomes expression within tissue CD127^{+} ILC1 as well[47]. This same study also showed that circulating ILC1 in peripheral blood lack a type 1 gene signature entirely, and in fact, share a genetic profile with T lymphocytes, including expression of *CD3E, CD3D, CD3G, CD4, CD5,* and *CD6* transcripts. Both this and an earlier study also detected TCR rearrangements in peripheral blood and tonsil ILC1, suggesting either a contamination with T cells, or that the gating strategy is insufficient to identify ILC1 in these tissues[47,48]. The opinion that the CD127^{+} ILC1 is in fact not a separate lineage has also been expressed[45,84]. With regards to the CD127^{-} CD103^{+} ieILC1, a direct comparison of these cells to classical CD56^{+} NK cells from the tonsil yielded only few differentially regulated genes as ieILC1 specific, and instead a large shared signature of canonical NK cell genes such as *GZMA, GZMB, PRF1, KLRF1* (encoding NKp80)*, KLRC1* (encoding NKG2A) as well as of ILC3 associated transcripts *KIT* (encoding CD117) and *IL1R1*[85,86]. Further studies, in particular developmental lineage tracing investigations, will be necessary to elucidate the differences between human NK cells and ILC1.

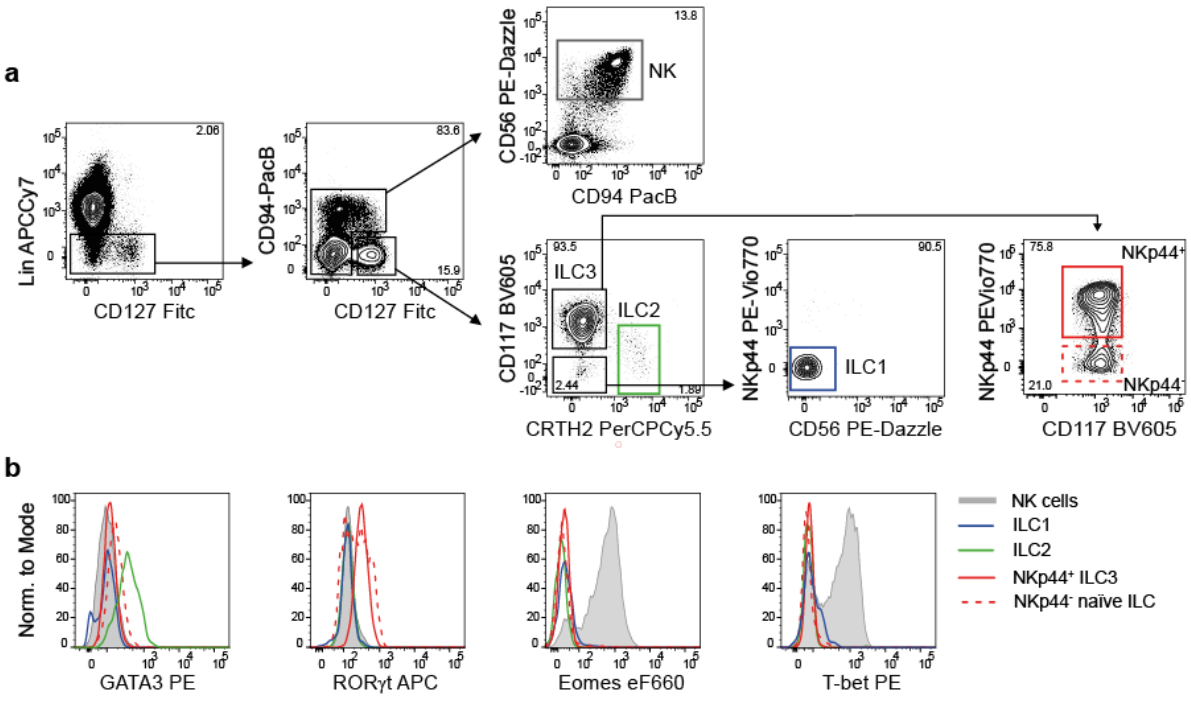

Figure 6: Identification of all ILC subsets in human tonsil. (**a**) Representative surface protein gating strategy of all ILC subsets in human tonsil. After magnetic depletion of CD3$^+$ T cells, cells were gated as viable CD3$^-$ CD14$^-$ CD19$^-$ FcεRIα$^-$ CD123$^-$ BDCA3$^-$ (Lin$^-$) and either CD94$^{+/lo}$ CD127$^{-/lo}$ CD56$^+$ NK cells (grey); CD94$^-$ CD127^{hi} CRTH2$^+$ ILC2 (blue); CD94$^-$ CD127^{hi} CD117$^-$ CRTH2$^-$ NKp44$^-$ CD56$^-$ ILC1 (blue); CD94$^-$ CD127^{hi} CD117$^+$ CRTH2$^-$ NKp44$^+$ ILC3 (red, solid); or CD94$^-$ CD127^{hi} CD117$^+$ CRTH2$^-$ NKp44$^-$ naïve ILC (red dashed). Gate numbers reflect population frequencies. (**b**) Representative expression of transcription factors of human ILC subsets as gated in (a). As published in Cossarizza...**Hernandez DC**... *et al*., 2021[84].

1.3 ILC development in the context of human hematopoiesis

1.3.1 Early events during lymphopoiesis

Though the process of hematopoiesis, the generation of all blood cells, was postulated as early as 1909 by Russian biologist Alexander Maximow[88], the canonical evidence originated as a consequence of lethal radiation in the atomic era leading to bone marrow failure, which could be rescued post injection of bone marrow cells from non-irradiated donors[89]. Since then, the field of human hematopoiesis has expanded rapidly and the journey from progenitor to lymphocyte has been revealed as a tightly regulated and hierarchical process. The derivation of all blood cells lies in the hematopoietic stem cell (HSC) compartment, which shares the features of self-renewal and multi-lineage differentiation. In humans, HSCs and their downstream progenitors (jointly termed hematopoietic progenitor cells (HPCs), henceforth)

exhibit expression of the surface phosphoglycoprotein CD34, originally described to mediate cellular adhesion to P- and E-selectin expressed by stroma cells in adult bone marrow. Importantly, $CD34^+$ HPCs derived from bone marrow, umbilical cord blood, and mobilized peripheral blood have the ability to repopulate the hematopoietic compartment after hematopoietic stem cell transplant (HSCT)[90–94]. Mouse HPCs can lack CD34 expression, and evidence puts forward that $CD34^-$ HPCs exist in humans as well[95,96], however, frequencies suggests that > 99% of HPCs in human cord blood are $CD34^+$.

The establishment of blood and immune systems from HPCs is conserved across vertebrates and begins early on during embryogenesis[97]. In humans, multipotent $CD34^+$ HPCs are detected in the aorta-gonad-mesonephros at around weeks 3-4 of gestation, and shortly thereafter seed the liver, which becomes the primary hematopoietic organ during embryonic development[97]. It is posited that HPCs home to the bone marrow just before birth, where hematopoiesis dominates from thereon into adult life[98]. The scarcity and difficulty in assessing both fetal tissues and the adult bone marrow niche make human hematopoietic stages challenging to study, pinpointing the urgent necessity of modelling these processes *in vitro*.

Studies in both human and mice exposed that lymphopoiesis follows the basic stages of cellular differentiation, in that the properties of self-renewal and multipotency are lost in a series of steps as HPCs progressively restrict lineage commitment and ultimately commit to a single-cell fate (reviewed in Doulatov *et al.*, 2012[90]). This sequential differentiation course from $CD34^+$ HPCs to differentiated effector cells is a primarily irreversible process during steady state conditions. As $CD34^+$ HPCs advance through the developmental pathway to lymphocytes, they first differentiate into multipotent progenitor cells (MPPs) which retain both lymphoid and myeloid potential. Thereafter, a significant lineage making decision is made, tightly regulated by transcription factor networks involving *BCL11A*, *GATA3, MEF2C, SPI1,* and *CEBPA* which restricts the subsequent differentiation into two fundamental branches: myeloid and lymphoid[99,100]. The myeloid branch of this bifurcation is headed by the common

myeloid progenitor (CMP) which can generate granulocytes (neutrophils, eosinophils, mast cells and basophils), monocytes, erythrocytes and megakaryocytes, while the common lymphoid progenitor (CLP) is the source of all lymphoid cells. In humans, the CLP is enriched within the heterogeneous pool of $CD34^+$ $CD45RA^+$ HPCs, which have preferential potential for B cell, conventional and unconventional T cell, and innate lymphoid cell generation including NK cells[90,100,101].

1.3.2 Mouse ILC development

Analogous to T and B lymphocytes, ILCs arise from the CLP, which has lost the ability to generate cells of the myeloid lineage. ILC ontogeny has been most extensively investigated in the mouse, where a population of integrin $\alpha4\beta7^+$ $Flt3^+$ $CD127^+$ cells within bone marrow and fetal liver CLPs, termed the α-lymphoid precursor (αLP) or ILC precursor (ILCP) has been described. These precursors were shown to give rise to ILC1, ILC2, and ILC3 including LTi cells, but not NK cells, suggesting that NK cells follow a distinct developmental path[23,102,103]. Expression of ILC-subset associated transcription factors (Eomes, T-bet, RORγt) are absent in the ILCP, which instead highly express inhibitor of DNA binding 2 (Id2), a helix-loop-helix transcriptional repressor that antagonizes E proteins necessary for T and B cell development, and whose absence is associated with a lack of ILC subsets[23,32,102,104]. However, contradictory reports have recently suggested that Id2 expressing progenitors do indeed give rise to NK cells together with all ILC subsets[105–107]; this inconsistency is likely due to varying mouse models and gene reporter strengths. This is supported by the strong promotion of Id2 expression by TF nuclear factor IL-3 (NFIL3), a factor essential for innate lymphocyte differentiation, in particular that of NK cells[107–109]. Downstream of the $Id2^+$ $\alpha4\beta7^+$ ILCP, increased expression of promyelocytic leukemia zinc finger (PLZF), an Id2 target involved in NKT cell development[110], marks a decrease in NK and LTi cell potential and a focus on potential for what is often termed “helper” ILC subsets: ILC1, ILC2, and ILC3[105,111]. This $PLZF^{hi}$ $Id2^+$ precursor is termed the common helper ILC progenitor (CHILP), and further restricts its differentiation potential by

upregulating GATA3 and TOX transcription networks, both associated to development of helper ILC lineages and not NK or LTi cells[53,112–115]. Although the pathway of ILC development in mice has been ardently investigated, the stage at which precursors seed tissue and terminally differentiate, both during fetal development and adulthood, remains unclear. ILC progenitors identified in the fetal liver may dominate ILC generation during embryogenesis, and their progeny might seed the tissue where they remain resident throughout life. It is suggested that these ILC progenitors from the fetal liver then home to the bone marrow shortly before birth, where they remain into adulthood. However, various reports have identified the presence of ILC progenitors already within fetal tissue, such as lung or intestine, suggesting that ILC progenitors may seed tissues during embryogenesis earlier than previously assumed[57,116–118]. Similarly, recent studies in adult mice have posited for the first time the idea that the tissue ILC compartment might be self -renewing and -maintaining, rather than reconstituted from central lymphoid tissues such as the bone marrow[116,118–120].

1.3.3 Human ILC development

CD34⁺ ILC precursors

Few studies have identified the precursor populations between the CLP and terminally differentiated ILCs in humans. It was suggested early on that human ILC progenitors lie within CD34⁺ HPCs, as human NK cells and/or ILC3, as well as ILC2-like cells, have been generated *in vitro* from this starting population in a handful of studies[121–124]. In recent years, ILC restricted progenitors were described within the CD34⁺ CD45RA⁺ CLP-containing population across a variety of tissues (**Figure 7**). In a pioneering study, the first human ILC restricted progenitor was identified in adult tonsil and intestinal lamina propria, but not in circulation, as a CD34⁺ CD45RA⁺ RORγt-expressing precursor (ILC3P), which gives rise preferentially to ILC3 *in vitro*, accordingly the dominant helper ILC subset in these tissues[125]. This suggested for the first time that adult human ILCs might be renewed and maintained within tissue sites, and not only in the hematopoietic niche of the bone marrow, as formerly supposed. Following this finding, an

NK lineage restricted CD34$^+$ CD45RA$^+$ progenitor which also expresses CD38, CD10, and CD7 (termed NKP) was identified in adult bone marrow and cord blood, as well as fetal liver, reflecting the circulating nature of NK cells. A small population of NKP was also detected in the tonsil, an NK cell rich site. The NKP generates functional NK cells *in vitro* as well as *in vivo,* as shown through transfers into immunodeficient mice[126]. In 2016, an IL-1R1$^+$ ILC progenitor able to generate all helper ILC subsets as well as NK cells was propositioned to sit within the CD34$^+$ CD45RA$^+$ RORγt$^+$ ILC3P previously described, implying that NK cells could develop from a RORγt$^+$ precursor[127]. This was at odds with mouse data generated from RORγt deficient and fate map reporter mice, showing normal numbers of NK cells and no history of RORγt expression during NK cell development, respectively, as well as the finding that *RORC*-deficient individuals also harbour normal numbers of NK cells[23,128,129]. Most recently, another human ILCP was identified as CD34$^+$ α4β7$^+$ CD48$^+$ CD52$^+$; this population was not found *ex vivo* in umbilical cord blood or peripheral blood, and only after expansion in *in vitro* culture or a small subset in the tonsil[130]. Knowledge regarding the lymphopoiesis of human ILC family members remains scarce, in particular the connection between the CLP and terminally differentiated ILCs. In this regard, a comprehensive *in vitro* culture system would fundamentally

enable the study of human ILC differentiation, and aid in filling in the gaps in knowledge that are currently present in the field.

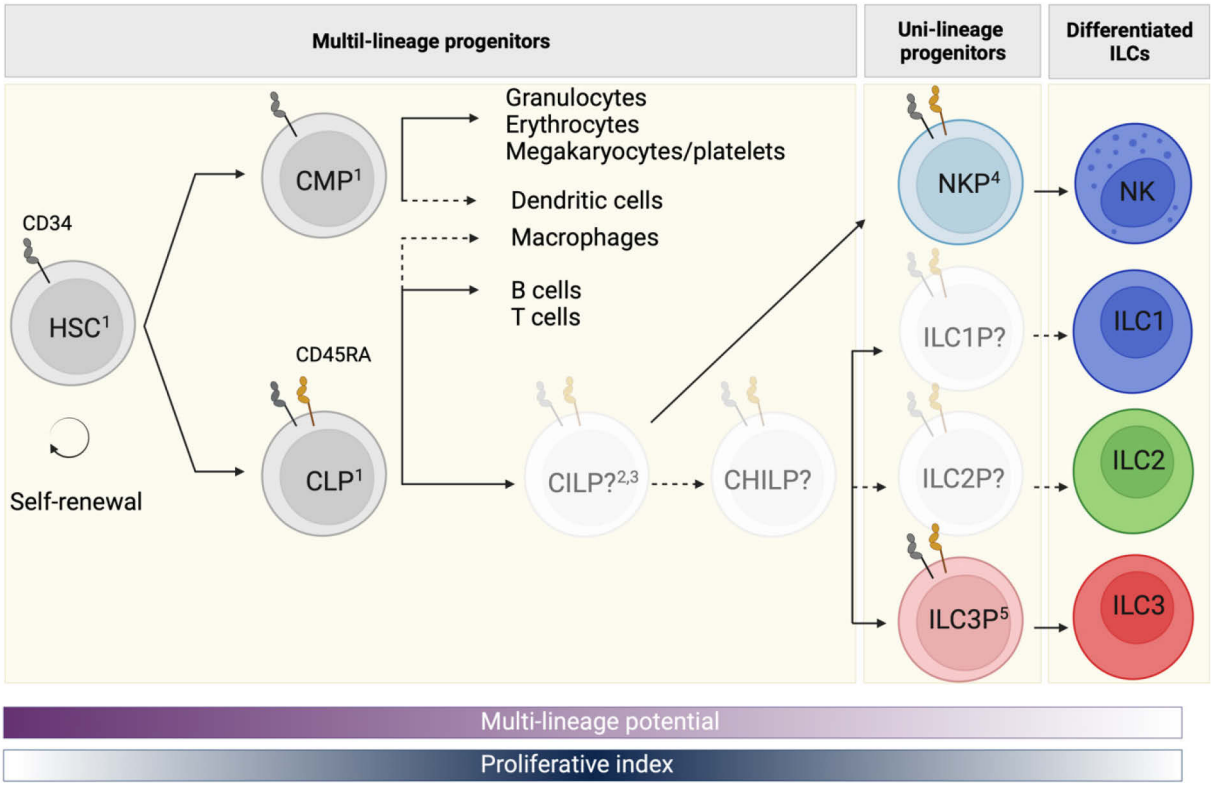

Figure 7: Proposed roadmap to human ILC development. Human ILC development and its gaps are schematized. All human cell generation starts from the self-renewing CD34$^+$ hematopoietic stem cell (HSC) pool, from which multi-lineage potential decreases as daughter cells differentiate into further and further restricted progenitors. A major lineage making decision toward either myeloid or lymphoid fates first takes place. The CD34$^+$ common myeloid progenitor (CMP) gives rise to granulocytes, erythrocytes, megakaryocytes and platelets, while the CD34$^+$ CD45RA$^+$ common lymphoid progenitor (CLP) has the ability to engender B cells and T cells as well as all ILC subsets. The generation of dendritic cells and macrophages has been observed from both CMPs and CLPs, and requires further investigation. In the mouse, a common ILC progenitor (CILP) able to give rise to all ILC subsets including NK cells has been described, as well as a common helper ILC progenitor (CHILP) which itself rises from the CILP, and lacks NK cell potential. The counterparts of the CILP and the CHILP have yet to be described in humans. Committed human ILC progenitors able to give rise to only NK cells (NKP) or ILC3 (ILC3P) have been described, and not for ILC1 or ILC2. 1. Doulatov *et al.,* 2012. 2. Scoville *et al.,* 2016. 3. Tufa *et al.,* 2021. 4. Renoux *et al.,* 2015. 5. Montaldo *et al.,* 2014.

CD34$^-$ ILC precursors

A recent development in the ILC field has nudged ILC development research out of the CD34$^+$ court. In 2017, Lim and colleagues investigated what at the time were termed peripheral blood ILC3, which consisted of CD127$^+$ CD117$^+$ ILCs with low levels of lineage identifying transcripts including *RORC* (encoding for RORγt) and little capacity to secrete cytokines after stimulation,

but with epigenetically poised cytokine loci[128]. They observed that after *in vitro* culture with cytokines, akin to polarization of naïve $CD4^+$ T cells, these cells would give rise to functionally capable ILC subsets including $Eomes^+$ NK cells, and obtained similar results through transfer of these putative human ILC precursors into immunodeficient mice. This $CD34^-$ $CD117^+$ ILC precursor was found circulating in cord blood and adult peripheral blood, as well as in lung and tonsil tissue. This circulating ILCP has since been revealed to be a highly heterogeneous innate lymphoid population, which clusters most closely to ILC3 populations in transcriptomic analysis, and thus might include mature ILC3 as well as uncommitted ILCP populations. In 2018, it was suggested that expression of CD56 can divide this population into a $CD56^+$ NK/ILC3 precursor and a $CD56^-$ ILC2 precursor[131], and a study in 2019 further expanded on this concept and narrowed down the $CD56^-$ ILC2-skewed progenitor as expressing KLRG1, a marker known to be expressed by ILC2 in both mice and humans[112,132,133]. It was proposed that this circulating progenitor derives from the $CD34^+$ CLP pool, enters tissue and therein differentiates into the appropriate ILC subset based on signals from the microenvironment[128,134,135]. However, the developmental relationship between $CD34^+$ HPCs and this circulating $CD34^-$ ILCP remains to be formally described.

The fact that this population of mainly circulating ILC precursors lacks expression of markers associated with hematopoietic progenitor cells such as CD34, and instead express a strong transcriptional ILC signature has led voices in the field to suggest a nomenclature more in line with that of T cells, in that these may be a naïve ILC subset. The discussion on ILC progenitor versus naïve ILC has also highlighted the need for additional markers for the identification of *bona fide* ILC3 in circulation and tissues, as CD117 alone is not sufficient[47].

1.3.4 Developmental requirements for ILCs

In humans, hematological perturbations or deficiencies can provide insight into hematopoietic decisions and the requirements thereof, questions that in mice can be answered in a more targeted way with genetic modification techniques. In these ways, it was shown that the

development and maintenance of helper ILC subsets (ILC1, ILC2, and ILC3) requires signaling through the common γ-chain (γc; also known as IL-2Rγ), which constitutes part of the IL-2, IL-4, IL-7, IL-9, IL-15 and IL-21 receptor complexes[136]. IL-7, produced by stromal cells, epithelial cells and fibroblasts, signals through its receptor IL-7Rα (CD127) together with IL-2Rγ, and is expressed on all helper ILC subsets and committed ILC progenitors[32,33,112,137]. As observed in *Il7rα* deficient mice, IL-7 is heavily implicated in the differentiation and maintenance of ILC2, ILC3 and LTi cells[137,138]. The necessity of IL-7 for ILC2 and ILC3 differentiation is supported by the observation that individuals with a mutation in the IL-7R gene (*IL7R*) have decreased numbers of these subsets but not of NK cells[137,139]. The decreased, but not absent, numbers of ILCs in these individuals could be accounted for by a recently described IL-7R-independent mechanism for ILC2 and ILC3 development through IL-15[140], suggesting there exists a small redundancy in the requirement for IL-7 which potentially rescues total ILC deficiency. Interestingly, patients with mutations in *IL2RG (*encoding IL-2Rγ) or *JAK3,* involved in IL-2Rγ signaling, lack detectable lymph nodes, suggesting that complete abolishment of IL-7 and IL-15 signaling results in impaired LTi cell generation and lymph node organogenesis in humans[141–143]. The few studies available of human helper ILC generation *in vitro*, in particular ILC3, have only been possible with the provision of IL-7 signaling[123,125,128,144].

IL-7 signaling may not be a prerequisite for NK cell and ILC1 development, as they remain present in IL-7Rα deficient humans and mice, but they do share a requirement for IL-15[23,137,139,140,145]. Both NK cells and ILC1 express IL-2RB (also known as CD122), through which IL-15 signals together with IL-2Rγ, and are greatly reduced in IL-15 and IL-15R deficient mice[23,146,147]. Similarly, individuals with a defect in IL-2RB present with severe viral infections and lack of NK cell development[148]. Further, IL-15 receptor signaling during both NK cell development and maintenance is tightly regulated by Id2, one of the key TFs modulating ILC fates during ILC commitment[149], making it a crucial factor for human NK cell generation *in vitro*[150].

Moreover, the Notch signaling pathway, conserved across species and a major regulator of cell fates, has also been heavily implicated in innate lymphocyte differentiation. Mouse studies have linked NCR$^+$ ILC3 to a requirement of Notch for their development and maintenance, as seen through decreased numbers in mice lacking the Notch signaling adaptor RBP/J[71,151,152]. In particular, T-bet expression, which is critical for the development of the NCR$^+$ ILC3 subset, is dependent on Notch signaling[71,153]. Unlike NCR$^+$ ILC3, studies using inhibitors have shown that fetal LTi cell generation does not require Notch[102], although a contrasting study suggests that Notch signaling is instead required earlier in the progenitor cascade to engage the LTi developmental pathway through the promotion of fetal liver α4β7$^+$ LTi progenitors[103]. Human IL-22 producing RORγt$^+$ ILC3 have been reported to be generated *in vitro* in both the presence and absence of Notch signaling[125,154], although expression of lineage identifying TF RORγt was observed to be higher in the absence of Notch ligand[154]. As for ILC2, *in vitro* studies have shown a Notch signaling requirement for the development of mouse ILC2 and human ILC2-like cells, a requirement which can be by-passed through TCF-1 activity[121,155,156]. Its role *in vivo,* however, remains under investigation.

Other factors involved in ILC development, in particular for *in vitro* generation of ILCs, include stem cell factor (SCF) and fms-like tyrosine kinase-3 ligand (Flt3-L) through their corresponding receptors CD117 and Flt3, both expressed in the CD34$^+$ HPC compartment. SCF and Flt3-L have been shown to promote early lymphopoiesis through induction of proliferation and differentiation of CD34$^+$ HPCs, as well as regulate their responsiveness to IL-7 and IL-15[157]. SCF in particular has also been shown essential for human ILC3 development *in vitro*[125]. A mixture of these factors, together with polarizing cytokines such as IL-12, IL-1β, IL-23, IL-25 and IL-33 has been utilized to optimize ILC generation, though protocols remain heterogeneous and variable between studies.

1.4 Co-culture systems to support human hematopoiesis

Studying human hematopoiesis has often relied on xenograft mouse models that lack major homeostatic signals and often need human cytokine supplementation. Due to these caveats, both *in vitro* and *ex vivo* models are utilized when investigating human hematopoiesis and often need to be carried out in parallel. At the forefront of these *in vitro* models are co-culture systems, which were used as early as the 1970s to evaluate lineage potential of human bone marrow cells co-cultured with peripheral blood leukocytes[158]. A large body of evidence indicates that the microenvironment surrounding the progenitor niche is profoundly involved in providing signals that regulate progenitor cell self-renewal and differentiation[159]. To simulate a progenitor niche *in vitro*, co-culture systems employ a stromal cell layer (so called feeder cells) to provide cell-to-cell contact and deliver a myriad of signals such as IL-7, SCF, and CXCL12, which support and regulate differentiation[160,161]. These stromal co-culture systems are among the most successful systems for *in vitro* recapitulation of lymphopoiesis. OP9 cells, the most prolifically used feeder cell line to support lymphoid generation, derives from the bone marrow stroma of *op/op* mice which harbour a mutation in the *CSF-1* gene, leading to impaired myeloid development[162]. This cell line was used to aid *in vitro* B cell generation for the first time, but it wasn't until its transfection with Notch ligands Delta-like 1 (DL1) or DL4 to introduce Notch signaling and inhibit B cell differentiation, that T cell generation became possible[163–165]. Due to its versatility and simplicity, and as a result of the conserved nature of Notch signaling, this OP9/DL1 system allows for both murine and human lymphopoiesis and has been at the forefront of T and B cell generation for decades. It has been crucial to not only understand developmental stages of lymphocytes, but also to allow perturbations of these pathways in order to gain further insight into lymphocyte biology[166–169].

1.5 The trials and tribulations of *in vitro* ILC generation

One of the primary characteristics of innate lymphocytes is their absence of responses in the context of self, meaning that unlike T and B cells, ILCs develop in the absence of positive or negative selection in a primary lymphoid organ such as the thymus or bone marrow. This

remarkable feature places ILC differentiation as an excellent candidate for *in vitro* investigations. Following the success of T cell differentiation studies, ILC differentiation from murine and human progenitors has been attempted using the OP9 and/or OP9-DL1, -DL4 co-culture system[23,111,156,170,123–128,131,132].

In vitro ILC generation has thus far aimed at identifying the differentiation potential of putative ILC progenitors from various compartments, and have used differing cytokines and culture conditions, feeder cell lines and time courses. Further confounding the issue, the readouts of these *in vitro* cultures used to define the ILC generation potential of putative progenitors differ wildly across studies. Cytokine expression is often used in these studies as the sole factor to identify NK/ILC1/ILC2/ILC3 lineages, other studies use only surrogate surface markers, a few use transcription factor data, and even less utilize a thorough multifaceted analysis including various aspects of lineage identification. With the additional convolution of ILC plasticity[171], analysis of human ILC lineage and differentiation must be stringent and multifaceted, in order to recapitulate intricate developmental processes. Thus far, the identity of the cells generated in these cultures has not been directly compared and validated with that of ILC subsets obtained *ex vivo*. Lastly, a systematic dissection of the signals required for optimal lineage decisions is often missing. These problems are not restricted to the investigation of ILC progenitors, but are a general issue permeating studies on differentiation of human cell lineages. Overall, although these investigations have provided critical information on ILC biology and expanded the ability for human ILC studies beyond scarce tissue samples, the cacophony of studies and protocols in the field render data hard to compare and can lead to wrongly assigned identities and confusion in the progenitor hierarchy.

2 Aim

The identification and differentiation of ILC subsets is a constantly developing research area, however, human ILC investigations are plagued by common difficulties such as insufficient cell numbers and scarce availability of tissue samples. Hence, to provide a strong backbone to stimulate developmental human ILC research and clarify ILC biology, the aim of this PhD thesis was:

To establish a comprehensive and reliable platform for generation of all human innate lymphoid cell subsets *in vitro*

3 Materials and Methods

3.1 Human Tissue samples

From Charité Universitätsmedizin Berlin, the following samples were obtained: cord blood; tonsils from patients undergoing tonsillectomies; intestinal samples from patients undergoing intestinal resection due to inflammatory bowel disease or other non-inflammatory disorders; liver samples from patients with liver carcinoma or other inflammatory liver diseases. Peripheral blood leukocytes were isolated from buffy coats of heathy adults provided by the German Red Cross (DRK, Berlin). All samples were processed within 24 hours. The institutional review boards of the Charité Universitätsmedizin Berlin approved the protocols and all probands gave their written informed consent according to the Declaration of Helsinki. All studies were approved by the Ethics Committee of the Charité Universitätsmedizin Berlin.

Table 1: Biological sample sourcing.

Biological samples	Source
Liver samples	Non affected, liver carcinoma
Tonsil	Tonsillectomy
Peripheral blood	Buffy coats, German Red Cross
Intestinal samples	Non affected, intestinal resection
Cord blood	Collected after childbirth
Bone marrow	Hip replacement surgery

3.2 Cell lines

OP9 or OP9-DL1 cell lines, of unspecified sex, purchased at ATCC or provided by Prof. Dr. Juan-Carlos Zúñiga-Pflücker from the University of Toronto (Toronto, Canada), respectively, were maintained in DMEM GlutaMAX media supplemented with 20% FCS (Corning), 100 U/ml penicillin (Thermo Fisher Scientific)., 0.1 mg/ml streptomycin (Thermo Fisher Scientific). and 50 µM β-Mercaptoethanol (Thermo Fisher Scientific).

Table 2: Cell lines utilized

Cell lines	Tissue	Source	Identifier
OP9	Mouse bone marrow stroma	ATCC	CRL-2749
OP9-DL1	Mouse bone marrow stroma	Dr. Juan-Carlos Zúñiga-Pflücker	N/A

3.3 Cell Isolation and sorting

Cord blood samples were obtained diluted in phosphate buffered saline (PBS) with ethylenediaminetetracetic acid (EDTA) (20 mM). Mononuclear cell (MNC) suspensions were isolated from all tissues by Ficoll density gradient centrifugation. Bone marrow and tonsil tissues were thoroughly dissociated in sterile phosphate buffered saline (PBS) with bovine serum albumin (BSA) and 2mM EDTA and pressed through a 70 µm strainer prior to Ficoll density gradient. Intestinal samples from inflamed and non-inflamed tissues were washed in 1mM DTT, followed by 3 washes in 0.7mM EDTA, and treated with Collagenase A solution (0.15mg/ml) for 12-16hrs prior to Percoll gradient separation. For cord blood and bone marrow: $CD34^+$ populations were enriched for using magnetic-activated cell sorting (MACS). The CD34 MicroBead UltraPure Kit was used in conjunction with LS or MS columns as per the manufacturer's instructions (Miltenyi). $CD34^+$ HPC were FACS-sorted from CD34 enriched fractions as Lin^- (LD^- $Fc\varepsilon R^-$ $sCD3\varepsilon^-$ $CD14^-$ $CD19^-$ $CD11c^-$ $CD123^-$) $CD45RA^+CD34^+$. Sorting was performed on a FACSAria I (BD Bioscience) with a 70um nozzle.

Table 3: Cell isolation reagents.

Reagents	Source	Identifier
EDTA	Sigma	Cat. No. #PHR2586
DTT	ThermoFisher	Cat. No. #R0861
HBSS-/-	Gibco	Cat. No. #14065-056
Collagenase A	Roche	Cat. No. # 10103578001
RMPI	Gibco	Cat. No. # 61870036
FCS	ThermoFisher	Cat. No. #16010159
P/S	ThermoFisher	Cat. No. # 15140122

Ficoll-Paque PLUS	Cytiva	Cat. No. #17144003
Percoll	Cytiva	Cat. No. #17089101
BSA	PAN Biotech GmbH	P06-1391500

3.4 Cell Culture

OP9 and OP9-DL1 cells were maintained for a maximum of 6 weeks and passaged when they reached 80-90% confluency. One day prior to $CD34^+$ sorting, $2x10^3$ OP9 or OP9-DL1 cells per well were seeded on round bottom 96 well plates (Greiner Bio One), to concentrate the low numbers of $CD34^+$ cells. The following day, FACS-sorted $CD34^+$ cells (bone marrow: $2x10^3$ cells/ well, cord blood: $1x10^3$ cells/ well) were plated onto approximately 80% confluent stromal cell monolayers in MEMα GlutaMAX media (Thermo Fisher Scientific). Media was supplemented with 10% human AB serum, 100 U/ml penicillin, 0.1 mg/ml streptomycin, and cytokine mix. Cytokine mix consisted of SCF, Flt3-L, IL-7, and IL-15 when stated (all 20 ng/ml) and IL-3 (all cultures: 5 ng/ml) (Miltenyi). After one week IL-3 supplementation was stopped. After two weeks Flt3-L was reduced to 5 ng/ml. Medium and cytokines were refreshed every 3-4 days by replacing half of the media containing 1x concentration of cytokines. At the end of week 1, 2, and 3, cells were replated onto fresh OP9 or OP9-DL1 onto flat bottom plates. To replate, cells were collected by forceful pipetting and passed through a 50 µm filter (Sysmex) to remove OP9/OP9-DL1 cells, wells and filter were washed 2x with PBS, cells were counted and up to 50000 cells/well were replated. For plasticity experiments, cells in conditions OP9+IL-15 and DL1 were supplemented with IL-1β and IL-12 (50 ng/ml each; Miltenyi) for 5 days prior to stimulation for 6 hr at 37°C with PMA (20 ng/ml), ionomycin (1 µg/ml) (both Sigma) and IL-23 (50 ng/ml; Miltenyi).

Table 4: Cell culture reagents.

Cytokines for cell culture	Source	Identifier
Human IL-7	Miltenyi	Cat. No.: 130-095-362
Human IL-15	Miltenyi	Cat. No.: 130-095-765

Human IL-3	Miltenyi	Cat. No.: 130-095-070
Human IL-12	Miltenyi	Cat. No.: 130-096-705
Human IL-1b	Miltenyi	Cat. No.: 130-093-563
Human SCF	Miltenyi	Cat. No.: 130-096-695
Human Flt3-L	Miltenyi	Cat. No.: 130-096-479
MEMα GlutaMAX	ThermoFisher	Cat. No.: 32561-029
DMEM	ThermoFisher	Cat. No.: 61965-026
Penicillin-Streptomycin	ThermoFisher	Cat. No. # 15140148
b-mercaptoethanol	ThermoFisher	Cat. No. #21985023
FCS	Corning	Cat.No. #35-079-CV
Human male AB serum	Sigma	Cat. No. #H4522
96 well cell culture plate, U-bottom	Greiner bio-one	Cat. No. #650180
96 well cell culture plate, F-bottom	Greiner bio-one	Cat. No. #655161
CO_2 incubator	Binder	Cat. No. #9040-0039

3.5 Flow cytometry

For phenotyping, cells were collected by forceful pipetting and passed through a 50 µm filter to remove OP9/OP9-DL1 cells, wells and filter were washed 2x with PBS. Surface marker antibodies were diluted in 50 µl PBS and cells stained for 15 min at 37°C. After washing, biotin was stained with fluorochrome labelled streptavidin for 10 min at 4°C. Afterwards, cells were fixed for 35 min at room temperature, permeabilized and TF were stained at room temperature for 45 min using the Foxp3 / Transcription Factor Staining Buffer Set (eBioscience). Cells were resuspended in 200 µl of PBS/BSA for measuring. For detection of intracellular cytokine expression cells were stimulated for 6 hr at 37°C with PMA (20 ng/ml), ionomycin (1 µg/ml) (both Sigma) and IL-23 (50 ng/ml; Miltenyi). Golgi Stop (1:1500) and Golgi Plug (1:1000) (both BD Bioscience) were added after 1 hr to all samples. Samples were then stained as described above, with the exception of a 1:1 dilution of the fixation buffer with PBS, to preserve the cytokine staining. Measurements were performed on an LSRFortessa or a FACSymphony (BD Bioscience) and data analyzed with FlowJo v.10.6.01 software (TreeStar) and Cytobank software[172]. All flow cytometry analysis was performed according to the Guidelines for the use of flow cytometry and cell sorting in immunological studies[87].

Table 5: Flow cytometry resources.

Antibodies	Source	Identifier
Anti-human CD123 APC-ef780 Clone: 6H6	eBioscience	Cat. #47-1239-42
Anti-human CD14 APC-ef780 Clone: 61D3	eBioscience	Cat. #47-0149-42
Anti-human CD19 APC-ef780 Clone: HIB19	eBioscience	Cat. #47-0199-42
Anti-human CD3 APC-ef780 Clone: SK7	eBioscience	Cat. #47-0036-42
Anti-human FcεRIα APC-Vio770 Clone: CRA1	Miltenyi	Cat. #130-105-457
Fixable Viability Dye eFluor780 (LD)	eBioscience	Cat. #65-0865-18
Anti-human CD94 Pacific Blue Clone: XA185	In house	N/A
Anti-human CD117 BV605 Clone: 104D2	Biolegend	Cat. #313218
Anti-human CD117 BV711 Clone: 104D2	Biolegend	Cat. #313230
Anti-human CD161 BV785 Clone: HP-3G10	Biolegend	Cat. #339930
Anti-human CD16 PerCP-Cy5.5 Clone: 3G8	Biolegend	Cat. #302027
Anti-human CD25 BV421 Clone: BC96	Biolegend	Cat. #302630
Anti-human CD45 AF700 Clone: HI30	Biolegend	Cat. #304024
Anti-human CD5 BV510 Clone: L17F12	Biolegend	Cat. #364018
Anti-human CD5 PE-Cy7 Clone: L17F12	Biolegend	Cat. #364008
Anti-human CD56 BV605 Clone: HCD56	Biolegend	Cat. #318334
Anti-human CRTH2 Biotin Clone: BM16	Miltenyi	Cat. #130-091-239
Anti-human CXCR3 BV711 Clone: G025H7	Biolegend	Cat. #353732
Anti-human IL-1R1 PE Clone: Polyclonal	R&D	Cat. #AB269P
Anti-human KLRG1 FITC Clone: REA261	Miltenyi	Cat. #130-103-640
Anti-human Neuropilin-1 PE Clone: AD5-17F6	Miltenyi	Cat. #130-090-533
Anti-human Nkp30 PE Clone: AF29-2D12	Miltenyi	Cat. #130-092-483
Anti-human Nkp44 Biotin Clone: P44-8	Biolegend	Cat. #325106
Anti-human Nkp46 PE Clone: 9E2	Miltenyi	Cat. #130-092-607
Anti-human RANKL PE Clone: MIH24	Biolegend	Cat. #347504
Anti-human Eomes PerCP-ef710 Clone: WD1928	eBioscience	Cat. #46-4877-42
Anti-human CD3 BV605 Clone: SK7	Biolegend	Cat. #344836
Anti-human CD3 APC Clone: OKT3	eBioscience	Cat. #17-0037-42
Anti-human Eomes APC Clone: WD1928	eBioscience	Cat. #50-4877-41
Anti-human Eomes FITC Clone: WD1928	eBioscience	Cat. #11-4877-42
Anti-human GATA3 PE-Vio615 Clone: REA174	Miltenyi	Cat. #130-109-115

Anti-human RORγt APC Clone: REA278	Miltenyi	Cat. #130-103-838
Anti-human T-bet PE-Cy7 Clone: 4B10	Biolegend	Cat. #644824
Anti-human T-bet PE Clone: ebio4b10	eBioscience	Cat. #12-5825-82
Streptavidin PerCP-Cy5.5	eBioscience	Cat. #46-4317-80
Anti-human IFNγ BV650 Clone: 4S.B3	eBioscience	Cat. #502537
Anti-human IL-13 PE Clone: JES10-5A2	Miltenyi	Cat. #130-092-964
Anti-human IL-17A BV605 Clone: Mab11	Biolegend	Cat. #512325
Anti-human IL-17F A488 Clone: Poly5166	Biolegend	Cat. #516603
Anti-human IL-22 PerCP-ef710 Clone: 22URTI	eBioscience	Cat. #46-7229-42
Anti-human IL-8 EF450 Clone: 8CH	eBioscience	Cat. #48-8088
Transcription factor staining buffer set	eBioscience	Cat. No. #00-5523-00
LSR Fortessa	BD	N/A
FlowJo™ Software v10.6.2	FlowJo LLC	N/A

3.6 Cytotoxicity assay

NK/ILC1 subsets were sorted as described in **Figure 13** and rested overnight in complete medium prior to stimulation. K562 target cells were stained with CellTrace Violet (ThermoFisher) and co-cultured with purified NK/ILC1 subsets at a ratio of 2:1 or 5:1.To control for spontaneous cell death, target cells were cultured in parallel in the absence of NK cells. After 6 hr, cell suspensions were stained for viability of target cells using Fixable Viability Dye eFluor780 (ThermoFisher) and were analyzed by flow cytometry. Percent cytotoxicity was calculated as follows: (% dead target cells in experimental condition – % dead target cells in spontaneous control) / (100% – % dead target cells in spontaneous control) × 100.

3.7 Bulk RNA sequencing

From a total of 5 donors, cells were differentiated until end of week 4 and subsets were sorted as: ILC3 as $CD45^{+}Lin^{-}CD161^{+}RANKL^{+}CRTH2^{-}CD94^{-}NKP44^{+}$; $CD94^{+}$ NK/ILC1 as $CD45^{+}$ Lin^{-} $CD161^{+}$ $RANKL^{-}$ $CRTH2^{-}$ $CXCR3^{+}$ $CD94^{+}$; $CD94^{-}$ NK/ILC1 as $CD45^{+}$ Lin^{-} $CD161^{+}$ $RANKL^{-}$ $CRTH2^{-}$ $CXCR3^{+}$ $CD94^{-}$; ILC2 as $CD45^{+}$ Lin^{-} $CD161^{+}$ $CRTH2^{+}$ $CD94^{-}$; $CD161^{-}$ non-ILC control as $CD45^{+}$ Lin^{-} $CD161^{-}$ $CD5^{+}$. RNA was isolated using RNeasy Plus Micro Kit (QIAGEN) when

cell numbers were < $5x10^5$ and Nucleospin RNAII kit (Macherey-Nagel) when cell numbers were > $5x10^5$. RNA quality was determined on a Bioanalyzer using the RNA 6000 Pico Kit (Agilent). Illumina libraries were prepared using Smart-Seq v4 mRNA Ultra Low Input RNA Kit (Clontech) and Nextera XT DNA Sample Preparation Kit (Illumina), with 10 ng of purified cDNA, according to the manufacturer's instructions. Libraries were paired-end sequenced (2 × 75 bp) on an Illumina NextSeq500 device. Raw sequence reads were mapped to human GRCh37/hg19 genome with TopHat2[173] in very-sensitive settings for Bowtie2[174] and using Gencode.19 [175] as reference. Gene expression was quantified by featureCounts[176] and analyzed using DESeq2 R-Package[177], in particular size factor normalization and rlog-transformation. Principle Component Analyses (PCA) were performed separately for: $CD161^-CD5^+$, NK/ILC1, $CD5^-$ ILC2, ILC3; NK/ILC1, $CD5^-$ ILC2, ILC3; and NK/ILC1, $CD5^-$ ILC2, $CD5^+$ ILC2, ILC3; as well as NK/ILC1 generated in OP9+IL-15 and DL1+IL-15 based on the above unscaled rlog-transformed values. Differential expression analysis was performed separately for ILC3 vs ILC2, ILC2 vs NK/ILC1, and in ILC3 vs NK/ILC1 and $CD161^+$ vs $CD161^-$ using the above size factor normalization based on all samples. Genes with an adjusted p-value (Wald-Test) ≤ 0.05 and the fold change ≥ 1.3 were considered significantly differentially expressed. Heat maps for selected genes were generated using z-scores of rlog-transformed read counts, clustered by maximum and minimum expression per gene.

3.8 Single-cell RNA sequencing

Cells were FACS-sorted as $CD45^+$ cells which were Lin^- (CD14, CD123, FcERa, Viability dye), combined with the following 34 CITE-Seq 34 antibodies: CD117, CD304 (Neuropilin-1), CD254 (RANKL), CD336 (NKp44), CD196 (CCR6), CD34, CD7, CD127 (IL-7Rα), CD1a, CD5, CD3 (SK7), CD4, CD8a, TCRα/β, TCRγ/δ, CD183 (CXCR3), CD94, NKp80, CD335 (NKp46), CD294 (CRTH2), CD278 (ICOS), HLA-DR, integrinβ7, CD49d (α4), CD19, CD161, CD2, KLRG1, CD56, CD16, Siglec-7, KIR2DL1, KIR2DL2, KIR3DL1. Cells were individually hashtagged per donor and per condition. Cells were loaded in the ChromiumTM Controller for partitioning single cells into nanoliter-scale Gel Bead-In-Emulsions (GEMs) aiming for a

recovery of 12,000 cells. Single Cell 3′ reagent kit v3.1 was used for reverse transcription, cDNA amplification and library construction of gene expression libraries (10x Genomics) according to the manufacturer's instructions. TotalSeq-A libraries were prepared following the protocol for 10x Single Cell 3′ Reagent Kit v3.1 provided by BioLegend, including primer sequences and reagent specifications. All libraries were quantified using a QubitTM 2.0 Fluorometer (ThermoFisher) and quality was tested on a 2100 Bioanalyzer with High Sensitivity DNA kit (Agilent). Libraries were sequenced on a NovaSeq 6000 S1 Flow cell (CeGaT GmbH Tübingen), read configurations were set to 28 (R1), 9 (i7), 91 (R2). Antibody and hashtag libraries were amplified using the KAPA HiFi ready mix with primers containing Illumina Small RNA RPIx sequences and Truseq D70x_s, respectively.

Data processing.

Transcriptome data was demultiplexed and mapped to the GRCh38 transcriptome with Cell Ranger v3.0.2. ADT and HTO libraries were demultiplexed with bcl2fastq v2.20.0.422, pseudoaligned with kallisto v0.46.0[178] to a mismatch matrix generated with kite (https://github.com/pachterlab/kite) and counted with bustools v0.39.2[179]. Downstream analysis was mainly performed with Seurat v3.2.3[180]. After mapping and demultiplexing, we observed an unexpected overloading of the library reaction requiring a stringent filtering strategy to remove low quality cells and doublets. Only cells which were found in ADT, HTO and transcriptome libraries were retained for analysis. Doublets marked by more than one hashtag were filtered out and supported identification of suitable cut-offs for filtering. Cells were further filtered by counts ($5000 < x < 12{,}500$) and percent mitochondrial reads ($x < 10$ %). Transcripts were normalized with scran v1.14.6[181]. ADT and HTO libraries were normalized by centered log-ratio normalization. The 90th percentile of normalized hashtag counts was set as threshold for demultiplexing. Cell cycle scores were assigned and regressed out during scaling. The 3000 most variable features identified with the vst-method were used for principal component analysis (PCA). Upon inspection of principal component (PC) loadings and elbowplot, the first 17 PCs were used for calculation of UMAP and the neighborhood graph for

clustering. For visualization of the heterogeneity generated from the different culture conditions, the relatively overrepresented DL1 condition from one of the donors was randomly downsampled to match the frequencies of the other conditions. Clusters were annotated based on the expression of marker genes and proteins and subsetted for more detailed analysis of ILC subpopulations. To better appreciate heterogeneity within these clusters, PCA was recalculated per subset and the number of PCs used for UMAP projection and clustering again determined based on PC loadings (ILC1: 11, ILC2: 10, ILC3: 10). Differential gene expression analyses were performed using the Wilcoxon test with a log fold-change threshold of 0.25 and a minimum expression frequency of 0.1.

Table 6: RNA-sequencing reagents.

Reagent	Source	Identifier
NucleoSpin® RNA Mini Kit	Macherey-Nagel	Cat. No.: #740955.50
RNeasy Plus Micro Kit	Qiagen	Cat. No.: #74034
Nextera XT DNA library preparation kit	Illumina	Cat. No.: #FC-131-1024
TotalSeq™-A0061 CD117	Biolegend	Cat. No.: #313241
TotalSeq™-A0406 CD304 (Neuropilin-1)	Biolegend	Cat. No.: #354525
TotalSeq™-A0356 CD254 (TRANCE, RANKL)	Biolegend	Cat. No.: #347509
TotalSeq™-A0802 CD336 (NKp44)	Biolegend	Cat. No.: #325117
TotalSeq™-A0143 CD196 (CCR6)	Biolegend	Cat. No.: #353437
TotalSeq™-A0054 CD34	Biolegend	Cat. No.: #343537
TotalSeq™-A0066 CD7	Biolegend	Cat. No.: #343123
TotalSeq™-A0390 CD127 (IL-7Rα)	Biolegend	Cat. No.: #351352
TotalSeq™-A0402 CD1a	Biolegend	Cat. No.: #300133
TotalSeq™-A0138 CD5	Biolegend	Cat. No.: #300635
TotalSeq™-A0049 CD3 (SK7)	Biolegend	Cat. No.: #344847
TotalSeq™-A0922 CD4	Biolegend	Cat. No.: #317451
TotalSeq™-A0080 CD8α	Biolegend	Cat. No.: #301067
TotalSeq™-A0224 TCRα/β	Biolegend	Cat. No.: #306737
TotalSeq™-A0139 TCRγ/δ	Biolegend	Cat. No.: #331229
TotalSeq™-A0140 CD183 (CXCR3)	Biolegend	Cat. No.: #353745
TotalSeq™-A0867 CD94	Biolegend	Cat. No.: #305521
TotalSeq™-A0923 NKp80	Biolegend	Cat. No.: #346709

TotalSeq™-A0101 CD335 (NKp46)	Biolegend	Cat. No.: #331943
TotalSeq™-A0102 CD294 (CRTH2)	Biolegend	Cat. No.: #350127
TotalSeq™-A0171 CD278 (ICOS)	Biolegend	Cat. No.: #313555
TotalSeq™-A1018 HLA-DR/DP/DQ	Biolegend	Cat. No.: #361717
TotalSeq™-A0214 integrin β7	Biolegend	Cat. No.: #321227
TotalSeq™-A0576 CD49d (integrin α4)	Biolegend	Cat. No.: #304337
TotalSeq™-A0050 CD19	Biolegend	Cat. No.: #302259
TotalSeq™-A0149 CD161	Biolegend	Cat. No.: #339945
TotalSeq™-A0367 CD2	Biolegend	Cat. No.: #309229
TotalSeq™-A0153 KLRG1	Biolegend	Cat. No.: #367721
TotalSeq™-A0084 CD56	Biolegend	Cat. No.: #392421
TotalSeq™-A0083 CD16	Biolegend	Cat. No.: #302061
TotalSeq™-A0902 Siglec-7	Biolegend	Cat. No.: #339217
TotalSeq™-A0420 KIR2DL1	Biolegend	Cat. No.: #339515
TotalSeq™-A0592 KIR2DL2	Biolegend	Cat. No.: #312615
TotalSeq™-A0599 KIR3DL1	Biolegend	Cat. No.: #312723
Single Cell 3′ reagent kit v3.2	10x Genomics	Cat. No. # PN-1000121
Chromium™ Controller	10x Genomics	N/A
Qubit™ 2.0 Fluorometer	ThermoFisher	N/A
Qubit™ dsDNA HS Assay Kit	ThermoFisher	Cat. No #Q32854
BioAnalyzer 2100	Agilent	Cat. No #G2939BA
Bioanalyzer High Sensitivity DNA Analysis	Agilent	Cat. No #5067-4626
NextSeq500/550 HighOutput Kit v2.5	Illumina	Cat. No #20024907
NextSeq500 sequencer	Illumina	N/A

Table 7: Single-cell sequencing algorithms.

Deposited data	Reference	GEO Accession number
Cell Ranger v3.0.2	[182]	https://support.10xgenomics.com/single-cell-gene-expression/software/pipelines/latest/using/count
CITE-seq-Count	[183]	
R Studio v4.0.0		https://rstudio.com/
Seurat v3.0.2	[180]	
Scran	[181]	

3.9 Gene Set Enrichment Analysis (GSEA)

ILC1, ILC2, ILC3 and NK signatures were defined based on single-cell RNA-sequencing transcriptomes of human tonsil ILCs. Raw transcript counts were obtained from GEO (accession number GSE70580)[48], assembled to gene counts and further processed by the Seurat 2.3.4 R-package[184]. In particular, data was normalized, patient specific effects were regressed out using the ScaleData and variable genes were identified using FindVariableGenes in default parameter setting. Sparse Partial Least Squares Discriminant Analysis (sPLS-DA) was performed on the variable genes using the mixOmics R-package[185] on ILC1, ILC2 and ILC3 and NK-cells including three components and keeping 200, 200 and 300 variable genes. Cells were separated by positive values in component 1 for ILC3, positive values in component 2 for NK, positive values in component 3 for ILC2 and negative values in component 3 for ILC1. Signature genes were defined according to their loading on the respective components. That is, loading on component 1 > 0, and 0 on component 2 and 3 for ILC3 signature, loading on component 2 > 0, and 0 on component 1 and 3 for NK, loading on component 3 > 0 and 0 on component 2 and 1 for ILC2 signature and finally loading on component 3 < 0 and 0 on component 2 and 1 for ILC1.

For $CD127^-$ ILC1 signature, raw gene counts from $CD127^-$ ILC1, $CD127^+$ ILC3, $CD56^{bright}$, $CD56^{dim}CD57^+$ and $CD56^{dim}CD57^-$ were obtained were obtained from GEO (accession number GSE112813)[86] and further processed by the DESeq2 R-Package, including size factor normalization and rLog transformation. A sPLS-DA was performed on rLog-transformed values, leading to no clear definition of signature genes. Therefore, a different strategy was transduced by performing pairwise comparisons between each subgroup and ILC3. Signature genes were defined by the top 100 up or down regulated differentially expressed protein coding genes, as judged by a p-value (Wald-Test) ≤ 0.05 for statistical significance and fold change. To avoid high fold changes for lowly expressed genes 10 artificial reads were added to each gene count. Gene Set Enrichment Analysis (GSEA)[186] was performed by the GSEA software based on human ILC1, ILC2, ILC3 and NK signatures between each cell-subset and the

corresponding rest (GEO GSE70580 and GSE112813). Gene set enrichment analyses were performed by Dr. Pawel Durek at the DRFZ.

3.10 Statistical analysis

Data are presented as mean ± standard error of the mean (SEM). Sample sizes for each experiment are included in the figure legends. Statistical tests used are stated in each figure legend, adjusted p value significance was classified as such: * p≤0.05; ** p≤0.01; *** p≤0.001; when tested, non-significance was stated as “ns”. Statistical analyses were performed using Prism v.8 software.

Table 8: Sequencing data deposition.

Deposited data	**Source (reference)**	**GEO Accession number**
Raw and analyzed bulk RNAseq data	This work ([187])	GSE141504
Raw and analyzed single-cell RNAseq data	This work ([187])	GSE171114
Single-cell RNAseq data of tonsil ILCs	([48])	GSE70580
RNAseq data of tonsil CD127^{-} ILC1	([86])	GSE112813

4 Results

4.1 *In vitro* culture of cord blood CD34⁺ CD45RA⁺ HPCs efficiently engenders CD161⁺ ILCs

Previous studies addressing human ILC generation have mainly focused on testing the differentiation potential of putative ILC-committed progenitors from varying compartments, using disparate sets of signals. In order to systematically identify the signals required for ILC versus other lymphocyte lineage fate-making decisions, CD34⁺ CD45RA⁺ HPCs from cord blood were isolated. This pool of HPCs is described to be enriched in CLPs which hold the potential to differentiate towards all lymphocyte subsets, including T and B cells[188,189]. The culture system consisted of CD34⁺ CD45RA⁺ HPCs co-cultured on either OP9 or DL1-transfected OP9 (hereafter referred to as DL1) stromal cells in the presence of IL-7, Flt3-L, SCF, with the addition of IL-3 only for the first week, which have been shown to sustain early lymphopoiesis[168,189]. This common cytokine mix was supplemented with or without IL-15, which can support the growth of NK cells and ILC3[123–125,150]. The culture conditions utilized throughout the study are schematically depicted in **Figure 8**.

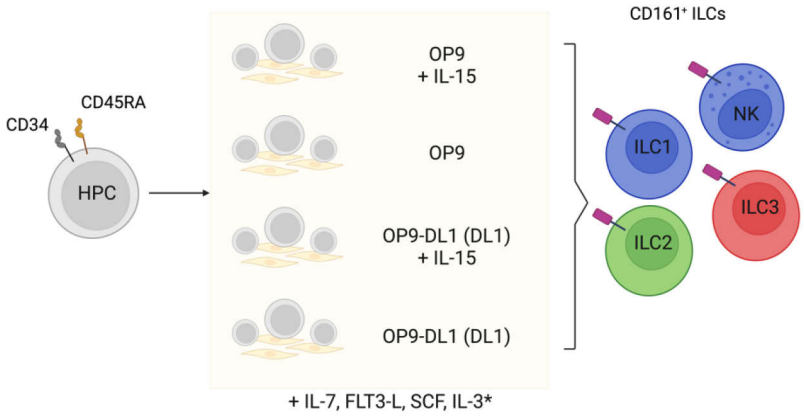

Figure 8: Schematic of culture conditions.
CD34⁺ CD45RA⁺ HPCs were sorted and co-cultured on either OP9 or DL1 stromal cells. All conditions were supplemented with IL-7, Flt3-L and SCF. IL-15 was additionally supplemented in conditions OP9+IL-15, and DL1+IL-15. CD161⁺ ILCs were identified and analyzed at end point. *IL-3 was provisioned only for the first week.

As high IL-7 concentrations impact the surface expression of its receptor, CD127, on human lymphocytes[190], ILCs were identified as CD45⁺ Lin⁻ (surface CD3ε⁻, CD14⁻, CD19⁻, CD123⁻, FcεRIα⁻, Viability dye⁻) cells which expressed low to high surface CD161, as expressed on all

human ILC subsets, including NK cells[2,4,58,191]. Cord blood $CD34^+$ $CD45RA^+$ HPCs were sorted using fluorescence-activated cell sorting to an average purity of 94.48% and with effectively no $CD161^+$ ILC or $CD5^+$ T cell contamination (**Figure 9a**). Percentage of $CD161^+$ ILCs was 0 on the first day of culture and progressively increased from week 1 to week 4, at which point cells were taken for further in-depth analysis (**Figure 9a,b**). The fold expansion at week 4 of conditions OP9+IL-15, DL1+IL-15 and DL1 were found to be comparable, showing that all conditions provide comparable proliferation potential (**Figure 9c**). Mean frequency of $CD161^+$ ILCs in conditions supplemented with IL-15, namely OP9+IL-15 and DL1+IL-15, were 96.59% and 92.66% respectively, while condition DL1 without IL-15 had a mean frequency of 52.54% (**Figure 9d**), and simultaneously showcased a $CD161^-$ $CD5^+$ population with a mean frequency of 33.04% (**Figure 9e**). Interestingly, the frequencies of this non-ILC $CD161^-$ $CD5^+$ population inversely correlated to that of $CD161^+$ ILCs derived from the same condition (**Figure 9f**). Condition OP9 without IL-15 was similarly tested and found to have lower fold expansion and reduced frequency of $CD161^+$ ILCs and thus, was not further pursued (**Figure 9g,h**).

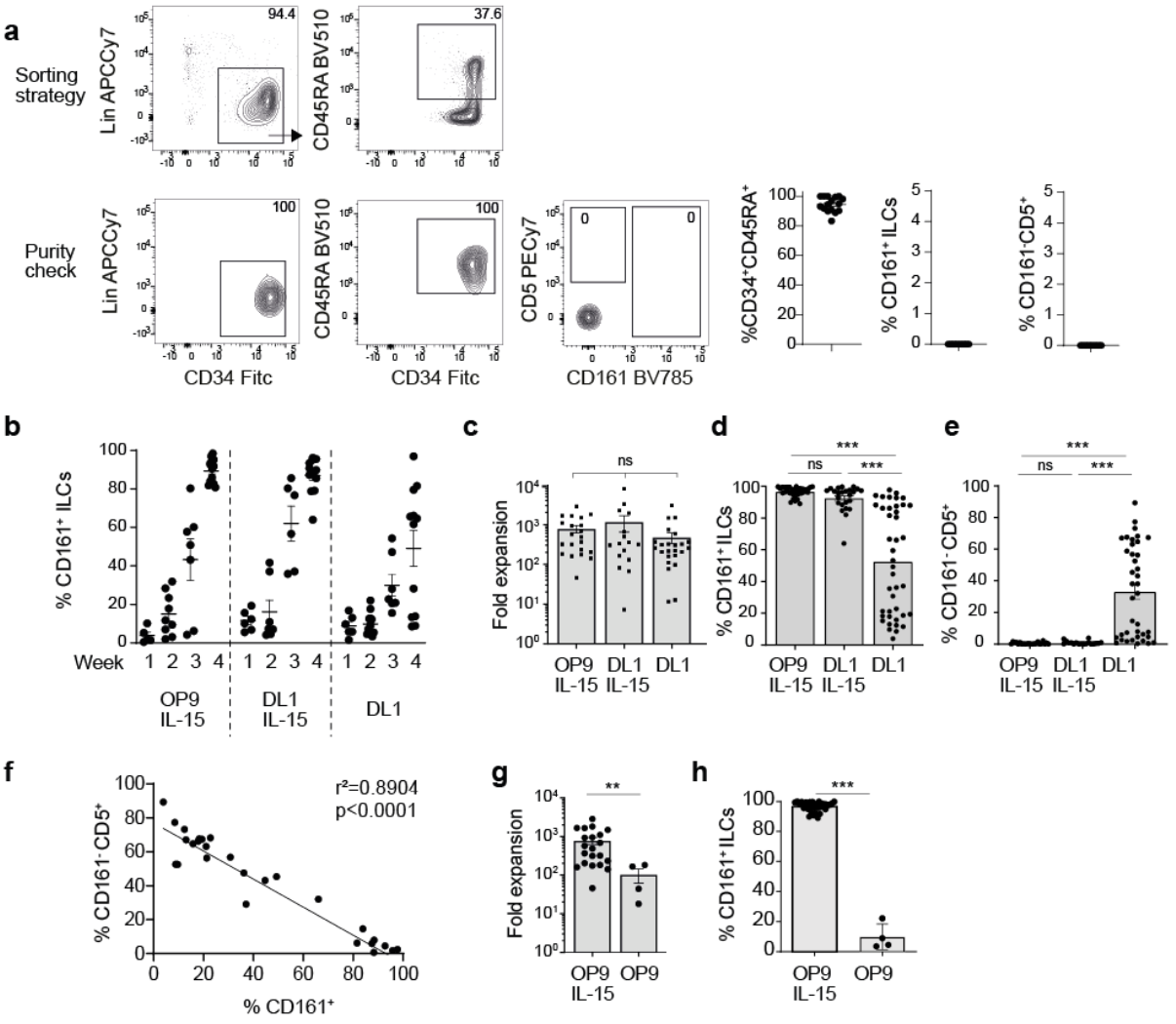

Figure 9: Human CD34⁺ HPCs generate CD161⁺ ILCs within 4 weeks of culture. (**a**) Representative sorting strategy of CD34⁺ CD45RA⁺ HPCs and frequencies of CD34⁺ CD45RA⁺ HPCs (n=16; 8 independent experiments), CD161⁺ ILCs (n=13, 4 independent experiments) and CD5⁺ lymphocytes (n=13; 4, independent experiments) within sorted cells. (**b**) Frequency of CD161⁺ ILCs generated in each condition, at week 1, 2, 3, and 4 of culture (20 independent experiments). (**c**) Fold expansion of live cells at week 4, relative to day 0 (n=16-24; 19 independent experiments). (**d**) Percent of CD161⁺ ILCs within CD45⁺ Lin⁻ (Lin: surface CD3ε (sCD3ε), CD14, CD19, CD123, FcεRIα, viability marker) cells at week 4 (n=25-42; 27 independent experiments). (**e**) Percent of CD161⁻ CD5⁺ subset within CD45⁺ Lin⁻ cells at week 4 (n=18-39; 23 independent experiments). (**f**) Linear regression between frequencies of CD161⁻ CD5⁺ and CD161⁺ cells from condition DL1 at week 4 (n=37). (**g**) Fold expansion of live cells (n=4-21, 17 independent experiments) and (**e**) percent of CD161⁺ ILCs in OP9+IL-15 and OP9 (n=4-36). Statistical analyses in **c, d, e** Kruskal-Wallis test with Dunn's multiple comparisons test; **g, h** were performed using Mann-Whitney test * p≤0.05; ** p≤0.01; *** p≤0.001; ns: not significant.

4.2 CD34⁺ CD45RA⁺ HPCs require distinct signals to generate all ILC subsets *in vitro*

To assess the phenotype of the ILCs generated in an unbiased way, flow cytometric data from all conditions at week 4 were pooled and visualized with Stochastic Neighbor Embedding (viSNE) to reduce data onto two dimensions (viSNE1 and viSNE2)[172,192]. Using effector

cytokines, TFs, and surface markers previously designated as lineage-defining, three major subsets were identified (**Figure 10a**). One group was governed by expression of IFN-γ, Eomes, T-bet, and CD94, indicative of a type 1 NK/ILC1 lineage. An IL-13-, GATA3-, and CRTH2-expressing group was suggestive of an ILC2 identity, while a third IL-22- and RORγt-driven group was indicative of type 3 innate cells, ILC3. By analyzing ILCs generated from each condition separately, OP9+IL-15 was observed to optimally engender RORγt^{+} RANKL^{+} ILC3 expressing high surface CD117 as reported in their *ex vivo* counterparts (**Figure 10b,c**), which produced effector cytokine IL-22 after stimulation (**Figure 10d**). ILC3 generation was strongly reduced in the absence of IL-15 as well as upon provision of Notch signaling (**Figure 10b,d**). Conversely, the rise of a GATA3^{hi} CRTH2^{+} ILC2 population able to secrete IL-13 upon stimulation was observed selectively in the presence of Notch signaling and the absence of IL-15, i.e. condition DL1 (**Figure 10b,d**). This data falls in line with previous studies associating Notch signaling to ILC2 generation[121,155,156]. A heterogeneous IFNγ producing population of NK/ILC1 with expression of T-bet and/or Eomes was observed preferentially in conditions with IL-15 supplementation, with the highest frequency in condition DL1+IL-15 (**Figure 10b,d**). Consistent with prior reports that show direct regulation of *Tbx21* (encoding T-bet) transcription by Notch signaling[193,194], T-bet was observed to be upregulated in NK/ILC1 generated in DL1+IL-15, showcasing not only Eomes^{+} T-bet^{+} cells but also a T-bet single positive population (**Figure 10b,e**). Identification of the ILC subsets generated in each condition through expression of lineage demarcating TFs or effector cytokines are summarized in **Figure 10f,g**, which collectively show that generation of NK/ILC1 is optimal in conditions supplemented by IL-15, ILC2 in condition DL1, and ILC3 in OP9+IL-15. Together, these data show that all ILC subsets can be generated *in vitro* as identified using surface markers, TFs, and cytokines. However, this data importantly point out that more than one culture condition and distinct signals are required for differentiation of all ILC lineages. Furthermore, the identification of ILC subsets based solely on cytokine expression grossly underestimates the generation potential of any given condition.

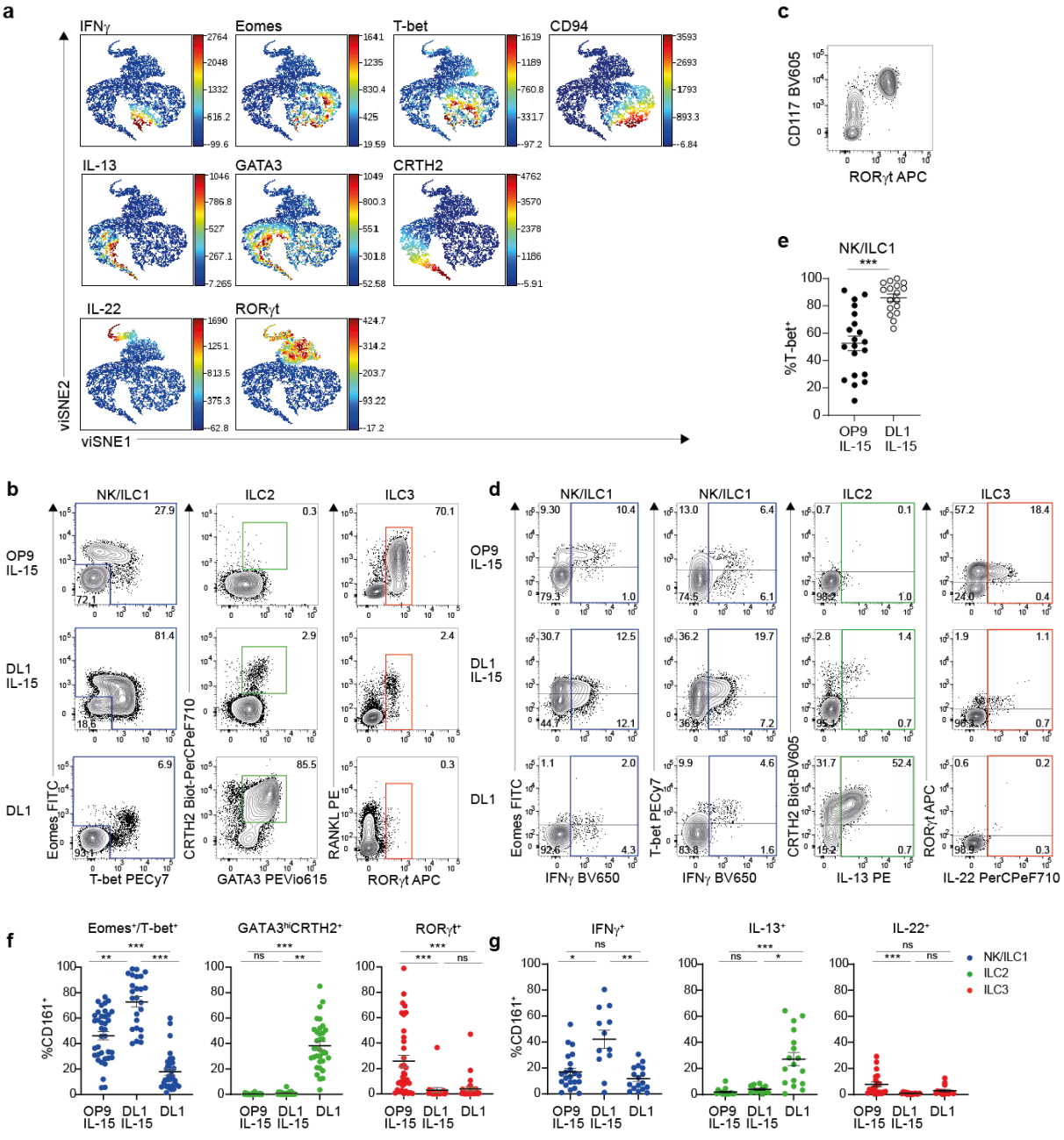

Figure 10: CD34⁺ CD45RA⁺ HPCs require distinct signals to generate all ILC subsets *in vitro*. (**a**) viSNE of CD161⁺ ILCs from all conditions concatenated, after PMA/Iono/IL-23 stimulation as depicted in **d**; for each marker, the median intensity was quantified and depicted as a heat map, where the scale represents max/min expression of each individual marker. (**b**) Representative expression of TF and surrogate surface markers within CD161+ ILCs at week 4, coloured gates show identification of subsets by TFs (NK/ILC1, blue; ILC2, green; ILC3 red). (**c**) CD117 and RORγt expression in CD161⁺ ILCs from OP9+IL-15 at week 4. (**d**) Representative expression of IFNγ, IL-13, and IL-22 within CD161⁺ ILCs at week 4, after PMA/Iono/IL-23 stimulation, coloured gates show identification of subsets by cytokines (NK/ILC1, blue; ILC2, green; ILC3 red). (**e**) Frequency of T-bet expressing NK/ILC1 (gated as shown in **b**) (n=17-20, 17 independent experiments). (**f**) Quantification of ILC subset generation by staining of TFs, as depicted in **b** (Eomes⁺/T-bet⁺: n=25-37, 27 independent experiments; GATA3^{hi} CRTH2⁺: n=25-34, 26 independent experiments; RORγt⁺: n=29-35, 26 independent experiments). (I) Quantification of ILC subset generation by staining of cytokines, as depicted in g (IFNγ⁺: n=12-22, 17 independent experiments; IL-13⁺: n=12-17, 14 independent experiments; IL-22⁺: n=14-22, 18 independent experiments). Statistical analyses in **e** were performed using Mann-Whitney test; **f, g** Kruskal-Wallis test with Dunn's multiple comparisons test; * p≤0.05; ** p≤0.01; *** p≤0.001; ns: not significant.

Once ILC lineages were identified through cytokines, TFs and surface makers, the kinetics of ILC subset generation were explored. Using ILC-subset identifying TFs as the most reliable form of identification, we followed ILC lineage generation through time and found it to rise steadily from week 1 to 4 (**Figure 11a**). Upregulation of ILC subset-identifying TFs occurred consistently between week 2 and 3, at which point the dominant ILC subset(s) in each condition became clear (**Figure 11a**). This pattern did not change prior to this time point, suggesting no overgrowth of one subset at the expense of another. Next, the possibility of donor-specific bias toward particular ILC subsets was tested. The ILC subset generation across all conditions was evaluated from each individual donor, and no significant correlation could be observed between different conditions for any ILC subsets generated (**Figure 11b**). This suggests that even donors who may be predisposed to generate high frequencies of specific subsets will only do so in response to a set of highly defined signals.

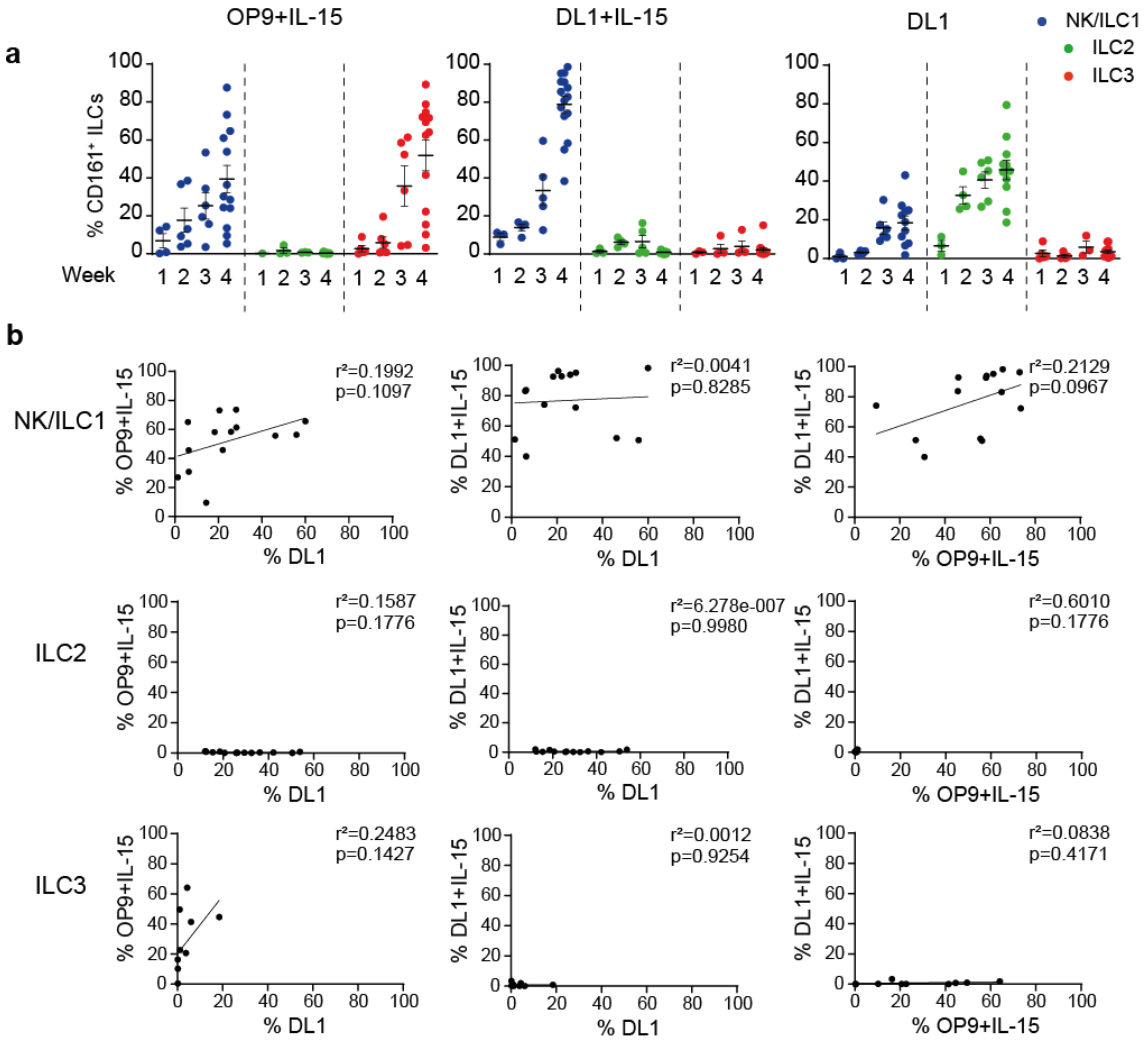

Figure 11: *In vitro* ILC generation is not competitive, nor donor biased. (**a**) Frequency of NK/ILC1 (blue), ILC2 (green), and ILC3 (red), as identified by TFs (gated as shown in Figure 10b), in each condition, at week 1, 2, 3, and 4 (n=3-15, 10 independent experiments). (**b**) Linear regressions showing frequencies of specified ILC subset generation as identified by TFs (top row: NK/ILC1; middle row: ILC2; bottom row: ILC3) in each condition at week 4 (n=10-14, 7-10 independent experiments).

4.3 *In vitro* generated ILCs represent stable lineages but undergo plastic differentiation upon provision of inflammatory signals

As human ILCs display varied plasticity when exposed to inflammatory conditions *in vitro*[52,83,191,195–200], functional plasticity was examined at steady state and after stimulation (**Figure 12a,b**). The lack of co-expression of TFs or of cytokines suggested the absence of hybrid ILC lineages such as GATA3^{hi} RORγt^{+} ILC2 described in human peripheral blood, or of RORγt^{+} T-bet^{+} ILC3 as described in mouse[200]. However, exposure of ILC2 or ILC3 to IL-1β and IL-12 before re-stimulation induced up-regulation of IFNγ expression (**Fig 12c-f**), suggesting their partial conversion under these conditions.

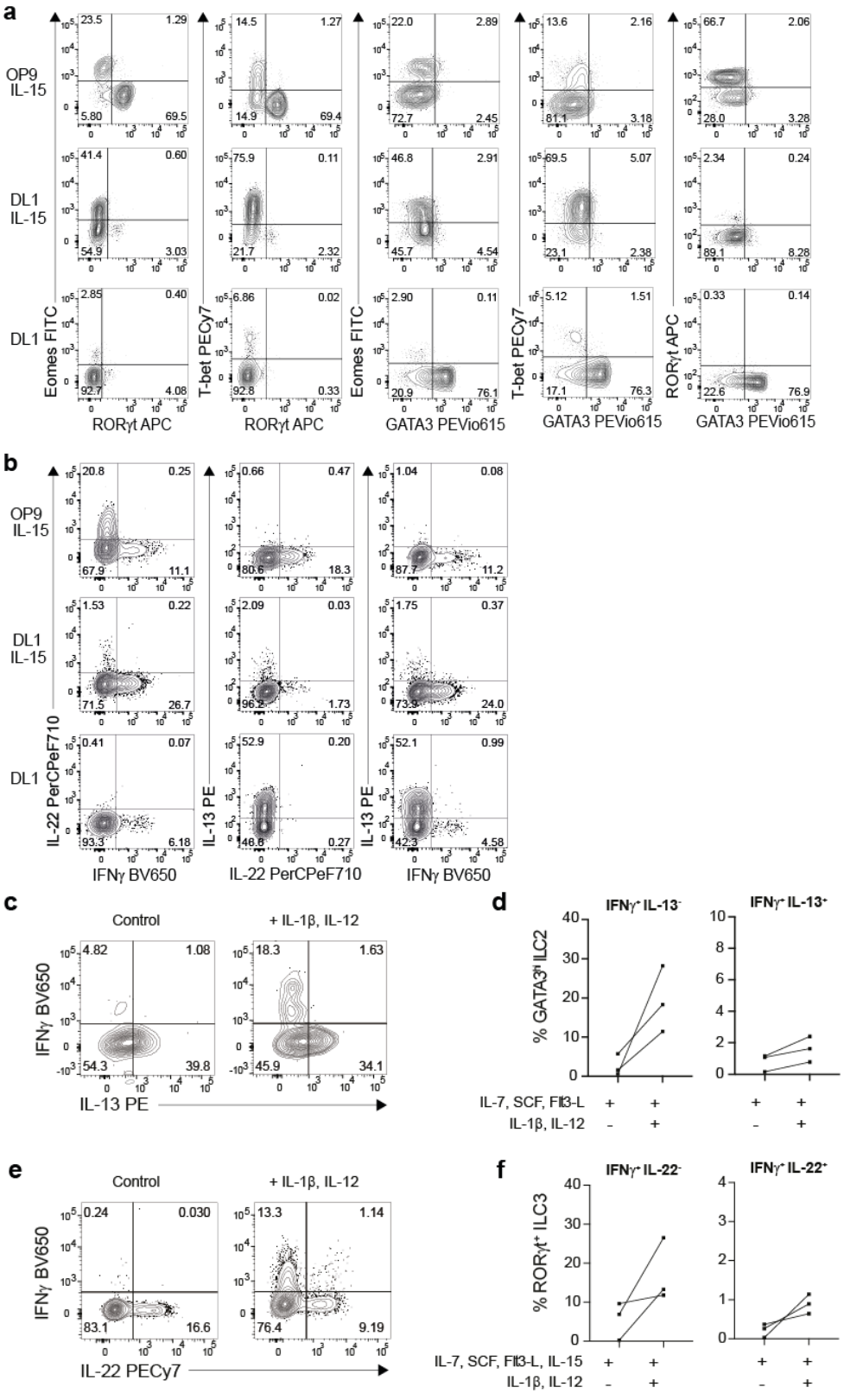

Figure 12: *In vitro* generated ILCs display clear effector programs at steady state. (**a**) Representative TF expression at week 4. (**b**) Representative cytokine expression after 6hr stimulation with PMA/Iono/IL-23 at week 4. (**c,d**) GATA3^{hi} ILC2 from condition DL1 and (**e,f**) RORγt^{+} ILC3 from condition OP9+IL-15 were generated and stimulated with IL-12 (50ng/ml) and IL-1β (50ng/ml) for 5 days prior to PMA/Iono/IL-23 stimulation and the indicated intracellular cytokines were measured. (n=3, 2 independent experiments).

4.4 CD161 expression marks acquisition of ILC lineage identifying transcriptome

To validate the lineage identity of the ILCs generated with further depth, $CD161^+$ ILC subsets were fluorescence-activated cell sorted from all conditions at week 4, based on the surface markers which best correlated to their hallmark TF (**Figure 13a**). ILC3 were sorted from condition OP9+IL-15 based on RANKL expression, which correlated to RORγt, and were further enriched by NKp44 (**Figure 13a-c**)**.** As a certain degree of heterogeneity in Eomes and T-bet expression was observed in NK/ILC1, we utilized expression of two surface markers to dissect these populations (**Figure 13a,b**). CXCR3 was used to identify cells of NK/ILC1 lineage, as it correlated to both Eomes and/or T-bet expression (**Figure 13b,d**). From this $CXCR3^+$ population, $CD94^+$ cells were found to be enriched for Eomes expression specifically, so both $CXCR3^+CD94^-$ and $CXCR3^+CD94^+$ cell subsets were sorted (**Figure 13e,f**). Finally, ILC2 were sorted from condition DL1 as $CRTH2^+$ cells, which correlated with $GATA3^{hi}$ expression (**Figure 13a,b,g**), as well as a $CD161^-CD5^+$ population exclusively engendered in this condition (**Figure 9e**; **Figure 13a,b**), as an internal control.

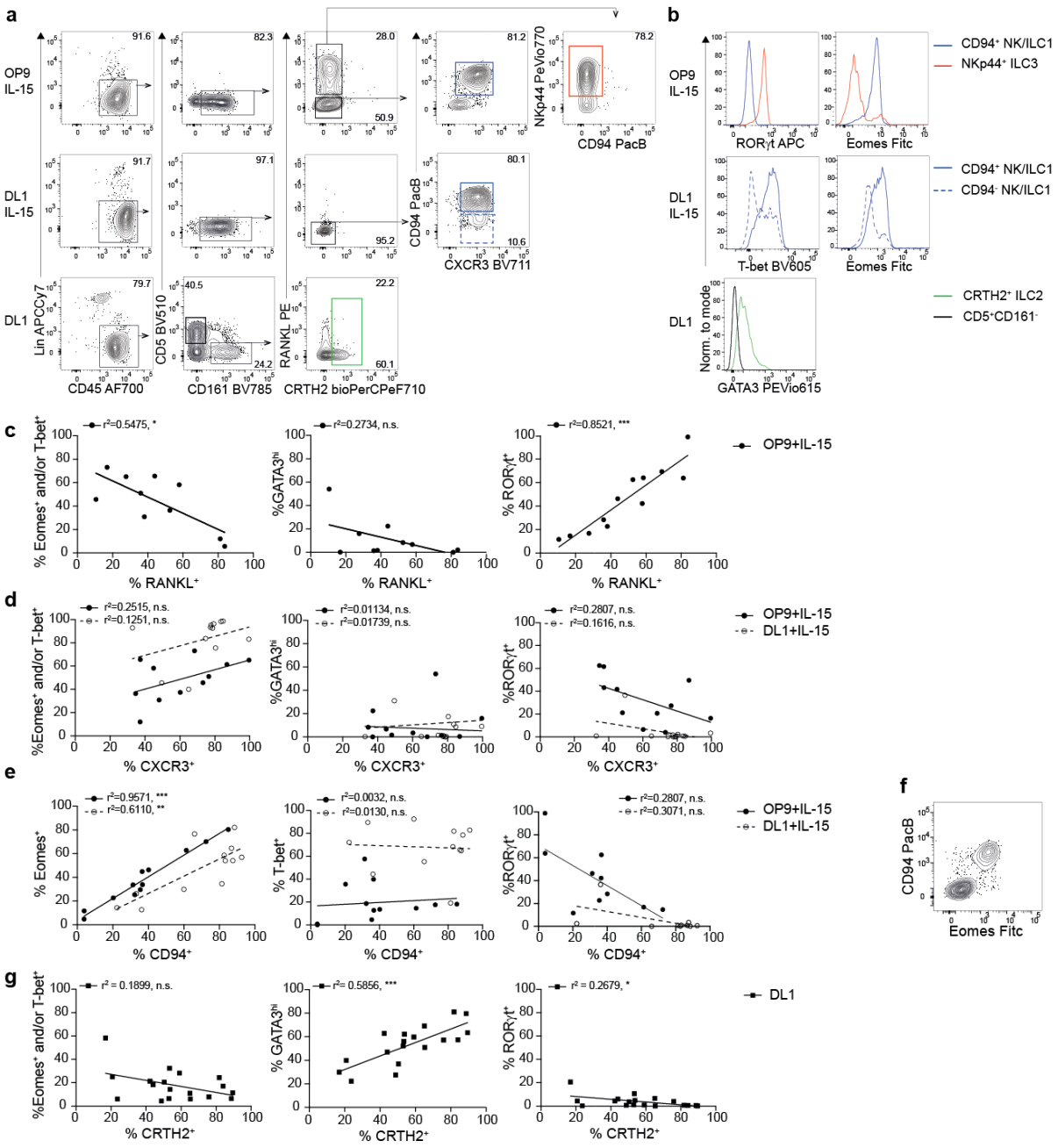

Figure 13: ILC subsets can be identified *in vitro* through surrogate surface markers, correlating to their respective transcription factors. (**a**) Representative sorting strategy for bulk RNA sequencing, based on surrogate surface markers; ILC3 as CD45$^+$ Lin$^-$ CD161$^+$ RANKL$^+$ CRTH2$^-$ CD94$^-$ NKp44$^+$ (red); CD94$^+$ NK/ILC1 as CD45$^+$ Lin$^-$ CD161$^+$ RANKL$^-$ CRTH2$^-$ CXCR3$^+$ CD94$^+$ (blue, solid); CD94- NK/ILC1 as CD45$^+$ Lin$^-$ CD161$^+$ RANKL$^-$ CRTH2$^-$ CXCR3$^+$ CD94$^-$ (blue, dashed); ILC2 as CD45$^+$ Lin$^-$ CD161$^+$ CRTH2$^+$ CD94$^-$ (green); CD161$^-$ non-ILC control as CD45$^+$ Lin$^-$ CD161$^-$ CD5$^+$ (black). (**b**) Representative TF expression in ILC subsets sorted as depicted in **a**. (**c-e**, **g**) Linear regressions between the indicated markers within cells in the different conditions were performed at a 95% confidence interval (n=10-18. 9-13 independent experiments). (**f**) Representative expression of CD94 and Eomes in OP9+IL-15 at week 4. * p≤0.05; ** p≤0.01; *** p≤0.001.

Bulk RNA sequencing was then performed on isolated ILC subsets. Using principal component analysis (PCA) to visualize relations amongst sorted subsets, the separation of 4 groups was observed, with no major influence by donor or culture condition (**Figure 14a,b**).

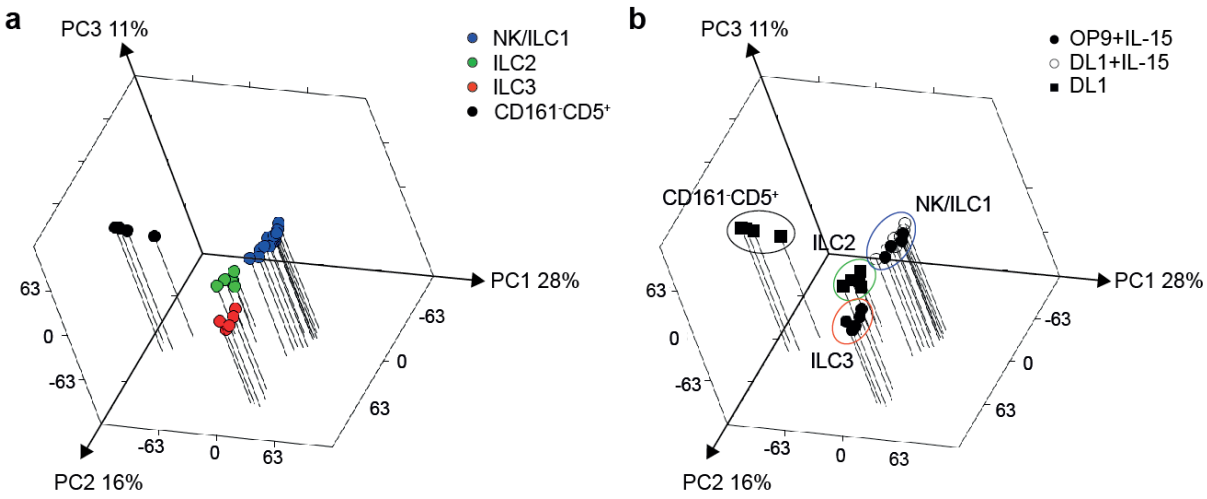

Figure 14: Bulk RNA sequencing clearly separates CD161$^+$ and CD161$^-$ populations. From a total of 5 donors, cells were differentiated until end of week 4 and subsets were sorted as shown in Figure 13a. (**a,b**) 3D PCA plots of CD161$^+$ ILC subsets and CD161$^-$ cells, coloured by subset (**a**) or by culture condition (**b**).

In particular, PC1 resolved separation between CD161$^+$ and CD161$^-$ CD5$^+$ subsets. Several canonical ILC development genes were found to be selectively upregulated in the CD161$^+$ subsets, not only *KLRB1* (encoding CD161, which was sorted for) but *ID2, NFIL3, ZBTB16* (encoding PLZF), *ITGB7* (encoding integrin β7) and *IL2RB* (**Figure 15a,b**), previously described to be present in all mature human ILCs[48].

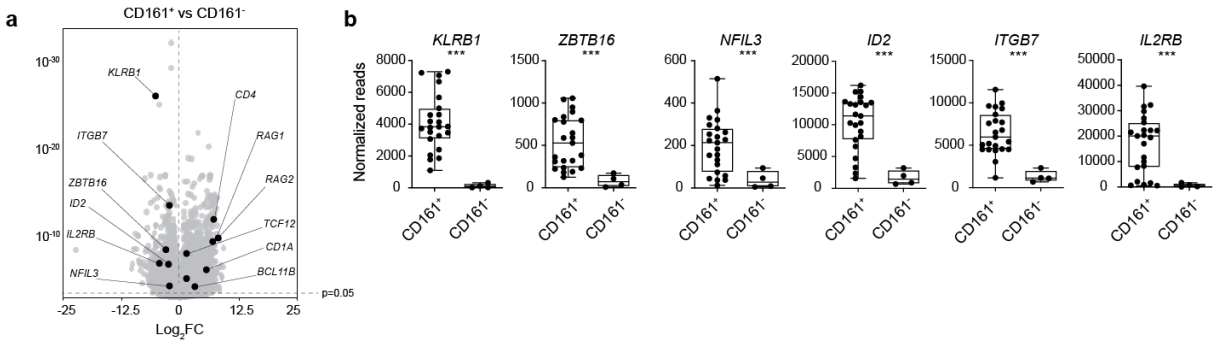

Figure 15: CD161 marks acquisition of ILC transcriptional profile. (**a**) Comparison of gene expression as a fold change (FC) between CD161$^+$ subsets (n=28) and CD161$^-$ subsets (n=4); dashed line on y-axis depicts adjusted p-value of 0.05; black dots represent selected differentially expressed genes with a FC ≥ 1.3. (**b**) Normalized reads of selected transcripts in CD161$^+$ and CD161$^-$ subsets. Statistical test in **b**: Wald Test; * p≤0.05; ** p≤0.01; *** p≤0.001

Conversely, the CD161$^-$ CD5$^+$ subset was enriched in genes associated to T cell lineage differentiation, such as *RAG1* and *RAG2, CD4, CD1A, CD6* and *PTCRA* (encoding the pre-TCRα) which were absent in CD161$^+$ subsets, as well as showcased higher transcripts of the TFs *TCF7, TCF3, TCF12* and zinc finger protein encoding *BCL11B*[201] (**Figure 16a**). Staining of intracellular CD3ε (iCD3ε), which has often been used as an identifier of T cell lineage commitment especially in cultures from HPCs[127,165], was found to not be selectively expressed in CD161$^-$ CD5$^+$ cells. Corresponding to previous data describing iCD3ε expression in innate compartments, both *ex vivo* and *in vitro*[48,202–205], we found iCD3ε to be also upregulated in CD161$^+$ ILCs in response to Notch signaling, especially in the absence of IL-15 (**Figure 16b**). These data suggest that although CD161$^+$ ILCs and T cell-committed CD161$^-$ CD5$^+$ cells can be simultaneously engendered in the same condition, acquisition of CD161 defines commitment towards ILCs and loss of T cell differentiation potential. These data also confirm that iCD3ε expression alone is not indicative of T cell commitment *in vitro.*

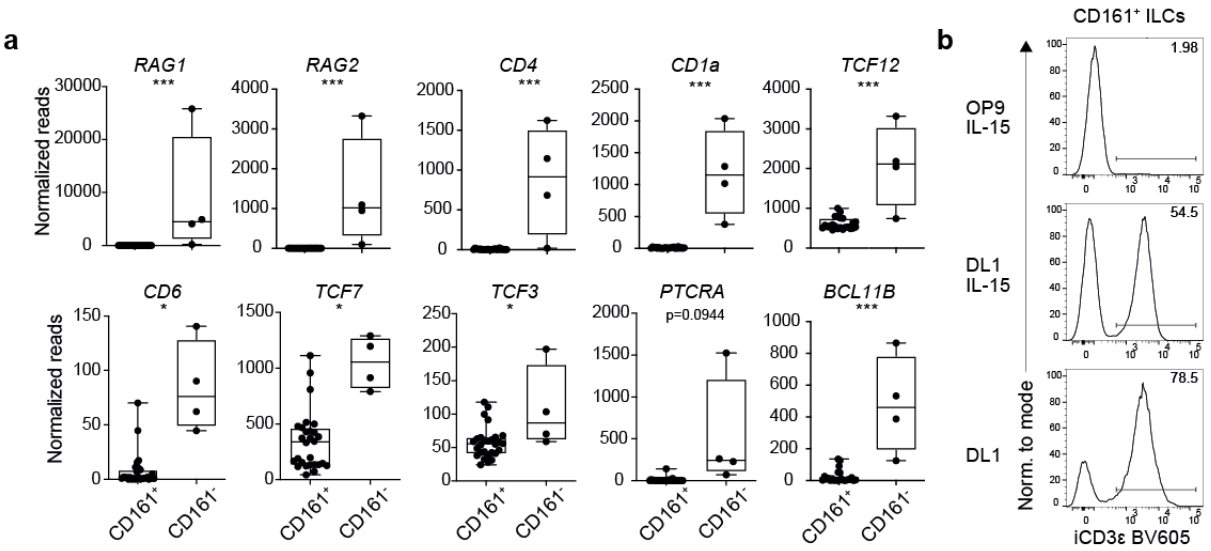

Figure 16: CD161$^-$ subset defined by T cell associated transcriptome. (**a**) Normalized reads of selected transcripts in CD161$^+$ and CD161$^-$ subsets. (**b**) Representative expression of iCD3ε within CD161$^+$ ILCs in each condition at week 4. Statistical test in **a**: Wald Test; * p≤0.05; ** p≤0.01; *** p≤0.001

Removing the CD161$^-$ CD5$^+$ non-ILC subset from the PCA analysis allowed a focus on the individual ILC subset profiles (**Figure 17a**). By comparing the genes which were differentially expressed in pairwise comparisons between each subset we determined the core identity genes of each ILC lineage, which were also the genes driving the first two major principal components (**Figure 17a,b**). For example, ILC3 genes were denoted as differentially expressed in ILC3 vs ILC2 as well as in ILC3 vs NK/ILC1 comparisons. Differentially expressed genes present in only one comparison (e.g. only in ILC3 vs ILC2 but not in ILC3 vs NK/ILC1) were not taken as subset identifying genes but were still considered for further analysis (**Figure 17c**). Both *KLRB1* and *ZBTB16* transcripts were present in all ILC subsets identified. *IL7R* transcripts, which unlike CD127 protein are not strongly downregulated in response to IL-7 signaling[190] were detectable in both ILC2 and ILC3, while lower in NK/ILC1, which in turn expressed high *IL2RB* transcripts (**Figure 17d**).

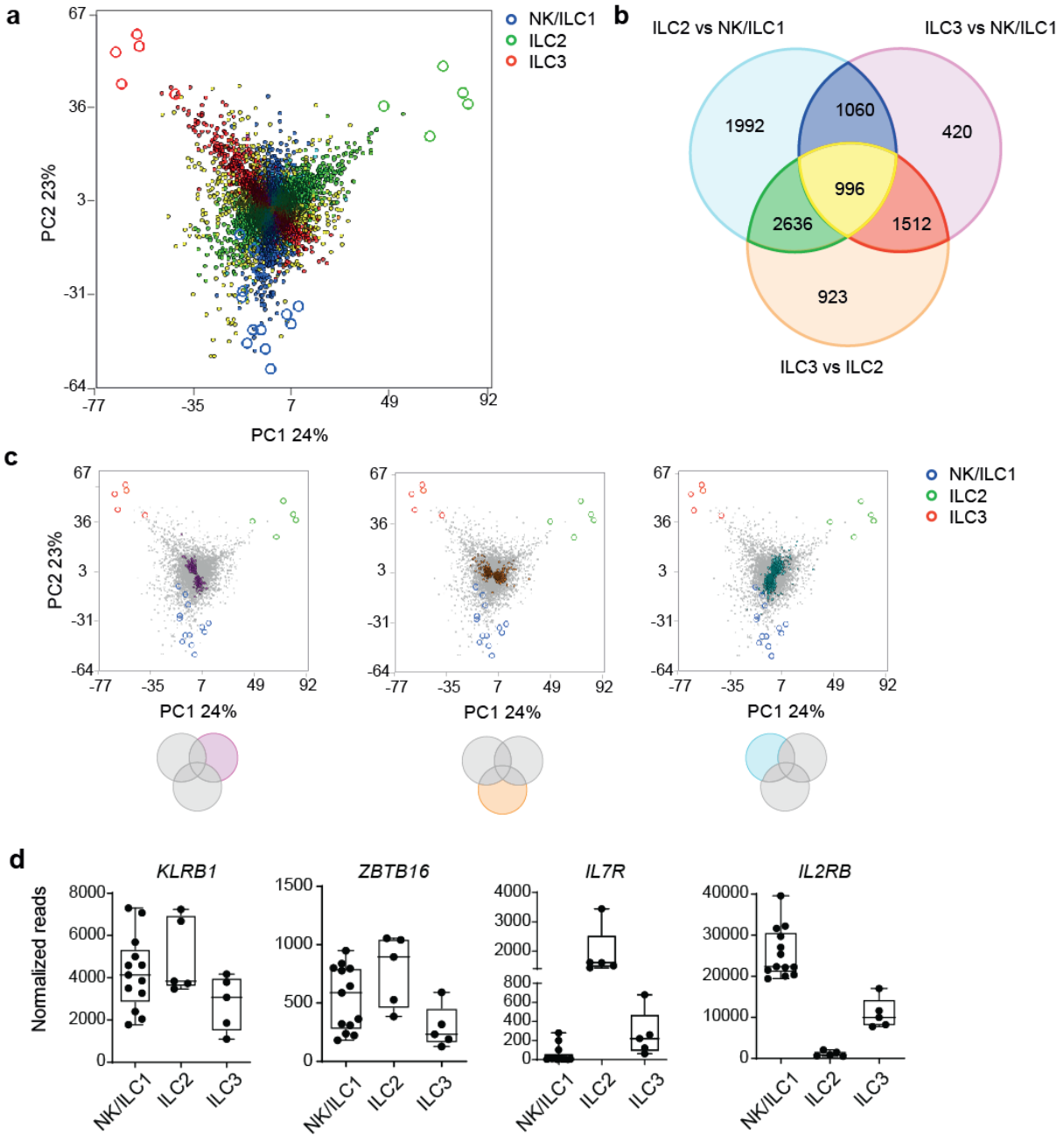

Figure 17: CD161⁺ ILC subsets display individual transcriptome profiles. (**a**) Biplot depicting PCA of CD161⁺ ILC subsets (large open circles), superimposed on genes driving the principal components (small filled circles). Genes are coloured as per diagram in **b**. (**b**) Venn diagram showing sets of significantly differentially expressed genes (DEGs) between comparisons of subsets. NK/ILC1 genes present on both comparisons are depicted as blue; ILC3 genes as red; ILC2 genes as green; genes differentially expressed in all subsets as yellow. (**c**) Biplot depicting PCA of ILC subsets (large open circles) and genes driving the principal (small filled circles) where the genes are coloured as per **a**. (**d**) Normalized reads of *KLRB1*, *ZBTB16*, *IL7R*, and *IL2RB* transcripts in NK/ILC1 (n=13), ILC2 (n=5) and ILC3 (n=5).

From this data set we can construe that not only do CD161⁺ CD45⁺ Lin⁻ cells generated *in vitro* from HPCs express a compelling ILC lineage profile, but ILC subsets within CD161⁺ cells are distinctive and showcase a robust lineage identity.

4.5 NKp44^{+} ILC3 generated *in vitro* largely recapitulate signatures of their *ex vivo* tonsil counterpart

Exploring the ILC3 phenotype, we found transcripts for ILC3 lineage defining genes such as *RORC*, *IL1R1*, *IL23R*, *NCR2* (encoding NKp44), *KIT* (encoding CD117) and *TNFSF11* (encoding RANKL) to be strong drivers of the principal components, and differentially expressed in ILC3 (**Figure 18a-c**). Further consolidating their mature lineage profile, ILC3 expressed transcripts for *IL22*, *IL26*, *IL8, IL4I1*, *LTA*, *LTB*, *CCR7* and *CCL20* (**Figure 18b**), as observed *ex vivo*[48,58,60,62,125]. Amongst differentially regulated ILC3 genes, RORγt, RANKL, CD117, IL-1R1, IL-8 and IL-22 were validated at protein level (**Figure 10a-c; Figure 18d**). Assessment of NKp44 showed that ILC3 generated are largely NKp44^{+} (**Figure 13a; Figure 18e**). Neuropilin-1 (NRP1), which has been described on NKp44^{+} ILC3 in the tonsil and associated with an LTi-like ILC3 phenotype in human[206], was observed on a small fraction of ILC3 generated (**Figure 18d**). NKp46, which in mice is present in a subset of T-bet expressing ILC3, was found to be low or absent in comparison to NK/ILC1 generated in the same condition (**Figure 18d**). Neither *IL17A* nor *IL17F* transcripts were detected, as previously described *ex vivo*[48], however, both IL-17A and IL-17F proteins were observed selectively in a small fraction of RORγt^{+} ILC3 after stimulation (**Figure 18d**).

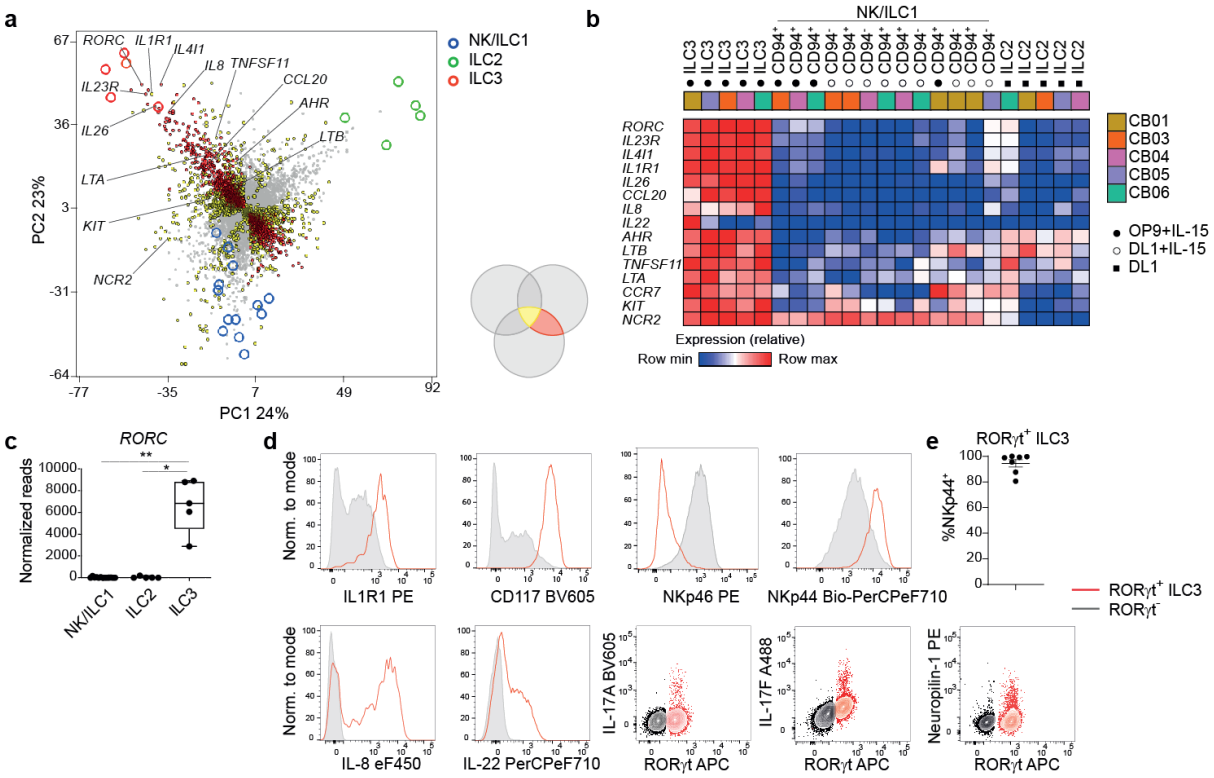

Figure 18: *In vitro* generated NKp44⁺ ILC3 showcase robust transcriptional, phenotypic, and functional ILC3 identifying profile. (**a**) Biplot depicting PCA of ILC subsets (large open circles) and differentially expressed genes specific to ILC3 (small closed circles), coloured as per Figure 16a. (**b**) Heatmap showing selected ILC3 signature genes; clustering by Z score, visualization depicting max/min expression of individual genes. (**c**) Normalized reads of RORC across all ILC subsets, n=5. Kruskal-Wallis test with Dunn's multiple comparisons test; * p≤0.05; ** p≤0.01; *** p≤0.001. (**d**) Representative expression of IL-1R1, CD117, NKp46, Neuropilin-1 and NKp44 within RORγt⁺ ILC3 and RORγt⁻ ILCs from OP9+IL-15. IL-8, IL-22, IL-17A, and IL-17F were measured after 6hr PMA/Iono/IL-23 stimulation (n>2, at least 2 independent experiments). (**e**) Percent of RORγt⁺ ILC3 from OP9+IL-15 expressing NKp44, n=7, 6 independent experiments.

To directly compare the transcriptome of our *in vitro* generated ILC3 to *ex vivo* ILC3, we performed gene set enrichment analysis (GSEA) using a publically available transcriptome data set of *ex vivo* isolated tonsil ILCs[48] (**Figure 19a**). We found the *in vitro* generated ILC3 to be most significantly positively enriched with tonsil ILC3, while most significantly dissimilar to tonsil conventional NK cells.

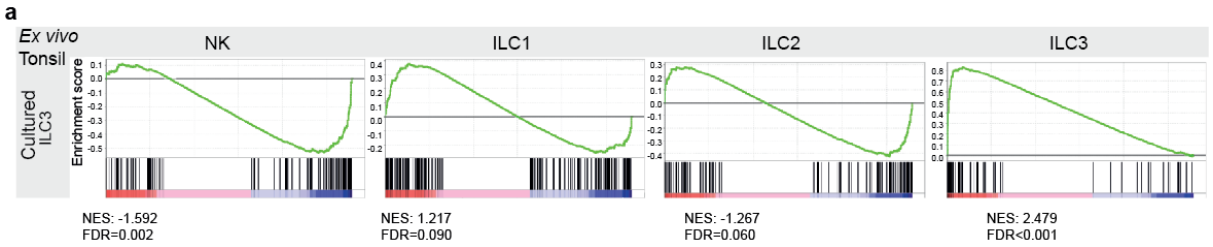

Figure 19: *In vitro* generated NKp44^{+} ILC3 share transcriptional profile with *ex vivo* isolated tonsil ILC3. (**a**) Gene set enrichment analysis comparing the *in vitro* ILC3 gene signature to that of tonsil ILCs, depicting normalized enrichment score (NES) and false discovery rate (FDR).

Together, these findings indicate that *in vitro* generated ILC3 support a functional transcriptomic and proteomic profile in line with signatures obtained from *ex vivo* ILC3.

4.6 CD5^{-} and CD5^{+} ILC2 generated *in vitro* display a global signature akin to that of tonsil ILC2

Next, the phenotype of the *in vitro* generated ILC2 was investigated with further depth. Generated ILC2 expressed recognizable ILC2 identifying transcripts such as *GATA3*, *PTGDR2* (encoding CRTH2), *KLRG1*, *HPGD*, *HPGDS* and *S1PR1,* which drove the PCA separation from other ILC subsets (**Figure 20a-c**). Similar to *GATA3*, *BCL11B* has been described as a critical TF not only for T cell lineage-fate decisions, but specifically for ILC2 as well[207–209]. Accordingly, within the ILC subsets, we observed high *GATA3* and *BCL11B* transcripts restricted to ILC2 (**Figure 20c**). Expression of *IL2RA* (encoding CD25), *IL1RL1* (encoding the IL-33 receptor) and *IL13* transcripts were also well represented in the ILC2 generated. Although not present systematically in every donor, *IL5*, *IL4*, *IL9* as well as *IL10* transcripts could be detected, showing the potential of ILC2 to produce these cytokines (**Figure 20b**), keeping with *ex vivo* data[53,210,211]. Consistent with *ex vivo* findings of lung, PB, and fetal gut ILC2, their *in vitro* generated counterpart expressed chemokine receptors *CCR2* and *CCR4*[4,49] (**Figure 20b**). KLRG1, CD25, NKp30, and high CD45 expression were confirmed at the protein level, together with IL-13 expression after stimulation (**Figure 20d**) as described previously[4,212].

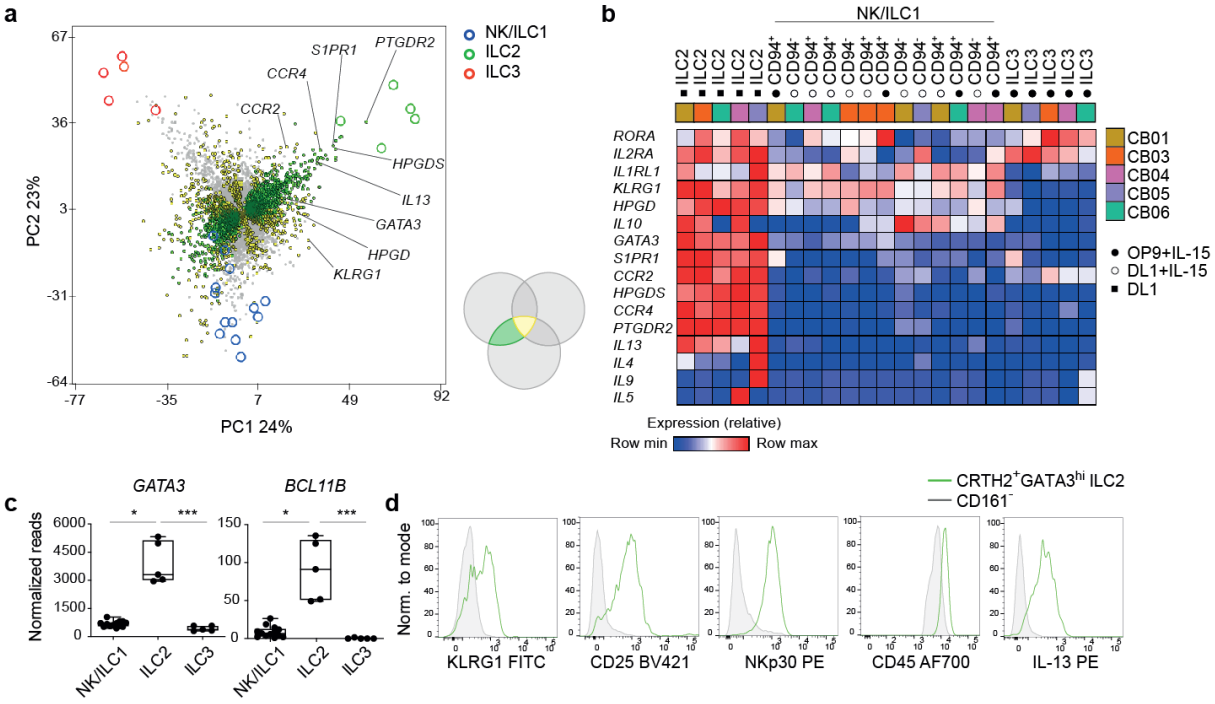

Figure 20: *In vitro* generated ILC2 showcase robust transcriptional, phenotypic, and functional ILC2 identifying profile. (**a**) Biplot depicting PCA of CD5$^-$ ILC subsets (large open circles) and differentially expressed genes specific to ILC2 (small closed circles), coloured as per Figure 16a. (**b**) Heatmap showing selected ILC2 signature genes; clustering by Z score, visualization depicting max/min expression of individual genes. (**c**) Normalized reads of *GATA3* and *BCL11B* in NK/ILC1 (n=13), ILC2 (n=5) and ILC3 (n=5). Kruskal-Wallis test with Dunn's multiple comparisons test; * p≤0.05; ** p≤0.01; *** p≤0.001. (**d**) Representative expression of KLRG1, CD25, NKp30, and CD45 in GATA3^{hi} CRTH2$^+$ ILC2 and CD161$^-$ non-ILCs from DL1. IL-13 was measured after PMA/Iono/IL-23 stimulation (n>2, at least 2 independent experiments).

GSEA using *ex vivo* isolated tonsil ILCs[48] exposed the *in vitro* generated ILC2 to have a significant positive enrichment with tonsil ILC2, showcasing parallels in their transcriptome, while showing significant negative enrichment with tonsil ILC3, ILC1 and NK cells (**Figure 21a**).

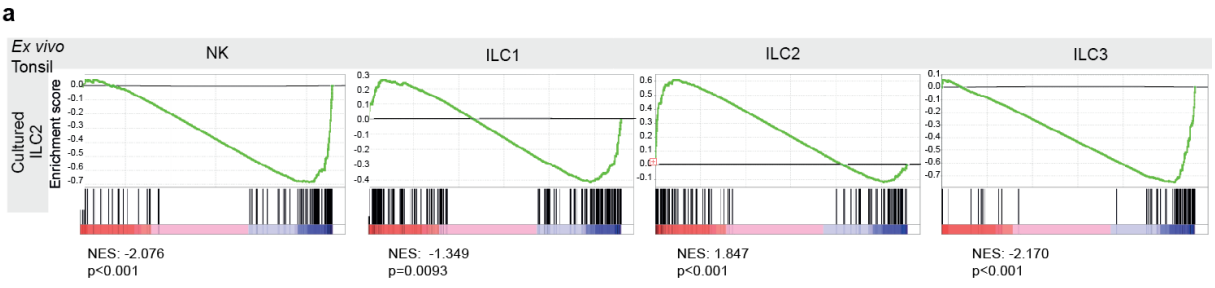

Figure 21: *In vitro* generated ILC2 share transcriptional profile with *ex vivo* isolated tonsil ILC2. (**a**) Gene set enrichment analysis comparing the *in vitro* ILC2 gene signature to that of tonsil ILCs, depicting normalized enrichment score (NES) and false discovery rate (FDR).

Notably, CD5, which has long been a marker of T cell precursors as well as a T cell identifier[213], has been recently described to mark functionally immature ILC2 and ILC3 in human cord blood and postnatal thymus[214]. Interestingly, CD5 expression was observed on a fraction of ILC2 generated (**Figure 22a**). Expression of ILC2 identifying transcripts *GATA3* and *IL13* were not significantly different between $CD5^+$ and $CD5^-$ ILC2 (**Figure 22b**)

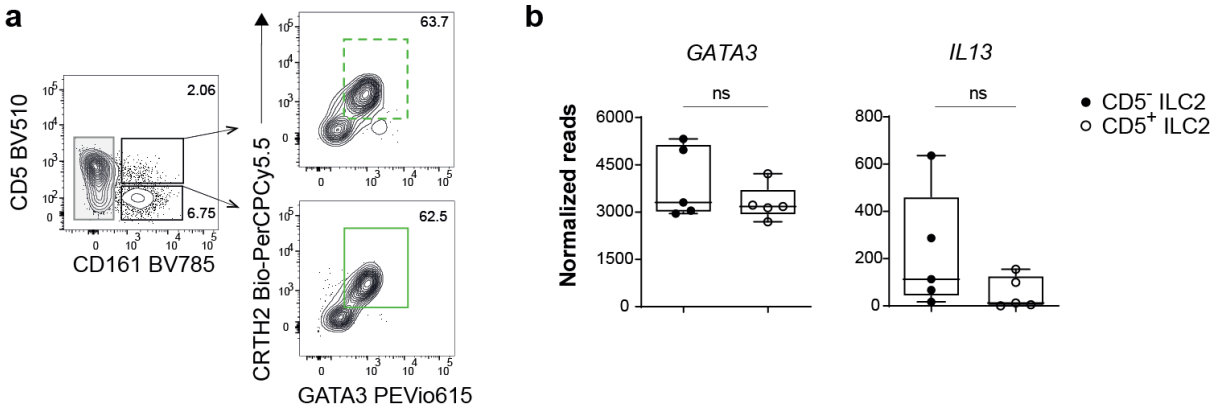

Figure 22: $CD5^+$ ILC2 are generated *in vitro* and have comparable *GATA3* and *IL13* transcripts. (**a**) Representative gating and expression of GATA3 and CRTH2 in $CD5^-$ and $CD5^+$ ILC2 subsets. (**b**) Normalized reads of *GATA3* and *IL13* transcripts in $CD5^-$ and $CD5^+$ ILC2, n=5. Statistical analyses in (**b**) Mann-Whitney test; * p≤0.05; ** p≤0.01; *** p≤0.001; ns: not significant.

We next compared the global transcriptional signatures of $CD5^-$ and $CD5^+$ subsets within the ILC2 population. PCA showed that $CD5^-$ and $CD5^+$ ILC2 clustered together and were distinctly demarcated from $CD161^-$ $CD5^+$ cells (**Figure 23a**), indicating that both $CD5^-$ and $CD5^+$ ILC2 subsets represent genuine ILC2 lineages, supported by the shared expression of several canonical ILC2 genes including *GATA3, IL13, PTGDR2, HPGD,* and *HPGDS* (**Figure 23b**). Protein expression of KLRG1, CD25, NKp30, GATA3, CRTH2, CD45 and IL-13 was also comparable between subsets (**Figure 22a; 23c**).

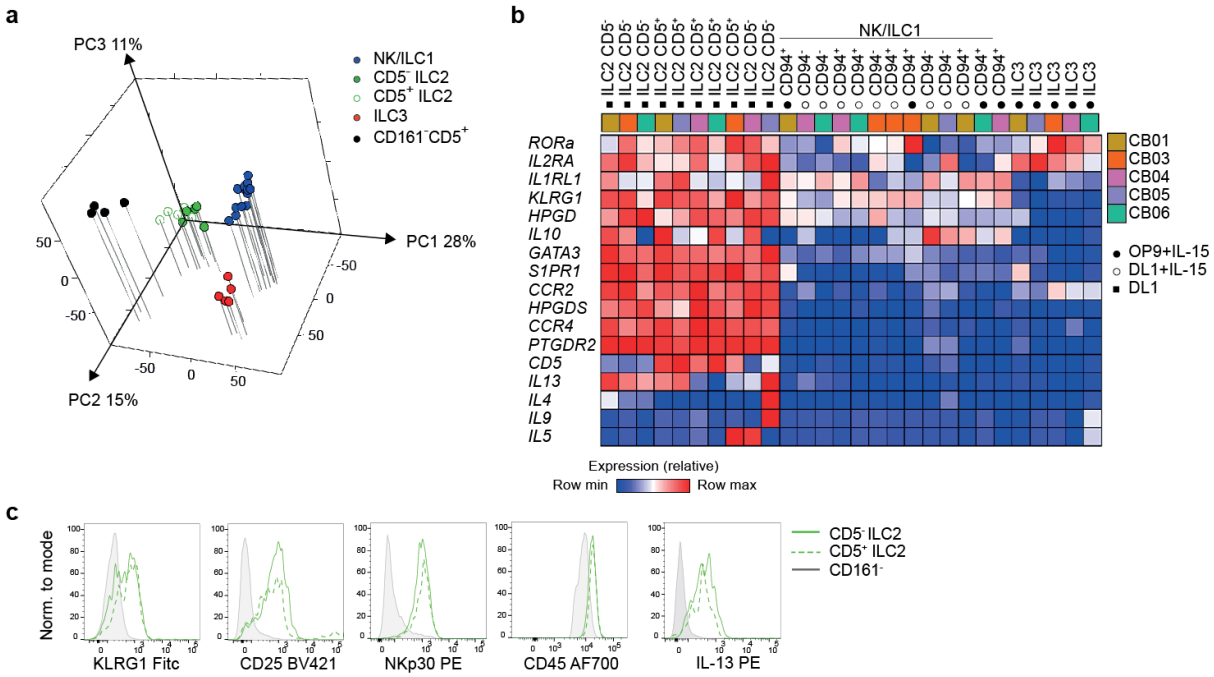

Figure 23: CD5⁺ ILC2 generated *in vitro* retain ILC2 transcriptomic and protein profile. (**a**) PCA plot of all ILC subsets, including CD5⁻ and CD5⁺ ILC2, and CD161⁻ CD5⁺ cells. (**b**) Heatmap showing selected ILC2 signature genes; clustering by Z score, visualization depicting max and min expression of individual genes. (**e**) Representative expression of the indicated markers in CD5⁻ and CD5⁺ ILC2, as well as CD161⁻ non-ILCs from DL1. IL-13 was measured after 6hrs PMA/Iono/IL-23 stimulation.

Temporally following CD5 expression in ILC2 showed it to decrease, suggesting CD5 as being transiently expressed (**Figure 24a**). To exclude a donor-specific bias of ILC2 differentiation, frequencies of the CD161⁻CD5⁺ population and CD5$^{+/-}$ ILC2 were investigated. Donors which generated high frequencies of ILC2, similarly generated high frequencies of CD161⁻CD5⁺ cells (**Figure 24b**). This suggests that T cell differentiation comes at expense of ILC fate (**Figure 9f**), but not necessarily of ILC2. Conversely, CD5 was absent in ILC lineages (NK/ILC1 and ILC3) generated in different culture conditions (**Figure 24c**).

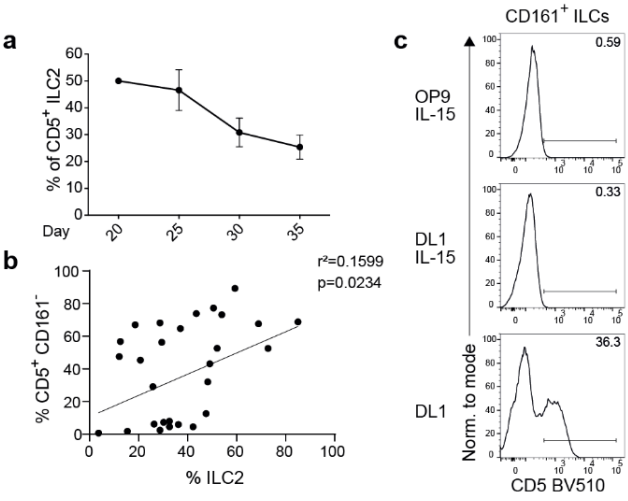

Figure 24: CD5 is transiently expressed in ILC2. (**a**) Kinetics of CD5 expression within GATA3^{hi} CRTH2⁺ ILC2 from DL1, n=2-5, 8 independent experiments. (**b**) Linear regression of frequencies of CD5⁺ CD161⁻ and CD161⁺ ILC2 from condition DL1 (n=31, 20 independent experiments). (**c**) Expression of CD5 within CD161⁺ ILCs in every condition, at week 4.

Collectively, these data demonstrate that *in vitro* generated ILC2 are phenotypically on par with *ex vivo* isolated ILC2, and reveal that previously touted T cell antigens such as iCD3ε, CD5 are insufficient to distinguish ILCs from adaptive lineages, especially in *in vitro* differentiation systems.

4.7 *In vitro* generated NK/ILC1 pool exhibit a global type 1 signature

Finally, we scrutinized the *in vitro* generated CD94^{+} and CD94^{-} NK/ILC1 by diving into the PCA cluster that emerged from the transcriptome data. Differentially regulated genes which drove the NK/ILC1 signature generated in either OP9+IL-15 or DL1+IL-15, as compared to ILC2 and ILC3, included canonical NK cell receptors such as *NCR1*, *NCAM1*, *FCGR3A* (encoding CD16), and *KLRF1* (encoding NKp80), cytotoxicity mediating genes *GZMA*, *GZMB*, and *PRF1,* TFs *EOMES* and *TBX21,* as well as signaling mediators *IL12RB2*, *CCL5*, and *IFNG* (**Figure 25a-c**).

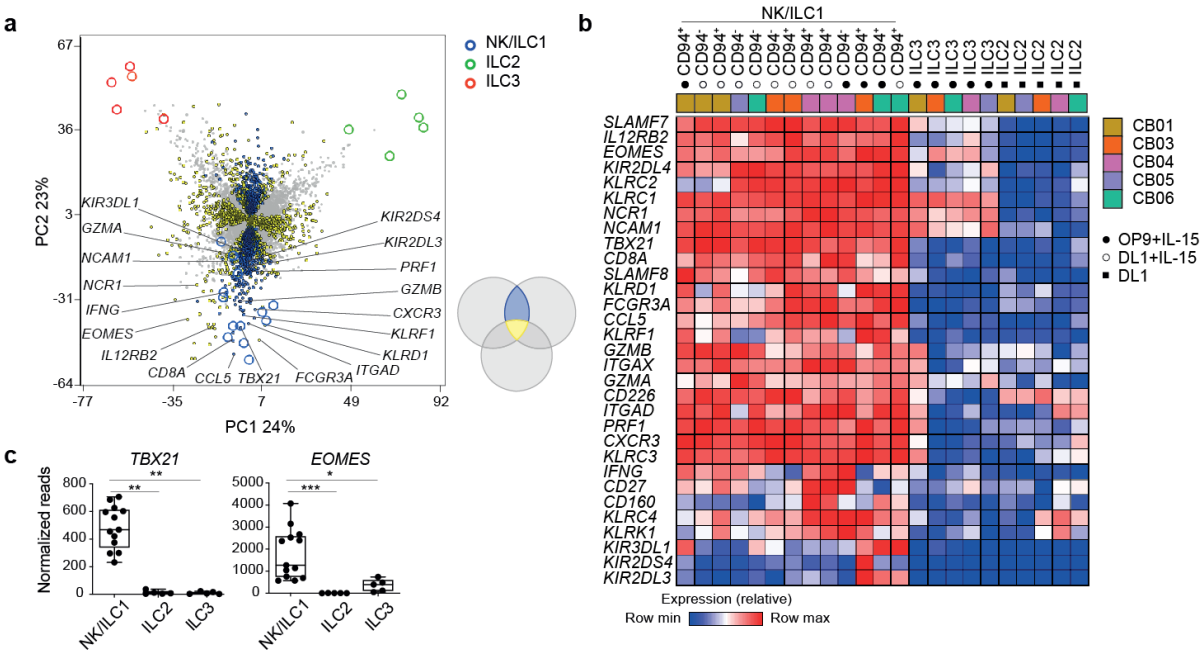

Figure 25: *In vitro* generated NK/ILC1 showcase a robust transcriptional type 1 gene signature. (**a**) Biplot depicting PCA of ILC subsets (large open circles) and differentially expressed genes specific to NK/ILC1 (small closed circles), coloured as per Figure 16a. (**b**) Heatmap showing selected NK/ILC1 signature genes; clustering by Z score, visualization depicting max/min expression of individual genes. (**c**) Normalized reads of *TBX21* and *EOMES* in CD94$^{+/-}$ NK/ILC1 (n=13), ILC2 (n=5) and ILC3 (n=5). Indicated comparisons depicted in **c** were performed using a Kruskal-Wallis test with Dunn's multiple comparisons test; * p≤0.05; ** p≤0.01; *** p≤0.001.

We next attempted to untangle the differences within this cluster to dissect NK cells from ILC1. Since CD94$^-$ NK/ILC1 enriched for T-bet single-positive cells and CD94 has been previously used to distinguish NK cells from ILC1 in *in vitro* cultures[127], we hypothesized this population to be more akin to ILC1 than NK cells. Although CD94 expression preferentially enriched for Eomes$^+$ cells both in OP9+IL-15 and DL1+IL-15 (**Figure 13e,f**), no cluster separation between CD94$^+$ and CD94$^-$ subsets or OP9+IL-15 and DL1+IL-15 conditions emerged by performing a PCA on the isolated NK/ILC1 subsets. Instead, the samples clustered by donor (**Figure 26a**), suggesting that the similarities within the NK/ILC1 subsets generated in either condition were greater than the differences in Eomes and CD94 expression. Comparing CD94$^+$ and CD94$^-$ subsets, only minor differences in *EOMES* and *TBX21* transcripts were observed (**Figure 26b**). CD56 and NKp46 protein levels were similar in Eomes$^+$ and Eomes$^-$ cell subsets, while there was a trend of higher CD16 expression in Eomes$^+$ cells (**Figure 26c,d**). In terms of effector cytokines, *IFNG* and *TNF* transcripts were also comparable across subsets (**Figure 26e**). In general, intracellular expression of IFNγ after stimulation was slightly increased in DL1+IL-15 derived NK/ILC1 (**Figure 10g; Figure 26f**). No significant differences were noted in killing activity within the subsets, although a trend for NK/ILC1 generated in DL1+IL-15 to have increased effector functions, as also depicted for IFNγ production, was observed (**Figure 26g**). This goes together with previous reports showing that Notch signaling in CD34$^+$ cultures increased expression of maturation markers and amplifies toxicity from NK cells[215].

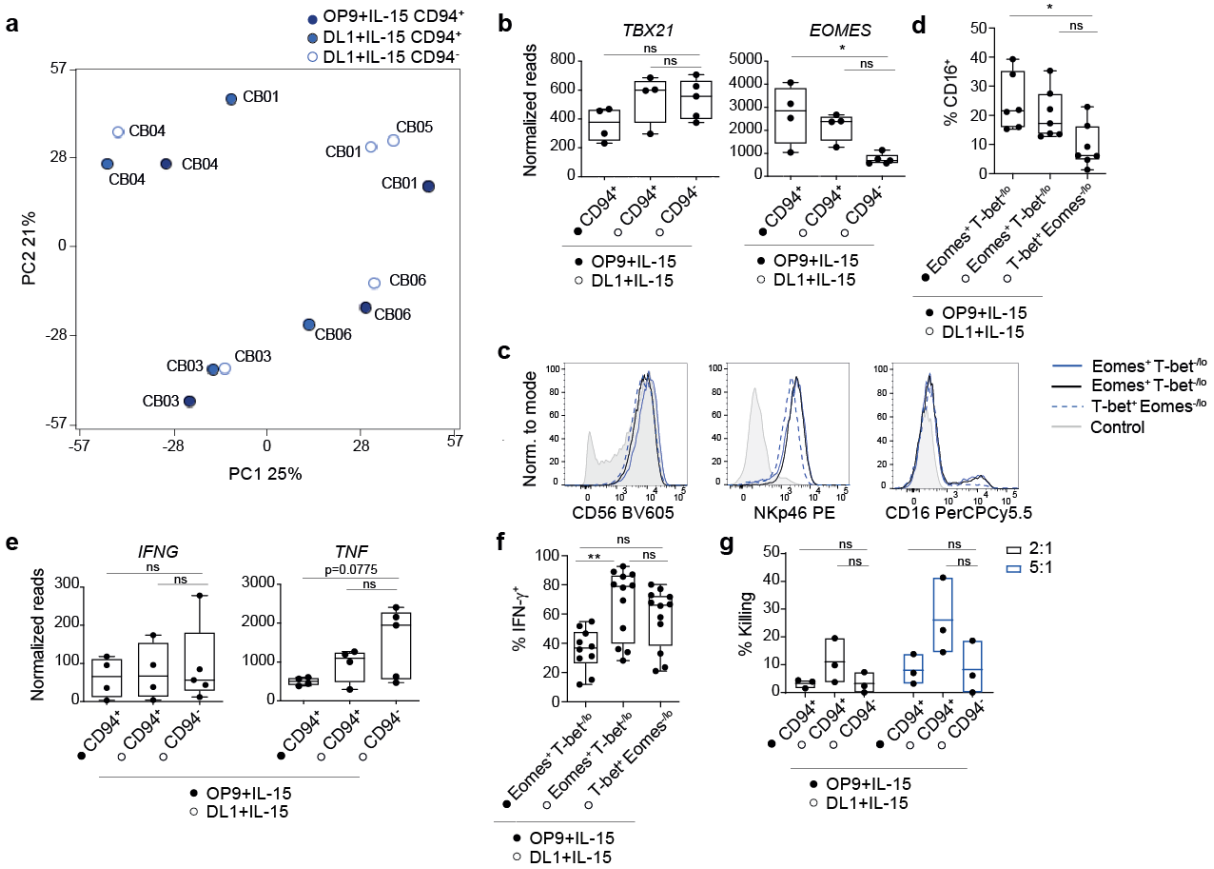

Figure 26: Eomes or CD94 expression do not clearly dissect NK/ILC1 heterogeneity *in vitro*. (**a**) Biplot depicting PCA of NK/ILC1 subsets sorted, donors annotated. (**b**) Normalized reads of *TBX21* and *EOMES* in CD94$^+$ NK/ILC1 from OP9+IL-15 (n=4), CD94$^+$ (n=4) and CD94$^-$ (n=5) NK/ILC1 from DL1+IL-15. (**c**) Representative expression of CD56, NKp46 and CD16 in Eomes$^+$ T-bet$^{-/lo}$ from OP9+IL-15 (blue, solid) and Eomes$^+$ T-bet$^{-/lo}$ (black) and T-bet+Eomes-/lo (blue, dashed) from DL1+IL-15. Control is Eomes$^-$ T-bet$^-$ from OP9+IL-15 (grey). (**d**) Fraction of CD16$^+$ cells across NK/ILC1 subsets: Eomes$^+$ T-bet$^{-/lo}$ from OP9+IL-15 (n=6) and Eomes$^+$ T-bet$^{-/lo}$ (n=7) and T-bet$^+$ Eomes$^{-/lo}$ from DL1+IL-15 (n=7), 5 independent experiments. (**e**) Normalized reads of *IFNG* and *TNF* in CD94$^+$ NK/ILC1 from OP9+IL-15 (n=4), CD94$^+$ (n=4) and CD94$^-$ (n=5) NK/ILC1 from DL1+IL-15. (**f**) Fraction of IFNγ$^+$ cells within NK/ILC1 subsets: Eomes$^+$ T-bet$^{-/lo}$ from OP9+IL-15 (n=10) and Eomes$^+$ T-bet$^{-/lo}$ (n=12) and T-bet$^+$ Eomes$^{-/lo}$ (n=12) from DL1+IL-15, after 6hr PMA/Iono/IL-23 stimulation, 8 independent experiments. (**g**) NK/LC1 killing assessed as % of K562 target cells lysed at NK/ILC1 to target cell ratios 2:1 and 5:1 across NK/ILC1 subsets sorted; n=3, 1 independent experiment. Indicated comparisons depicted in **b, d, e, f, g,** were performed using a Kruskal-Wallis test with Dunn's multiple comparisons test; * p≤0.05; ** p≤0.01; *** p≤0.001; ns: not significant.

As a way to directly compare the phenotypes of our NK/ILC1 to *ex vivo* isolated NK and ILC1 we performed a GSEA using tonsil derived CD127$^-$ CD56$^+$ NK and CD127$^+$ non-cytotoxic ILC1[48] (**Figure 27a**). This revealed a stark similarity of the *in vitro* generated NK/ILC1 to tonsil NK, and not to CD127$^+$ ILC1. In contrast, when comparing to tonsil CD127$^-$ cytotoxic ILC1 originally described by Fuchs and colleagues[31,86], we observed a strong positive enrichment (**Figure 27b**).

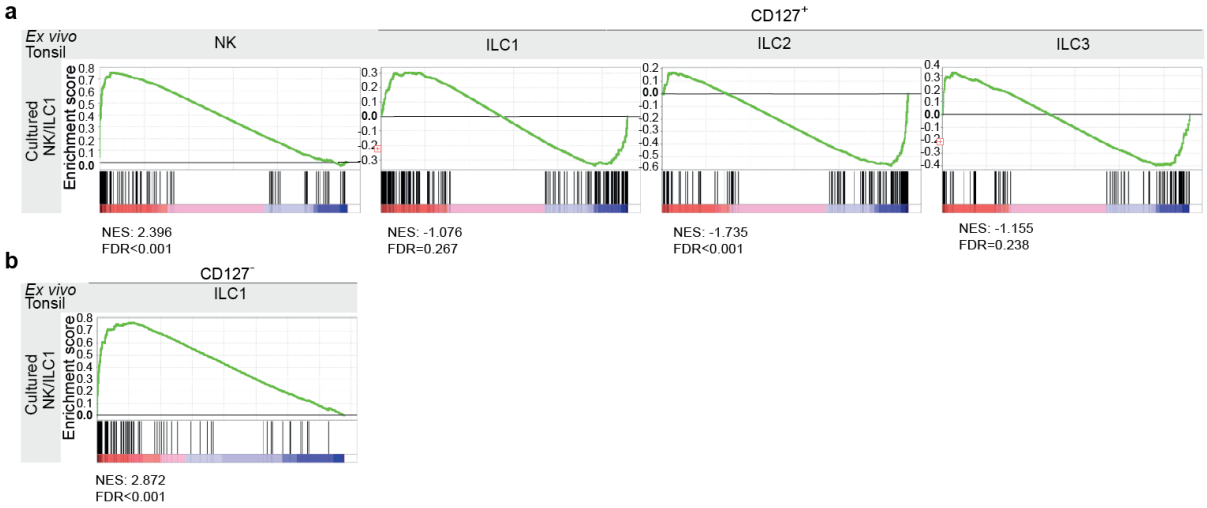

Figure 27: *In vitro* generated NK/ILC1 share transcriptional profile with *ex vivo* isolated tonsil NK cells and cytotoxic CD127$^-$ ILC1, but not with non-cytotoxic CD127$^+$ ILC1. (**a**,**b**) Gene set enrichment analysis comparing the *in vitro* NK/ILC1 gene signature to that of CD127$^+$ or CD127$^-$ tonsil ILCs respectively, depicting normalized enrichment score (NES) and false discovery rate (FDR).

In summary, these data confirm the presence of a global type 1 signature in NK/ILC1 subsets. However, the line between human NK and ILC1 identification and characteristics remains problematic, as the definitions of Eomes$^+$ NK and T-bet$^+$ ILC1 might fall apart under *in vitro* culture and should be reconsidered for future studies. In line with the variable identity of NK/ILC1 in the cultures, exploring *ex vivo* TF expression within CD56$^+$ or CD94$^+$ conventional NK cells reveals the multifaceted nature of Eomes and T-bet also within tissue sites (**Figure 28**), suggesting that a clear and convincing separation between human NK and ILC1 requires further study and semantic refinement.

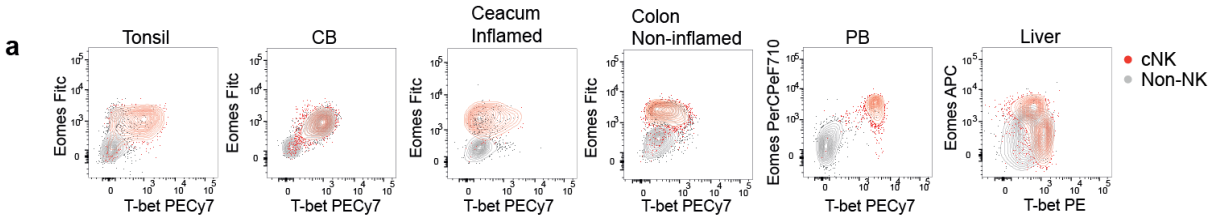

Figure 28: Eomes and T-bet expression is heterogeneous in conventional NK cells *ex vivo*. Representative expression of Eomes and T-bet across various organs. Red population represents conventional NK cells (in tonsil, liver, cord blood (CB): Lin$^-$ CD45$^+$ CD3$^-$ CD56$^+$ CD117$^{+/-}$; in PB: Lin$^-$ CD3$^-$ CD7$^+$ CD56$^+$ CD117$^{+/-}$; in caecum and colon: Lin$^-$ CD45$^+$ CD3$^-$ CD94$^+$), grey population represents non-NK (in tonsil, liver, CB, peripheral blood (PB): Lin$^-$ CD45$^+$ CD3$^-$ CD56$^-$; in caecum and colon: Lin$^-$ CD45$^+$ CD3$^-$ CD94$^-$).

4.8 Unbiased assessment of ILC transcriptional signatures and heterogeneity by single-cell RNA sequencing

To define the transcriptional landscape of the generated ILCs in an unbiased manner and to gain more detailed insights about potential heterogeneity within the obtained ILC subsets, single-cell RNA sequencing (scRNA-seq) was performed. To include possible transitional or differentiating cells with little to no CD161 expression, total $CD45^+$ Lin^- cells from each of the three conditions (OP9+IL-15, DL1+IL-15, and DL1) were sorting, omitting positive selection by CD161 expression. For simultaneous characterization of RNA and protein, we integrated oligo-conjugated antibodies into the single-cell sequencing workflow, also known as CITE-seq (Cellular Indexing of Transcriptomes and Epitopes by sequencing)[216], which allowed for the validation of ILC lineage transcriptional identities with surface protein expression on the same cells. A total of 10512 cells across all conditions were analyzed from 2 donors. Cells were embedded using uniform manifold approximation and projection (UMAP). After regressing cell cycle effects out, 4 main clusters emerged, distributed over the three conditions (**Figure 29a,b**). Of these clusters, cluster 1, 2 and 3 expressed CD161 signifying ILC lineages, whereas cluster 0 lacked CD161 and instead expressed CD5 and CD1a, suggesting a more T-cell like phenotype (**Figure 29c**).

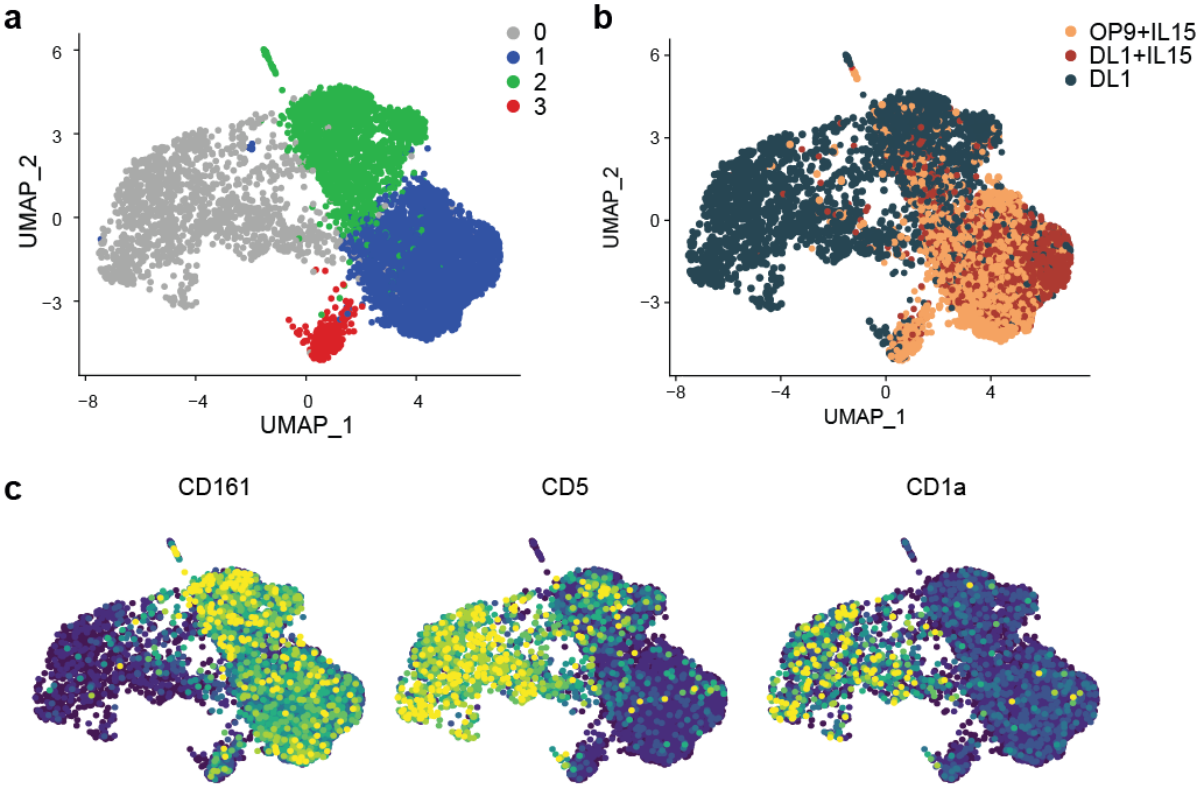

Figure 29: Assessment of single cell transcriptional signatures confirm ILC lineage clusters and a non-ILC CD161$^-$ population. From 2 donors, CD45$^+$ Lin$^-$ cells sorted from each of the three conditions. (**a**) UMAP dimensionality reduction projection, color-coded to present clusters identified. (**b**) UMAP dimensionality reduction projection, color-coded to present conditions from which individual cells are derived. (**c**) Expression of surface CD161, CD5, and CD1a protein from CITE-seq onto UMAP visualization in **a**.

Further analysis showed that cells belonging to cluster 0 expressed high levels of *RAG1*, *CD3G*, and *PTCRA* transcripts, as well as T-lymphocyte associated TFs *TCF12* and *BCL11B*, and markedly low *KLRB1* transcripts. This cluster, which rose exclusively from the DL1 condition, was equivalent to the CD161$^-$ CD5$^+$ population presented in the bulk RNA-seq (**Figure 30a,b**). Clusters 1, 2 and 3 displayed surface CD161, along with preferential expression of *KLRB1*, *ID2* and *ZBTB16* transcripts, and were identified as belonging to the ILC lineage, confirming with an unbiased approach the validity of CD161 as an ILC lineage marker in CD34$^+$ HPC cultures (**Figure 30a,b**). Expression of the master TFs *EOMES*, *GATA3* and *RORC* flagged the three main ILC clusters, NK/ILC1 (cluster 1), ILC2 (cluster 2) and ILC3 (cluster 3) (**Figure 30a,b**), respectively, while *TBX21* transcripts were hardly detectable in the scRNA-seq data set (**Figure 30c**). *IL7R* expression was observed preferentially in ILC2 and ILC3, while NK/ILC1 rather displayed high expression of *IL2RB* transcripts (**Figure 30a**).

Besides *RORC*, the ILC3 signature was driven by 134 differentially regulated genes, including *IL23R*, *IL1R1*, *IL26*, *NCR2* (**Figure 30b**) and belonged chiefly to cells engendered in condition OP9+IL-15 (**Figure 29b**), corroborating the phenotype delineated through both flow cytometry and bulk RNA-seq. The ILC2 signature, rising mainly from the DL1 condition (**Figure 29b**), was driven by 80 differentially regulated genes, including high *GATA3* and *HPGD*, which was consistent with the ILC2 phenotype described (**Figure 30b**). Finally, the NK/ILC1 cluster which was derived from conditions supplied with IL-15 (**Figure 29b**), showcased a robust type 1 signature driven by 142 differentially regulated genes, including high *EOMES*, *NCR1*, *NCAM1*, *PRF1*, *KLRC1* and *NKG7* transcripts (**Figure 30b**), in line with our bulk RNA-seq data. No clusters with an ILC profile lacking surface CD161 expression were found, confirming that surface CD161 expression marks acquisition of ILC lineage identifying transcriptome *in vitro.*

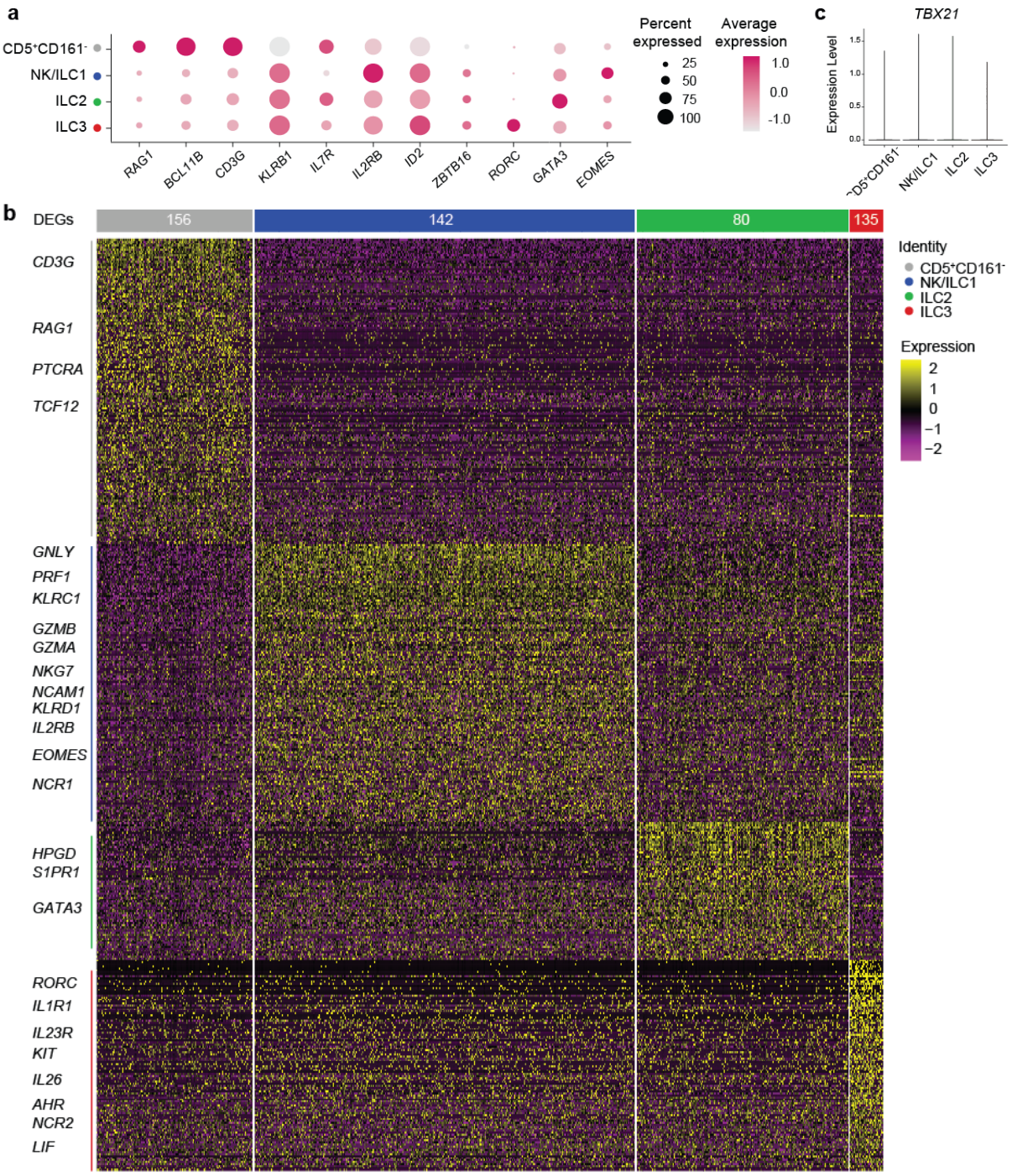

Figure 30: Single cell RNA sequencing confirms ILC lineage identities of NK/ILC1, ILC2 and ILC3. (**a**) Dotplot displaying expression of selected and previously described human T cell and ILC subset-specific markers in the different clusters. Color scale represents average expression, dot size visualizes fraction of cells within the cluster expressing the gene. (**b**) Violin plot presenting expression of *TBX21* transcripts in all clusters. (**c**) Heatmap presenting all differentially expressed genes (DEGs) within each cluster.

To evaluate heterogeneity within ILC subsets generated, each ILC cluster was dissected and further clustered using UMAP. Focusing on the ILC3 supercluster revealed two ILC3 subclusters, both of which showed comparable ILC3 lineage identifying transcripts *RORC*, *KIT*,

and *IL23R*. Interestingly ILC3 subcluster 1 was characterized by higher *IL1R1*, *IL26, LTA* and *LIF* transcripts, possibly compatible with a more activated cellular state (**Figure 31a,b**). Dissection of the ILC2 cluster revealed three subclusters which expressed comparable *GATA3* (**Figure 31c,b**). Both subcluster 0 and 1 exhibited similar *PTGDR2* expression, while subcluster 1 was characterized by high *IL1RL1* and *IL2RA*, and low *S1PR1* and *PTGER2* transcripts, consistent with a more activated phenotype. ILC2 subcluster 2 was conversely characterized by low *PTGDR2*, along with higher expression of some type 1 genes, including *KLRF1* and *EOMES* (**Figure 31c,d**), suggesting that this subcluster may have partially down-regulated type 2 and concomitantly up-regulated type 1 signatures, possibly in line with an ILC2/ILC1 phenotype. Finally, examination of the NK/ILC1 population exposed three subclusters driven by 80 d ifferentially regulated genes (**Figure 31e**). In contrast to the observed differences in protein expression, *EOMES* and *KLRD1* transcripts (encoding CD94) were comparable among the three subclusters, and did not enable a dissection of NK and non-cytotoxic ILC1 phenotype, in line with the bulk RNA-seq data. Higher expression of *FCGR3A* could be identified in subcluster 2, which might reflect heterogeneity within NK cell subsets, as observed *ex vivo* (**Figure 31f**).

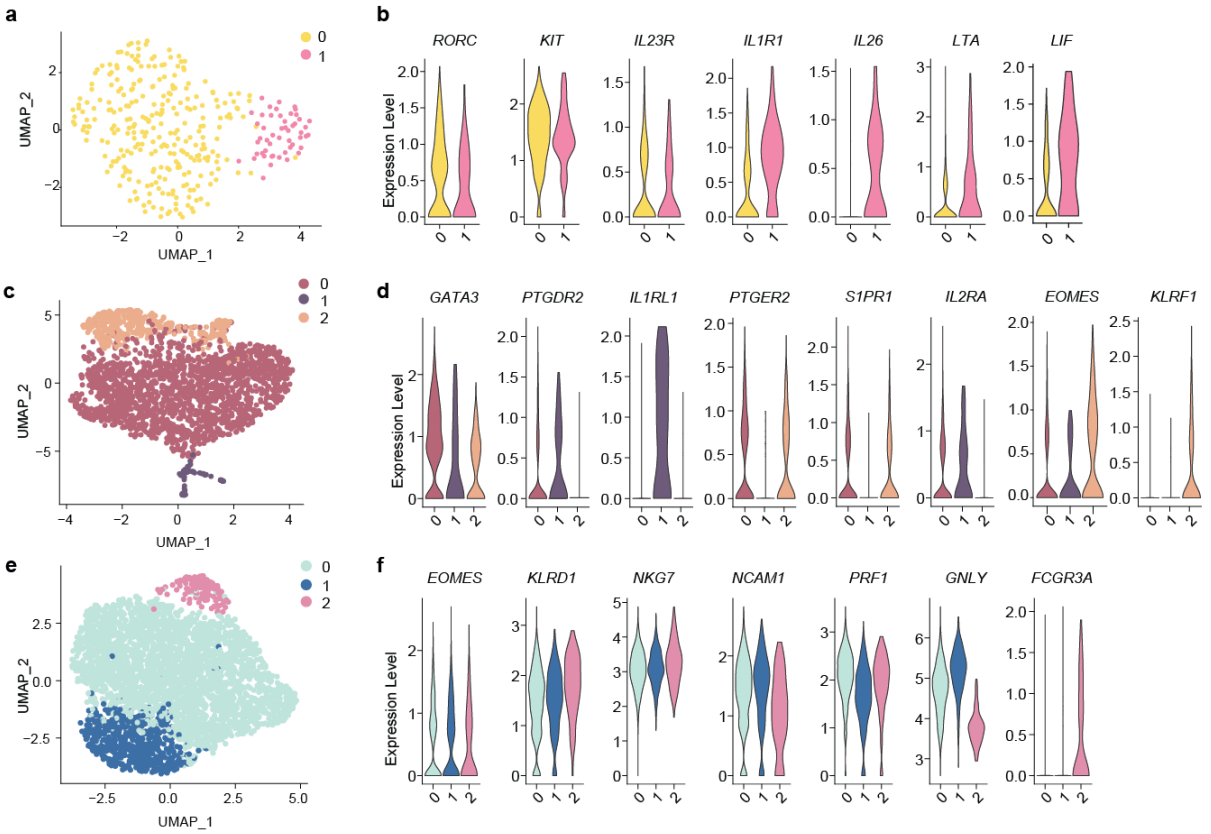

Figure 31: Single cell RNA sequencing reveals heterogeneity within *in vitro* generated ILC subsets. (**a**) UMAP dimensionality reduction of ILC3 clusters, color-coded to present subclusters. (**b**) Violin plots of *RORC, KIT, IL23R, IL1R1, IL26, LTA*, and *LIF* transcripts in ILC3 subclusters. (**c**) UMAP dimensionality reduction of ILC2 clusters, color-coded to present subclusters. (**e**) Violin plots of *GATA3, PTGDR2, IL1RL1, PTGER2, S1PR1, IL2RA, EOMES* and *KLRF1* transcripts in ILC2 subclusters. (**f**) UMAP dimensionality reduction of NK/ILC1 clusters, color-coded to present subclusters. (**g**) Violin plots of *EOMES, KLRD1, NKG7, NCAM1, PRF1, GNLY,* and *FCGR3A* transcripts in NK/ILC1 subclusters.

Collectively, using an unbiased sorting strategy independent of lineage identifying surface markers, this data validates the lineage identity of ILC subsets generated under different culture conditions. Furthermore, this data shows that even with provision of a stable set of signals, a certain degree of transcriptional heterogeneity can be obtained while generating ILCs *in vitro*, which however, does not enable clear distinction between NK and non-cytotoxic ILC1.

4.9 ILC lineages can be efficiently generated *in vitro* from bone marrow-derived CD34$^+$ HPCs

Next, the potential for CD34$^+$ CD45RA$^+$ HPCs from bone marrow of adult individuals to generate functional ILC subsets under the described conditions was tested. As in cord blood, all conditions, OP9+IL-15, DL1+IL-15, and DL1, had comparable fold expansion in bone marrow (**Figure 32a**). Supplementation with IL-15 in OP9+IL-15 and DL1+IL-15 resulted in a mean frequency of CD161$^+$ ILCs of 91.38% and 78.54% respectively. Also analogous to cord blood, DL1 showcased both a CD161$^+$ ILC and a CD161$^-$CD5$^+$ population, at mean frequencies of 41.87% and 21.67%, respectively (**Figure 32a-c**).

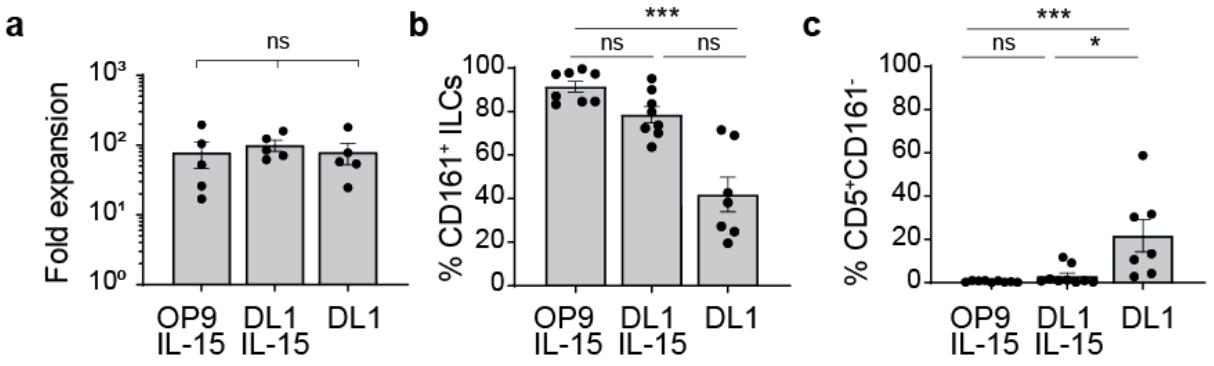

Figure 32: Human CD34$^+$ CD45RA$^+$ HPCs derived from bone marrow generate CD161$^+$ ILCs. (**a**) Fold expansion of live cells at week 4, relative to day 0 (n=5, 2 independent experiments). (**b**) Percent of CD161$^+$ ILCs within CD45$^+$ Lin$^-$ cells at week 4 (n=7-8, 5 independent experiments). (**c**) Percent of CD5$^+$ CD161$^-$ subset within CD45$^+$ Lin$^-$ cells at week 4 (n=7-8, 6 independent experiments).

In OP9+IL-15, two dominating ILC subsets could be identified, namely Eomes$^+$ and/or T-bet$^+$ NK/ILC1 which partially expressed CD94 and secreted IFNγ upon stimulation, and RORγt$^+$ ILC3 displaying surface CD117, which produced IL-22 (**Figure 33a-c**). Addition of Notch signaling upregulated T-bet expressing cells in NK/ILC1, as observed in cord blood (**Figure 33d**). As in cord blood, CRTH2$^+$ GATA3^{hi} ILC2 capable of expressing IL-13 were generated in condition DL1, although unlike cord blood, DL1+IL-15 appeared partly permissive to ILC2 generation (**Figure 33a,c**). Both CD5$^+$ and CD5$^-$ ILC2 were generated in DL1 and DL1+IL-15 (**Figure 33e**).

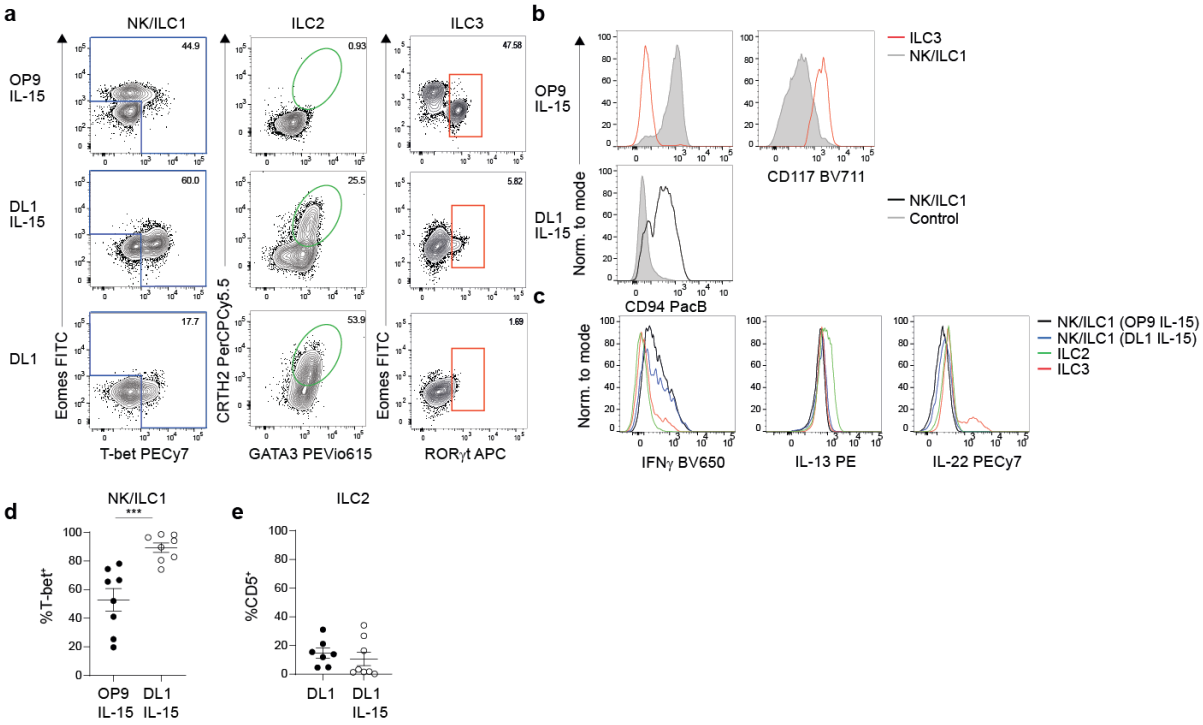

Figure 33: Mature and functional core ILC subsets can be generated from human bone marrow-derived CD34⁺ CD45RA⁺ HPCs. (**a**) Representative expression of transcription factors (TFs) and surface markers within CD161⁺ ILCs at week 4, colored gates show identification of subsets by TFs (NK/ILC1, blue; ILC2, green; ILC3, red). (**b**) Representative expression of CD117 and CD94 on NK/ILC1 and ILC3 (gated as in **a**) generated in the indicated conditions at week 4. For DL1+IL-15 Eomes⁻ /T-bet⁻ cells are depicted as control. (**c**) Representative expression of IFNγ, IL-13, and IL-22 within Eomes⁺ and/or T-bet⁺ NK/ILC1 from OP9+IL-15 (black), and from DL1+IL-15 (blue), RORγt⁺ ILC3s from OP9+IL-15 (red), and GATA3^{hi} CRTH2⁺ ILC2s from DL1 (green). (**d**) Frequency of T-bet⁺ cells within NK/ILC1 in the indicated conditions (n=8, 5 independent experiments). (**e**) Frequency of CD5⁺ cells within ILC2 from DL1 and DL1+IL-15 (gated as in **a**) n=7-8, 5 independent experiments. Statistical analysis (B) Mann-Whitney test; * p≤0.05; ** p≤0.01; *** p≤0.001.

The efficiency of ILC subset generation from bone marrow CD34⁺ CD45RA⁺ HPCs, as identified by transcription factors or by cytokine expression is quantified in **Figure 34a,b** respectively. As in cord blood, OP9+IL-15 was the most efficient culture condition for ILC3 generation (**Figure 34a,b**). However, while DL1+IL-15 appeared to be the most efficient condition to generate IFNγ-producing NK/ILC1 starting from cord blood CD34⁺ HPCs (**Figure 10f,g**), from bone marrow these differences were less pronounced (**Figure 34a,b**). ILC2 were most efficiently generated in condition DL1, with some permissibility in DL1+IL-15 as well (**Figure 34a,b**). This data suggests that the pathways regulating ILC differentiation are consistent in both cord blood and bone marrow circulating compartments, although tissue-driven differences between progenitors may affect ILC generation potential.

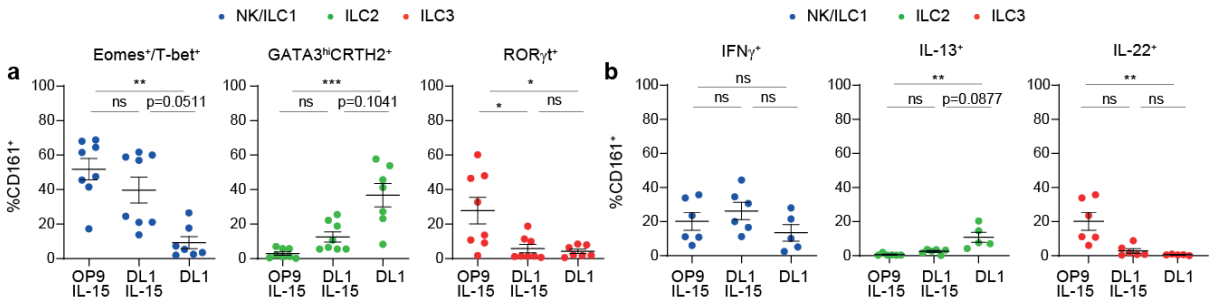

Figure 34: CD34⁺ CD45RA⁺ HPCs from bone marrow generate all core ILC subsets in response to specific conditions. (**a**) Quantification of ILC subset generation as identified by transcription factors (TFs) (Eomes⁺/T-bet⁺: n=7–8, 5 independent experiments; GATA3^{hi} CRTH2⁺: n=7–8, 5 independent experiments; RORγt⁺: n=7–8, 5 independent experiments). (**b**) Quantification of ILC subset generation as identified by cytokines (IFNγ⁺: n=5–6, 3 independent experiments; IL-13⁺: n=5–6, 3 independent experiments; IL-22⁺: n=5–6, 3 independent experiments). Statistical analyses were performed using a Kruskal-Wallis test with Dunn's multiple comparisons test; *p%0.5; **p%0.01; ***p % 0.001.

Collectively, these data show that *in vitro* differentiation from CD34⁺ CD45RA⁺ HPCs provides an effective and reliable method to test the potentiality of ILC progenitor pools. Moreover, the extensive phenotypic and transcriptional validation performed in this study highlights the similarities, as well as the inconsistencies, in ILC lineage generation, as compared to their *ex vivo* counterparts.

5 Discussion

The identification of ILCs in humans has led to serious advances in our understanding of homeostasis and inflammation. Studies from the last decade have revealed that mature ILCs differentiate from step-wise restricted ILC progenitors, and unlike T cells, are independent from thymic selection processes[105,125–128,131]. This remarkable feature allows for the recapitulation of the complete of ILC family *in vitro*, whereas generation of effector T cells directly from CD34$^+$ HPCs is an arduous process that does not physiologically mirror T cell development[168]. The system described in this work reliably enables the engenderment of fully differentiated and functional ILC lineages from CD34$^+$ CD45RA$^+$ HPCs from cord blood and bone marrow. This work ultimately shows that ILC subset differentiation can occur in the absence of IL-12, IL-18, IL-1β, IL-23, IL-33, or TSLP, cytokines often used to polarize naïve T cells into specific T helper subsets[23,106,111,217]. One of the key strengths of this study lies in the vast number of cultures presented, which despite a certain variability intrinsic to human studies, clearly indicate which culture conditions reliably engender the different ILC lineages.

5.1 Heterogeneity of the CD34$^+$ CD45RA$^+$ HPC pool

The data in this thesis, which shows the definitive generation of NK/ILC1, ILC2 and ILC3 subsets from cord blood and bone marrow derived CD34$^+$ CD45RA$^+$ HPCs, suggest that ILC programs might be partially pre-imprinted in either multi- or uni-potent ILC progenitors. It further suggests that individual ILC subsets may only emerge from these progenitors under specific conditions. *In vivo*, human ILC lineage differentiation from circulating (fetal liver, cord blood, bone marrow or peripheral blood derived) CD34$^+$ progenitors may be completed within tissue niches, where mature ILCs preferentially reside. In line with this concept ILC-, ILC2- and ILC3-committed progenitors have been described in tissues both in mice and humans[102,119,120,125,127,218]. One of the limitations of the human studies performed thus far is that the potential for ILC engenderment from CD34$^+$ precursors has been grounded on inadequate

and insufficient surface markers, and validation of the ILC progeny through transcription factor analysis and genetic profiling has been lacking. It remains to be conclusively ascertained whether the heterogeneous starting pool of CD34$^+$ CD45RA$^+$ HPCs used in this work holds common ILC progenitors or already pre-committed ILC1-, ILC2- or ILC3-specific progenitors. Only through additional detailed single-cell analysis of the transcriptome and epigenome of circulating and tissue CD34$^+$ CD45RA$^+$ progenitors will we be able to fully unveil the heterogeneity of this population, and explore whether it comprises of already pre-committed progenitors toward the different ILC lineages.

While human T cell-, B cell- and ILC-committed progenitors have been mainly identified within the CD34$^+$ HPC pool[125–127,169], a recent study from Lim and colleagues proposed a CD34$^-$ CD127$^+$ CD117$^+$ multi-potent ILC progenitor, found in adult tissues as well as circulating in peripheral blood[128,131]. Further characterization of this population highlights their heterogeneity and suggests that they may be a mix of transitional ILC populations[132] or may represent a more naïve ILC phenotype[47]. The developmental relationship between CD34$^+$ committed progenitors and these CD34$^-$ populations remain to be clarified. These two sources of ILC differentiation may not be mutually exclusive and both may play a role in constituting ILC pools in different tissues during distinct waves of ILC ontogeny.

5.2 Notch signaling skews ILC lineage differentiation programs in CD34$^+$ CD45RA$^+$ HPCs

The rise of the *RAG1/2* expressing CD161$^-$CD5$^+$ population in the presence of Notch signaling and the absence of IL-15 may occur due to differentiation of T cell lineage imprinted progenitors within the CD34$^+$ pool. The link between conditions favourable for growth of both ILC2 and T cells *in vitro* (namely Notch signaling and IL-7) has been previously reported, together with the notion that ILC2 can directly differentiate from committed thymic T cell precursors, *in vitro* and *in vivo*[121,156,218,219]. This link is further highlighted by the observed transient expression of T cell associated protein CD5 in ILC2, generated in the presence of DL1 and in the absence of IL-15

signaling. Interestingly, it was recently shown that IL-15 can induce granzyme B-mediated Notch1 cleavage, silencing Notch target genes[204], potentially explaining the antagonistic role of IL-15 in ILC2 lineage differentiation and the absence of ILC2 in conditions OP9+IL-15 and DL1+IL-15. In bone marrow, where an ILC2 pre-committed progenitor has been described in the mouse[112], condition DL1+IL-15 is also partially permissive to generation of ILC2, suggesting a fraction of precursors may have received initial Notch signals already *in vivo* and be thereby less sensitive to the action of IL-15 *in vitro*. In the mouse, Notch signaling has also been associated to promotion of a type 1 transcriptional program, as shown during T_H1 polarization through direct regulation of *Tbx21*[193,194]. Accordingly, the differentiation and maintenance of NKp46$^+$ ILC3 in the mouse, which express T-bet, is regulated by Notch[64,71,152,220]. Unlike the mouse, human NKp46$^+$ and/or NKp44$^+$ ILC3 do not express T-bet *ex vivo*, and can hence differentiate *in vitro* without external provision of Notch signaling. As shown here, Notch signaling in the system rather promotes generation of NK/ILC1 lineages and up-regulation of T-bet therein.

5.3 ILC lineage identification requires multifaceted analysis

One of the major highlights of this study lies in the validation of the different ILC lineages generated. The quality of lineage identification is pertinent not only for descriptive studies, but also for understanding the flexibility between lineages as it may impact the definition of plasticity. As seen in the IL-12 mediated ILC2-ILC1[52,83,198] or ILC3-ILC1 conversion[191] plasticity arises during challenge with inflammatory or polarizing signals, as also recapitulated in this work. Importantly, single-cell sequencing of ILCs generated in condition DL1 exposed what protein analysis did not: a subcluster partially retaining an ILC2 signature while exhibiting upregulation of type 1 genes, possibly indicating intrinsic ILC2 plasticity. While this putative ILC2/ILC1 subset could not be detected by TF staining, it may already be poised and account for the IFNγ production observed in ILC2 in response to IL-1β and IL-12 stimulation. Alternatively, as condition DL1 is suboptimal for NK/ILC1 engenderment due to the lack of IL-15, this population might simply reflect their aborted generation. Interestingly, a report from

2009 suggests that Notch activation can indeed promote an NK-like program from $CD34^+$ HPCs *in vitro* in the absence of IL-15, but that IL-15 is required for total maturation and to amplify cytotoxicity from these cells[215].

This finding further demonstrates that assigning cells generated *in vitro* or *in vivo* from putative progenitors to ILC lineages based on one cytokine or surface marker could lead to ambiguity in data interpretation. This study reveals the caveat that using only one condition to generate ILCs inherently biases lineage decision processes, as not all subsets can be generated with the same signals, and that multidimensional evaluation of the generated cells is absolutely required to assign lineage. This has implications on clonal assays, frequently utilized in ILC progenitor studies[111,125,127,128], in which only one condition can be tested per individual progenitor cell. A combination of single-cell and bulk cell assays will be critical in assessing the differentiation potential of candidate progenitors.

5.4 Limitations of the study

The robust potential for human ILC generation brought forth by this study lends itself to further exploration to study ILC fate-making decisions and differentiation. Hand in hand with potential for human ILC generation, it is pertinent to emphasise the limitations of such platforms. Of particular importance is the problematic identification of NK cell and ILC1 subsets. Previously, expression of Eomes has been used to demarcate NK cells among T-bet expressing Group 1 ILCs. However, mouse NK cell and ILC1 lineage assignment can be challenging in organs such as salivary glands, where prototypical phenotypes of NK cells and ILC1 fall apart[221,222]. In humans, Group 1 ILC lineage identities are even more debated[84,223], as there is great heterogeneity and variation of Eomes and T-bet expression across tissues, as shown in this and other studies[224], and may reflect tissue specific signals or cell maturity. A population fitting the minimal description of ILC1 ($T\text{-}bet^+$ $Eomes^{-/lo}$ $CD94^-$) is generated in these *in vitro* cultures, matching the populations identified as *bona fide* ILC1 in previous *in vitro* studies[127]. However, this “ILC1” population is here revealed to be transcriptionally similar to cytotoxic $CD127^-$ ILC1

and NK cells, which themselves are described to be heterogeneous. Nevertheless, it cannot be excluded that the strong cytotoxic signature detected in the NK/ILC1 might be enhanced by constant IL-15 provision in these cultures, as shown for T cells and NK cells, and may push the “ILC1” population generated toward a cytotoxic NK cell phenotyte[225,226]. Further, and as described earlier in this thesis, a recent study on blood and tonsil CD127$^+$ ILC1 has further shown that type 1 transcriptional features are missing in these cells *ex vivo*, whose core signature consist rather of T cell lineage associated transcripts[47], likely a T cell contamination. This makes direct comparisons between *in vitro* generated and *ex vivo* isolated ILC1 to ascertain lineage difficult. Overall, this suggests that identification of ILC1 generated *in vitro* through lack of CD94 or Eomes protein expression is insufficient to ascertain lineage, and that the differentiation potential of ILC progenitors has to be revisited.

Concerning faithful generation of ILC3, this system consistently recapitulates an NKp44$^+$ ILC3 signature akin to that of the tonsil, rather than NKp44$^-$ ILCs associated to a more naïve ILC phenotype. A human LTi cell signature was not detected either globally or at the individual cell level, in line with sequencing data from *ex vivo* isolated ILC3 from various adult compartments[47,48,59,60]. These limitations of the platform may not be inherently intrinsic, but rather reflect the lack of a clear *ex vivo* transcriptional signature, hindering their recapitulation *in vitro*.

5.5 Unresolved questions and future potential

Several lines of inquiry regarding the developmental trajectory of human ILCs remain open: Does a common ILCP that gives rise to all ILC subsets under the right conditions exist within the CD34$^+$ CD45RA$^+$ HPC pool? Are there subset specific ILC progenitors that are primed and pre-committed *in vivo*? What does the ILC developmental landscape look like during embryogenesis? What are the main transcriptional and epigenetic mechanisms regulating ILC development in humans? Regarding the culture system itself, examination of the effect of stromal cells on ILC differentiation is also of major interest. Do human stromal cell lines present

different signals than murine? Would use of tissue specific stromal cells, from tonsil or bone marrow for example, influence the phenotype and presentation of ILC differentiation?

This platform, which allows for the perturbation of ILC development between the stages of progenitor up to fully differentiated ILCs, presents a gateway to resolve many unanswered questions in the field. For instance, an ideal way to use this platform to explore the transcriptional networks regulating ILC development and gain of effector function, would be with genetic modification of the $CD34^+$ $CD45RA^+$ HPC pool to specifically target various players in differentiation. This could be done through lentiviral transduction, and the outcome on ILC subset engenderment can be henceforth evaluated. Additionally, candidate ILC progenitors identified through transcriptomic or epigenetic analysis *ex vivo* lend themselves to be tested in this platform, where the described culture conditions test for specific ILC subset potential. Of course, as *in vitro* potential does not necessarily correlate with *in vivo* activity, candidate progenitors which have been tested *in vitro* should also undergo transfers into xenograft models. In principle, as lineage restricted progenitors have decreased proliferative potential, expansion of candidate progenitors *in vitro* would also be pertinent to investigate. Finally, having a self-renewing source of ILCs which allow for genetic modification techniques can pave the road for potential adoptive transfer therapies.

5.6 Concluding remarks

To conclude, this work presents for the first time a tool for engenderment of the core ILC lineages from the relatively easily accessible $CD34^+$ $CD45RA^+$ HPC compartment. Prominently, experiments performed within the scope of this study exposed the caveat that individual conditions are required for specific ILC subset generation, namely hinging on Notch signaling and IL-15 provision. Additionally, this work revealed a link between conditions favourable for both human T-cell like and ILC2 lineages *in vitro*, and further showed that acquisition of CD161 separates canonical ILC signatures from T cell signatures *in vitro*. The recapitulation of the core ILC lineage identities presented here are corroborated by extensive

and consistent phenotypic, functional, and transcriptional interrogation, at both the global and single-cell level, which in other studies is based solely on cytokines or insufficient surrogate surface markers. Additionally, this platform tackles common problems in human ILC studies such as insufficient cell numbers and scarce availability of tissue samples.

Altogether, this work represents a critical resource to elevate human ILC research, and in particular serves as an important instrument to aid in clarifying human ILC biology and differentiation.

5.6 Graphical summary

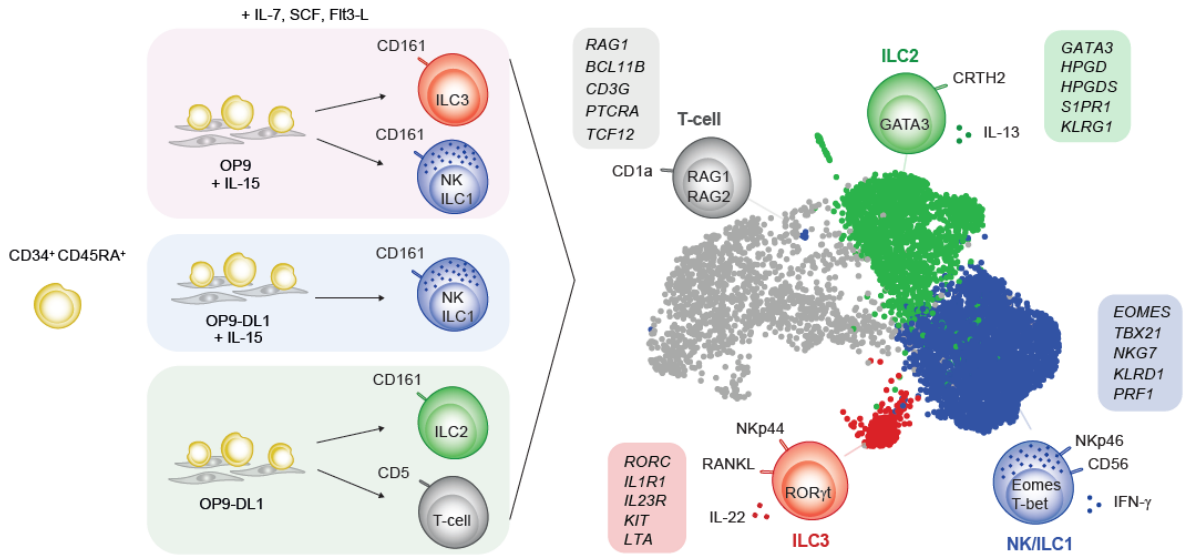

Figure 35: *In vitro* generation of human innate lymphoid cells from CD34⁺ CD45RA⁺ hematopoietic progenitors. Co-culture of CD34⁺ CD45RA⁺ hematopoietic progenitor cells with stromal cell line OP9, or OP9 transfected with DL1 to provide Notch signaling (OP9-DL1) in the presence of cytokines IL-7, SCF, and Flt3-L with or without IL-15, is sufficient to generate all core ILC subsets, which are identified by the acquisition of CD161. Condition OP9 with the addition of IL-15 generates RORgt⁺ NKp44⁺ ILC3 capable of secreting IL-22. A heterogeneous pool of Group 1 ILC (NK/ILC1), expressing Eomes, T-bet, NKp46 and capable of producing IFNγ are generated in the presence of IL-15, with or without the inclusion of Notch signaling, conditions OP9+IL-15 and DL1+IL-15. In the absence of IL-15 but in the presence of Notch signaling, condition DL1, two lineages arise: a T cell like population expressing RAG and CD1a transcripts, and ILC2, identified by GATA3, CRTH2 and IL-13 expression. Bulk and single cell transcriptomic analysis reveal robust ILC transcriptomes which correlate those found in their *ex vivo* counterparts.

6 References

1. Vivier E, Malissen B. Innate and adaptive immunity: Specificities and signaling hierarchies revisited. *Nat Immunol*. Published online 2005. doi:10.1038/ni1153
2. Vivier E, Artis D, Colonna M, et al. Innate Lymphoid Cells: 10 Years On. *Cell*. 2018;174(5):1054-1066. doi:10.1016/j.cell.2018.07.017
3. Vivier E, Tomasello E, Baratin M, Walzer T, Ugolini S. *Functions of Natural Killer Cells*. Vol 9. Nature Publishing Group; 2008:503-510. doi:10.1038/ni1582
4. Mjösberg J, Trifari S, Crellin NK, et al. Human IL-25-and IL-33-responsive type 2 innate lymphoid cells are defined by expression of CRTH2 and CD161. *Nat Immunol*. 2011;12(11):1055-1062. doi:10.1038/ni.2104
5. Gasteiger G, Fan X, Dikiy S, Lee SY, Rudensky AY. Tissue residency of innate lymphoid cells in lymphoid and nonlymphoid organs. *Science*. 2015;350(6263):981-985. doi:10.1126/science.aac9593
6. Moro K, Kabata H, Tanabe M, et al. Interferon and IL-27 antagonize the function of group 2 innate lymphoid cells and type 2 innate immune responses. *Nat Immunol*. 2015;17(1):76-86. doi:10.1038/ni.3309
7. Nussbaum JC, Van Dyken SJ, von Moltke J, et al. Type 2 innate lymphoid cells control eosinophil homeostasis. *Nature*. 2013;502(7470):245-248. doi:10.1038/nature12526
8. Huang Y, Mao K, Chen X, et al. S1P-dependent interorgan trafficking of group 2 innate lymphoid cells supports host defense. *Science (80-)*. 2018;359(6371):114-119. doi:10.1126/science.aam5809
9. Spits H, Artis D, Colonna M, et al. Innate lymphoid cells--a proposal for uniform nomenclature. *Nat Rev Immunol*. 2013;13(2):145-149. doi:10.1038/nri3365
10. Klose CSN, Artis D. Innate lymphoid cells as regulators of immunity, inflammation and tissue homeostasis. *Nat Immunol*. 2016;17(7):765-774. doi:10.1038/ni.3489
11. Ebbo M, Crinier A, Vély F, Vivier E. Innate lymphoid cells: Major players in inflammatory diseases. *Nat Rev Immunol*. 2017;17(11):665-678. doi:10.1038/nri.2017.86
12. Levine PH. Conference and workshop on cellular immune reactions to human tumor-associated antigens. Introduction. *Natl Cancer Inst Monogr*. Published online 1973.
13. Stehle C, Hernández DC, Romagnani C. Innate lymphoid cells in lung infection and immunity. *Immunol Rev*. Published online 2018. doi:10.1111/imr.12712
14. Voskoboinik I, Whisstock JC, Trapani JA. Perforin and granzymes: Function, dysfunction and human pathology. *Nat Rev Immunol*. Published online 2015. doi:10.1038/nri3839
15. Björkström NK, Ljunggren HG, Michaëlsson J. *Emerging Insights into Natural Killer Cells in Human Peripheral Tissues*. Vol 16. Nat Rev Immunol; 2016:310-320.

doi:10.1038/nri.2016.34

16. Dogra P, Rancan C, Ma W, et al. Tissue Determinants of Human NK Cell Development, Function, and Residence. *Cell*. 2020;180(4):749-763.e13. doi:10.1016/j.cell.2020.01.022
17. Chan A, Hong D-L, Atzberger A, et al. CD56 bright Human NK Cells Differentiate into CD56 dim Cells: Role of Contact with Peripheral Fibroblasts . *J Immunol*. 2007;179(1):89-94. doi:10.4049/jimmunol.179.1.89
18. Romagnani C, Juelke K, Falco M, et al. CD56 bright CD16 − Killer Ig-Like Receptor − NK Cells Display Longer Telomeres and Acquire Features of CD56 dim NK Cells upon Activation . *J Immunol*. 2007;178(8):4947-4955. doi:10.4049/jimmunol.178.8.4947
19. Chiossone L, Chaix J, Fuseri N, Roth C, Vivier E, Walzer T. Maturation of mouse NK cells is a 4-stage developmental program. *Blood*. 2009;113(22):5488-5496. doi:10.1182/blood-2008-10-187179
20. Vivier E, Nunès JA, Vély F. Natural killer cell signaling pathways. *Science (80-)*. Published online 2004. doi:10.1126/science.1103478
21. Sivori S, Vacca P, Del Zotto G, Munari E, Mingari MC, Moretta L. Human NK cells: surface receptors, inhibitory checkpoints, and translational applications. *Cell Mol Immunol*. Published online 2019. doi:10.1038/s41423-019-0206-4
22. Vilches C, Parham P. KIR: Diverse, rapidly evolving receptors of innate and adaptive immunity. *Annu Rev Immunol*. Published online 2002. doi:10.1146/annurev.immunol.20.092501.134942
23. Klose CSN, Flach M, Mohle L, et al. Differentiation of type 1 ILCs from a common progenitor to all helper-like innate lymphoid cell lineages. *Cell*. 2014;157(2):340-356. doi:10.1016/j.cell.2014.03.030
24. McKenzie ANJ, Spits H, Eberl G. Innate lymphoid cells in inflammation and immunity. *Immunity*. 2014;41(3):366-374. doi:10.1016/j.immuni.2014.09.006
25. McFarland A, A Y, SY W, et al. Multi-tissue single-cell analysis deconstructs the complex programs of mouse natural killer and type 1 innate lymphoid cells in tissues and circulation. *Immunity*. 2021;54(6):1320-1337.e4. doi:10.1016/J.IMMUNI.2021.03.024
26. Daussy C, Faure F, Mayol K, et al. T-bet and Eomes instruct the development of two distinct natural killer cell lineages in the liver and in the bone marrow. *J Exp Med*. 2014;211(3):563-577. doi:10.1084/jem.20131560
27. Vosshenrich CAJ, García-Ojeda ME, Samson-Villéger SI, et al. A thymic pathway of mouse natural killer cell development characterized by expression of GATA-3 and CD127. *Nat Immunol*. 2006;7(11):1217-1224. doi:10.1038/ni1395
28. Bernink JH, Peters CP, Munneke M, et al. Human type 1 innate lymphoid cells

accumulate in inflamed mucosal tissues. *Nat Immunol*. 2013;14(3):221-229. doi:10.1038/ni.2534

29. Krabbendam L, Heesters BA, Kradolfer CMA, et al. CD127+ CD94+ innate lymphoid cells expressing granulysin and perforin are expanded in patients with Crohn's disease. *Nat Commun*. 2021;12(1). doi:10.1038/S41467-021-26187-X
30. Forkel M, VanTol S, Höög C, Michaëlsson J, Almer S, Mjösberg J. Distinct Alterations in the Composition of Mucosal Innate Lymphoid Cells in Newly Diagnosed and Established Crohn's Disease and Ulcerative Colitis. *J Crohns Colitis*. 2019;13(1):67-78. doi:10.1093/ECCO-JCC/JJY119
31. Fuchs A, Vermi W, Lee JS, et al. Intraepithelial type 1 innate lymphoid cells are a unique subset of il-12- and il-15-responsive ifn-γ-producing cells. *Immunity*. 2013;38(4):769-781. doi:10.1016/j.immuni.2013.02.010
32. Moro K, Yamada T, Tanabe M, et al. Innate production of TH2 cytokines by adipose tissue-associated c-Kit+Sca-1+ lymphoid cells. *Nature*. 2010;463(7280):540-544. doi:10.1038/nature08636
33. Neill DR, Wong SH, Bellosi A, et al. Nuocytes represent a new innate effector leukocyte that mediates type-2 immunity. *Nature*. 2010;464(7293):1367-1370. doi:10.1038/nature08900
34. Price AE, Liang H-E, Sullivan BM, et al. Systemically dispersed innate IL-13-expressing cells in type 2 immunity. *Proc Natl Acad Sci U S A*. 2010;107(25):11489-11494. doi:10.1073/pnas.1003988107
35. Kabata H, Moro K, Koyasu S. The group 2 innate lymphoid cell (ILC2) regulatory network and its underlying mechanisms. *Immunol Rev*. 2018;286(1):37-52. doi:10.1111/IMR.12706
36. Roediger B, Weninger W. Group 2 Innate Lymphoid Cells in the Regulation of Immune Responses. *Adv Immunol*. 2015;125:111-154. doi:10.1016/BS.AI.2014.09.004
37. Halim TYF. Group 2 innate lymphoid cells in disease. *Int Immunol*. 2016;28(1):13-22. doi:10.1093/INTIMM/DXV050
38. Reynders A, Yessaad N, Vu Manh T-P, et al. Identity, regulation and in vivo function of gut NKp46+RORγt+ and NKp46+RORγt- lymphoid cells. *EMBO J*. 2011;30(14):2934-2947. doi:10.1038/emboj.2011.201
39. Spencer SP, Wilhelm C, Yang Q, et al. Adaptation of innate lymphoid cells to a micronutrient deficiency SD. *Science (80-)*. 2014;343(6169):432-437. doi:10.1126/science.1247606
40. Satoh-Takayama N, Kato T, Motomura Y, et al. Bacteria-Induced Group 2 Innate Lymphoid Cells in the Stomach Provide Immune Protection through Induction of IgA. *Immunity*. 2020;52(4):635-649.e4. doi:10.1016/j.immuni.2020.03.002

41. Mair F, Becher B. Thy1+ Sca1+ innate lymphoid cells infiltrate the CNS during autoimmune inflammation, but do not contribute to disease development. *Eur J Immunol*. 2014;44(1):37-45. doi:10.1002/eji.201343653
42. Gadani SP, Smirnov I, Smith AT, Overall CC, Kipnis J. Characterization of meningeal type 2 innate lymphocytes and their response to CNS injury. *J Exp Med*. 2017;214(2):285-296. doi:10.1084/jem.20161982
43. Fung ITH, Sankar P, Zhang Y, et al. Activation of group 2 innate lymphoid cells alleviates aging-associated cognitive decline. *J Exp Med*. 2020;217(4). doi:10.1084/jem.20190915
44. Krämer B, Goeser F, Lutz P, et al. Compartment-specific distribution of human intestinal innate lymphoid cells is altered in HIV patients under effective therapy. *PLoS Pathog*. 2017;13(5):e1006373. doi:10.1371/journal.ppat.1006373
45. Simoni Y, Fehlings M, Kløverpris HN, et al. Human Innate Lymphoid Cell Subsets Possess Tissue-Type Based Heterogeneity in Phenotype and Frequency. *Immunity*. 2017;46(1):148-161. doi:10.1016/j.immuni.2016.11.005
46. Xue L, Salimi M, Panse I, et al. Prostaglandin D2 activates group 2 innate lymphoid cells through chemoattractant receptor-homologous molecule expressed on TH2 cells. *J Allergy Clin Immunol*. 2014;133(4). doi:10.1016/j.jaci.2013.10.056
47. Mazzurana L, Czarnewski P, Jonsson V, et al. Tissue-specific transcriptional imprinting and heterogeneity in human innate lymphoid cells revealed by full-length single-cell RNA-sequencing. *Cell Res*. Published online 2021. doi:10.1038/s41422-020-00445-x
48. Björklund ÅK, Forkel M, Picelli S, et al. The heterogeneity of human CD127(+) innate lymphoid cells revealed by single-cell RNA sequencing. *Nat Immunol*. 2016;17(4):451-460. doi:10.1038/ni.3368
49. Weston CA, Rana BMJ, Cousins DJ. Differential expression of functional chemokine receptors on human blood and lung group 2 innate lymphoid cells. *J Allergy Clin Immunol*. 2019;143(1):410-413.e9. doi:10.1016/j.jaci.2018.08.030
50. Ricardo-Gonzalez RR, Van Dyken SJ, Schneider C, et al. Tissue signals imprint ILC2 identity with anticipatory function. *Nat Immunol*. 2018;19(10):1093-1099. doi:10.1038/s41590-018-0201-4
51. Schneider C, Lee J, Koga S, et al. Tissue-Resident Group 2 Innate Lymphoid Cells Differentiate by Layered Ontogeny and In Situ Perinatal Priming. *Immunity*. 2019;50(6):1425-1438.e5. doi:10.1016/j.immuni.2019.04.019
52. Lim AI, Menegatti S, Bustamante J, et al. IL-12 drives functional plasticity of human group 2 innate lymphoid cells. *J Exp Med*. 2016;213(4):569-583. doi:10.1084/jem.20151750
53. Mjösberg J, Bernink J, Golebski K, et al. The Transcription Factor GATA3 Is Essential

for the Function of Human Type 2 Innate Lymphoid Cells. *Immunity*. 2012;37(4):649-659. doi:10.1016/j.immuni.2012.08.015

54. Mebius RE, Rennert P, Weissman IL. Developing Lymph Nodes Collect CD4+CD3− LTβ+ Cells That Can Differentiate to APC, NK Cells, and Follicular Cells but Not T or B Cells. *Immunity*. 1997;7(4):493-504. doi:10.1016/S1074-7613(00)80371-4
55. Eberl G, Marmon S, Sunshine M-J, Rennert PD, Choi Y, Littman DR. An essential function for the nuclear receptor RORgamma(t) in the generation of fetal lymphoid tissue inducer cells. *Nat Immunol*. 2004;5(1):64-73. doi:10.1038/ni1022
56. Sun Z, Unutmaz D, Zou YR, et al. Requirement for RORgamma in thymocyte survival and lymphoid organ development. *Science*. 2000;288(June):2369-2373. doi:10.1126/science.288.5475.2369
57. Stehle C, Rückert T, Fiancette R, et al. T-bet and RORα control lymph node formation by regulating embryonic innate lymphoid cell differentiation. *Nat Immunol*. Published online 2021. doi:10.1038/s41590-021-01029-6
58. Cupedo T, Crellin NK, Papazian N, et al. Human fetal lymphoid tissue-inducer cells are interleukin 17-producing precursors to RORC+ CD127+ natural killer-like cells. *Nat Immunol*. 2009;10(1):66-74. doi:10.1038/ni.1668
59. Yudanin NA, Schmitz F, Flamar A-L, et al. Spatial and Temporal Mapping of Human Innate Lymphoid Cells Reveals Elements of Tissue Specificity. *Immunity*. 2019;50(2):505-519.e4. doi:10.1016/j.immuni.2019.01.012
60. Bar-Ephraim YE, Cornelissen F, Papazian N, et al. Cross-Tissue Transcriptomic Analysis of Human Secondary Lymphoid Organ-Residing ILC3s Reveals a Quiescent State in the Absence of Inflammation. *Cell Rep*. 2017;21(3):823-833. doi:10.1016/j.celrep.2017.09.070
61. Okada S, Markle JG, Deenick EK, et al. Impairment of immunity to Candida and Mycobacterium in humans with bi-allelic RORC mutations. *Science (80-)*. Published online 2015. doi:10.1126/science.aaa4282
62. Cella M, Fuchs A, Vermi W, et al. A human natural killer cell subset provides an innate source of IL-22 for mucosal immunity. *Nature*. 2009;457(7230):722-725. doi:10.1038/nature07537
63. Buonocore S, Ahern PP, Uhlig HH, et al. Innate lymphoid cells drive IL-23 dependent innate intestinal pathology. *Nature*. 2010;464(7293):1371-1375. doi:10.1038/nature08949
64. Lee JS, Cella M, McDonald KG, et al. AHR drives the development of gut ILC22 cells and postnatal lymphoid tissues via pathways dependent on and independent of Notch. *Nat Immunol*. 2011;13(2):144-151. doi:10.1038/ni.2187
65. Satoh-Takayama N, Vosshenrich CAJ, Lesjean-Pottier S, et al. Microbial flora drives

interleukin 22 production in intestinal NKp46+ cells that provide innate mucosal immune defense. *Immunity*. 2008;29(6):958-970. doi:10.1016/J.IMMUNI.2008.11.001

66. Sonnenberg GF, Monticelli LA, Elloso MM, Fouser LA, Artis D. CD4(+) lymphoid tissue-inducer cells promote innate immunity in the gut. *Immunity*. 2011;34(1):122-134. doi:10.1016/j.immuni.2010.12.009
67. Luci C, Reynders A, Ivanov II, et al. Influence of the transcription factor RORγt on the development of NKp46+ cell populations in gut and skin. *Nat Immunol*. 2009;10(1):75-82. doi:10.1038/ni.1681
68. Tomasello E, Yessaad N, Gregoire E, et al. Mapping of NKp46(+) Cells in Healthy Human Lymphoid and Non-Lymphoid Tissues. *Front Immunol*. 2012;3:344. doi:10.3389/fimmu.2012.00344
69. Donnelly RP, Sheikh F, Dickensheets H, Savan R, Young HA, Walter MR. Interleukin-26: An IL-10-related cytokine produced by Th17 cells. *Cytokine Growth Factor Rev*. Published online 2010. doi:10.1016/j.cytogfr.2010.09.001
70. Pascual-Reguant A, Köhler R, Mothes R, et al. Multiplexed histology analyses for the phenotypic and spatial characterization of human innate lymphoid cells. *Nat Commun*. 2021;12(1). doi:10.1038/s41467-021-21994-8
71. Rankin LC, Groom JR, Chopin M, et al. The transcription factor T-bet is essential for the development of NKp46+ innate lymphocytes via the Notch pathway. *Nat Immunol*. 2013;14(4):389-395. doi:10.1038/ni.2545
72. Sciumè G, Hirahara K, Takahashi H, et al. Distinct requirements for T-bet in gut innate lymphoid cells. *J Exp Med*. 2012;209(13):2331-2338. doi:10.1084/jem.20122097
73. Teunissen MB, Munneke JM, Bernink JH, et al. Composition of innate lymphoid cell subsets in the human skin: enrichment of NCR(+) ILC3 in lesional skin and blood of psoriasis patients. *J Invest Dermatol*. 2014;134(9):2351-2360. doi:10.1038/jid.2014.146
74. Hoorweg K, Peters CP, Cornelissen F, et al. Functional differences between human NKp44- and NKp44+ RORC+ innate lymphoid cells. *Front Immunol*. 2012;3(APR). doi:10.3389/fimmu.2012.00072
75. Glatzer T, Killig M, Meisig J, et al. RORγt+ Innate Lymphoid Cells Acquire a Proinflammatory Program upon Engagement of the Activating Receptor NKp44. *Immunity*. 2013;38(6):1223-1235. doi:10.1016/j.immuni.2013.05.013
76. Hepworth MR, Monticelli LA, Fung TC, et al. Innate lymphoid cells regulate CD4 + T-cell responses to intestinal commensal bacteria. *Nature*. 2013;498(7452):113-117. doi:10.1038/nature12240
77. Gury-BenAri M, Thaiss CA, Serafini N, et al. The Spectrum and Regulatory Landscape of Intestinal Innate Lymphoid Cells Are Shaped by the Microbiome. *Cell*. 2016;166(5):1231-1246.e13. doi:10.1016/j.cell.2016.07.043

78. Von Burg N, Chappaz S, Baerenwaldt A, et al. Activated group 3 innate lymphoid cells promote T-cell-mediated immune responses. *Proc Natl Acad Sci U S A*. 2014;111(35):12835-12840. doi:10.1073/pnas.1406908111
79. Lehmann FM, von Burg N, Ivanek R, et al. Microbiota-induced tissue signals regulate ILC3-mediated antigen presentation. *Nat Commun*. 2020;11(1). doi:10.1038/s41467-020-15612-2
80. Hepworth MR, Fung TC, Masur SH, et al. Group 3 innate lymphoid cells mediate intestinal selection of commensal bacteria-specific CD4+ T cells. *Science (80-)*. 2015;348(6238):1031-1035. doi:10.1126/science.aaa4812
81. Rao A, Strauss O, Kokkinou E, et al. Cytokines regulate the antigen-presenting characteristics of human circulating and tissue-resident intestinal ILCs. *Nat Commun*. 2020;11(1). doi:10.1038/s41467-020-15695-x
82. Krabbendam L, Nagasawa M, Spits H, Bal SM. Isolation of Human Innate Lymphoid Cells. *Curr Protoc Immunol*. 2018;122(1):e55. doi:10.1002/cpim.55
83. Bal SM, Bernink JH, Nagasawa M, et al. IL-1β, IL-4 and IL-12 control the fate of group 2 innate lymphoid cells in human airway inflammation in the lungs. *Nat Immunol*. 2016;17(6):636-645. doi:10.1038/ni.3444
84. Simoni Y, Newell EW. Dissecting human ILC heterogeneity: more than just three subsets. *Immunology*. 2018;153(3):297-303. doi:10.1111/imm.12862
85. Cella M, Gamini R, Sécca C, et al. Subsets of ILC3 − ILC1-like cells generate a diversity spectrum of innate lymphoid cells in human mucosal tissues. *Nat Immunol*. 2019;20(August):980-991. doi:10.1038/s41590-019-0425-y
86. Collins PL, Cella M, Porter SI, et al. Gene Regulatory Programs Conferring Phenotypic Identities to Human NK Cells. *Cell*. 2018;0(0):1-13. doi:10.1016/j.cell.2018.11.045
87. Cossarizza A, Chang HD, Radbruch A, et al. Guidelines for the use of flow cytometry and cell sorting in immunological studies (second edition). *Eur J Immunol*. 2019;49(10):1457-1973. doi:10.1002/eji.201970107
88. Maximow AA. The lymphocyte as a stem cell, common to different blood elements in embryonic development and during the post-fetal life of mammals. *Folia Haematol*. Published online 1909.
89. Lorenz E, Uphoff D, Reid TR, Shelton E. Modification of irradiation injury in mice and guinea pigs by bone marrow injections. *J Natl Cancer Inst*. Published online 1951. doi:10.1093/jnci/12.1.197
90. Doulatov S, Notta F, Laurenti E, Dick JEE. Hematopoiesis: A human perspective. *Cell Stem Cell*. 2012;10(2):120-136. doi:10.1016/j.stem.2012.01.006
91. Vogel W, Scheding S, Kanz L, Brugger W. Clinical Applications of CD34 + Peripheral Blood Progenitor Cells (PBPC) . *Stem Cells*. Published online 2000.

doi:10.1634/stemcells.18-2-87

92. Holyoake TL, Alcorn MJ. CD34 + positive haemopoietic cells:Biology and clinical applications. *Blood Rev*. Published online 1994. doi:10.1016/S0268-960X(05)80016-5
93. Baum CM, Weissman IL, Tsukamoto AS, Buckle AM, Peault B. Isolation of a candidate human hematopoietic stem-cell population. *Proc Natl Acad Sci U S A*. Published online 1992. doi:10.1073/pnas.89.7.2804
94. Kang Y, Chao NJ, Aversa F. Unmanipulated or CD34 selected haplotype mismatched transplants. *Curr Opin Hematol*. Published online 2008. doi:10.1097/MOH.0b013e32831366eb
95. Bhatia M, Bonnet D, Murdoch B, Gan OI, Dick JE. A newly discovered class of human hematopoietic cells with SCID- repopulating activity. *Nat Med*. Published online 1998. doi:10.1038/2023
96. Ishii M, Matsuoka Y, Sasaki Y, et al. Development of a high-resolution purification method for precise functional characterization of primitive human cord blood-derived CD34-negative SCID-repopulating cells. *Exp Hematol*. Published online 2011. doi:10.1016/j.exphem.2010.11.008
97. Jagannathan-Bogdan M, Zon LI. Hematopoiesis. *Dev*. Published online 2013. doi:10.1242/dev.083147
98. Lewis K, Yoshimoto M, Takebe T. Fetal liver hematopoiesis: from development to delivery. *Stem Cell Res Ther*. Published online 2021. doi:10.1186/s13287-021-02189-w
99. Gerstein RM. Deciding the decider: Mef2c in hematopoiesis. *Nat Immunol*. Published online 2009. doi:10.1038/ni0309-235
100. Doulatov S, Notta F, Eppert K, Nguyen LT, Ohashi PS, Dick JE. Revised map of the human progenitor hierarchy shows the origin of macrophages and dendritic cells in early lymphoid development. *Nat Immunol*. 2010;11(7):585-593. doi:10.1038/ni.1889
101. Haddad R, Guardiola P, Izac B, et al. Molecular characterization of early human T/NK and B-lymphoid progenitor cells in umbilical cord blood. *Blood*. Published online 2004. doi:10.1182/blood-2004-05-1845
102. Possot C, Schmutz S, Chea S, et al. Notch signaling is necessary for adult, but not fetal, development of RORγt+ innate lymphoid cells. *Nat Immunol*. 2011;12(10):949-958. doi:10.1038/ni.2105
103. Cherrier M, Sawa S, Eberl G. Notch, Id2, and RORγt sequentially orchestrate the fetal development of lymphoid tissue inducer cells. *J Exp Med*. 2012;209(4):729-740. doi:10.1084/jem.20111594
104. Yokota Y, Mansouri A, Mori S, et al. Development of peripheral lymphoid organs and natural killer cells depends on the helix-loop-helix inhibitor Id2. *Nature*. Published online

1999. doi:10.1038/17812

105. Xu W, Cherrier DE, Chea S, et al. An Id2RFP-Reporter Mouse Redefines Innate Lymphoid Cell Precursor Potentials. *Immunity*. 2019;50(4):1054-1068.e3. doi:10.1016/j.immuni.2019.02.022
106. Walker JA, Clark PA, Crisp A, et al. Polychromic Reporter Mice Reveal Unappreciated Innate Lymphoid Cell Progenitor Heterogeneity and Elusive ILC3 Progenitors in Bone Marrow. *Immunity*. 2019;51(1):104-118.e7. doi:10.1016/j.immuni.2019.05.002
107. Seillet C, Huntington ND, Gangatirkar P, et al. Differential Requirement for Nfil3 during NK Cell Development. *J Immunol*. 2014;192(6):2667-2676. doi:10.4049/jimmunol.1302605
108. Xu W, Domingues RG, Fonseca-Pereira D, et al. NFIL3 Orchestrates the emergence of common helper innate lymphoid cell precursors. *Cell Rep*. 2015;10(12):2043-2054. doi:10.1016/j.celrep.2015.02.057
109. Seillet C, Rankin LC, Groom JR, et al. Nfil3 is required for the development of all innate lymphoid cell subsets. *J Exp Med*. 2014;211(9):1733-1740. doi:10.1084/jem.20140145
110. Verykokakis M, Krishnamoorthy V, Iavarone A, Lasorella A, Sigvardsson M, Kee BL. Essential Functions for ID Proteins at Multiple Checkpoints in Invariant NKT Cell Development. *J Immunol*. Published online 2013. doi:10.4049/jimmunol.1301521
111. Constantinides MG, McDonald BD, Verhoef PA, Bendelac A. A committed precursor to innate lymphoid cells. *Nature*. 2014;508(7496):397-401. doi:10.1038/nature13047
112. Hoyler T, Klose CSN, Souabni A, et al. The Transcription Factor GATA-3 Controls Cell Fate and Maintenance of Type 2 Innate Lymphoid Cells. *Immunity*. 2012;37(4):634-648. doi:10.1016/j.immuni.2012.06.020
113. Aliahmad P, De La Torre B, Kaye J. Shared dependence on the DNA-binding factor TOX for the development of lymphoid tissue-inducer cell and NK cell lineages. *Nat Immunol*. Published online 2010. doi:10.1038/ni.1930
114. Seehus CR, Aliahmad P, Torre B De, et al. The development of innate lymphoid cells requires TOX-dependent generation of a common innate lymphoid cell progenitor. *Nat Immunol*. 2015;(April). doi:10.1038/ni.3168
115. Yagi R, Zhong C, Northrup DLL, et al. The Transcription Factor GATA3 Is Critical for the Development of All IL-7Rα-Expressing Innate Lymphoid Cells. *Immunity*. 2014;40(3):378-388. doi:https://doi.org/10.1016/j.immuni.2014.01.012
116. Bando JK, Liang H-EE, Locksley RM. Identification and distribution of developing innate lymphoid cells in the fetal mouse intestine. *Nat Immunol*. 2015;16(2):153-160. doi:10.1038/ni.3057
117. Simic M, Manosalva I, Spinelli L, et al. Distinct Waves from the Hemogenic Endothelium Give Rise to Layered Lymphoid Tissue Inducer Cell Ontogeny. *Cell Rep*. Published

online 2020. doi:10.1016/j.celrep.2020.108004

118. Oherle K, Acker E, Bonfield M, et al. Insulin-like Growth Factor 1 Supports a Pulmonary Niche that Promotes Type 3 Innate Lymphoid Cell Development in Newborn Lungs. *Immunity*. Published online 2020. doi:10.1016/j.immuni.2020.01.005
119. Zeis P, Lian M, Fan X, et al. In Situ Maturation and Tissue Adaptation of Type 2 Innate Lymphoid Cell Progenitors. *Immunity*. 2020;53(4):775-792.e9. doi:10.1016/j.immuni.2020.09.002
120. Ghaedi M, Shen ZY, Orangi M, et al. Single-cell analysis of RORα tracer mouse lung reveals ILC progenitors and effector ILC2 subsets. *J Exp Med*. 2020;217(3). doi:10.1084/jem.20182293
121. Gentek R, Munneke JM, Helbig C, et al. Modulation of Signal Strength Switches Notch from an Inducer of T Cells to an Inducer of ILC2. *Front Immunol*. 2013;4:334. doi:10.3389/fimmu.2013.00334
122. Freud AG, Becknell B, Roychowdhury S, et al. A human CD34(+) subset resides in lymph nodes and differentiates into CD56bright natural killer cells. *Immunity*. Published online 2005. doi:10.1016/j.immuni.2005.01.013
123. Tang Q, Ahn Y-OO, Southern P, Blazar BR, Miller JS, Verneris MR. Development of IL-22-producing NK lineage cells from umbilical cord blood hematopoietic stem cells in the absence of secondary lymphoid tissue. *Blood*. 2011;117(15):4052-4055. doi:10.1182/blood-2010-09-303081
124. Grzywacz B, Kataria N, Sikora M, et al. Coordinated acquisition of inhibitory and activating receptors and functional properties by developing human natural killer cells. *Blood*. 2006;108(12):3824-3833. doi:10.1182/blood-2006-04-020198
125. Montaldo E, Teixeira-Alves LG, Glatzer T, et al. Human RORγt+CD34+ cells are lineage-specified progenitors of group 3 RORγt+ innate lymphoid cells. *Immunity*. 2014;41(6):988-1000. doi:10.1016/j.immuni.2014.11.010
126. Renoux VM, Zriwil A, Peitzsch C, et al. Identification of a Human Natural Killer Cell Lineage-Restricted Progenitor in Fetal and Adult Tissues. *Immunity*. 2015;43(2):394-407. doi:10.1016/j.immuni.2015.07.011
127. Scoville SD, Mundy-Bosse BL, Zhang MH, et al. A Progenitor Cell Expressing Transcription Factor ROR??t Generates All Human Innate Lymphoid Cell Subsets. *Immunity*. 2016;44(5):1140-1150. doi:10.1016/j.immuni.2016.04.007
128. Lim AI, Li Y, Lopez-Lastra S, et al. Systemic Human ILC Precursors Provide a Substrate for Tissue ILC Differentiation. *Cell*. 2017;168(6):1086-1100.e10. doi:10.1016/j.cell.2017.02.021
129. Sanos SL, Bui VL, Mortha A, et al. RORγt and commensal microflora are required for the differentiation of mucosal interleukin 22-producing NKp46+ cells. *Nat Immunol*.

2009;10(1):83-91. doi:10.1038/ni.1684

130. Tufa DM, Yingst AM, Trahan GD, et al. Human innate lymphoid cell precursors express CD48 that modulates ILC differentiation through 2B4 signaling. *Sci Immunol*. Published online 2020. doi:10.1126/SCIIMMUNOL.AAY4218
131. Chen L, Youssef Y, Robinson C, et al. CD56 Expression Marks Human Group 2 Innate Lymphoid Cell Divergence from a Shared NK Cell and Group 3 Innate Lymphoid Cell Developmental Pathway. *Immunity*. 2018;49(3):464-476.e4. doi:10.1016/j.immuni.2018.08.010
132. Nagasawa M, Heesters BA, Kradolfer CMA, et al. KLRG1 and NKp46 discriminate subpopulations of human CD117 + CRTH2 − ILCs biased toward ILC2 or. *J Exp Med*. 2019;216(8):1762-1776. doi:10.1084/jem.20190490
133. Salimi M, Barlow JL, Saunders SP, et al. A role for IL-25 and IL-33–driven type-2 innate lymphoid cells in atopic dermatitis. *J Exp Med*. 2013;210(13):2939 LP - 2950. doi:10.1084/jem.20130351
134. Lim AI, Di Santo JP. ILC-poiesis: Ensuring tissue ILC differentiation at the right place and time. *Eur J Immunol*. Published online November 2, 2018. doi:10.1002/eji.201747294
135. Mjösberg J, Mazzurana L. ILC-poiesis: Making Tissue ILCs from Blood. *Immunity*. Published online 2017. doi:10.1016/j.immuni.2017.03.002
136. Rochman Y, Spolski R, Leonard WJ. New insights into the regulation of T cells by gamma(c) family cytokines. *Nat Rev Immunol*. 2009;9(7):480-490. doi:10.1038/nri2580
137. Vonarbourg C, Mortha A, Bui VL, et al. Regulated expression of nuclear receptor RORγt confers distinct functional fates to NK cell receptor-expressing RORγt+ innate lymphocytes. *Immunity*. 2010;33(5):736-751. doi:10.1016/j.immuni.2010.10.017
138. Mazzucchelli R, Durum SK. Interleukin-7 receptor expression: Intelligent design. *Nat Rev Immunol*. Published online 2007. doi:10.1038/nri2023
139. Puel A, Ziegler SF, Buckley RH, Leonard WJ. Defective IL7R expression in T-B+NK+ severe combined immunodeficiency. *Nat Genet*. Published online 1998. doi:10.1038/3877
140. Robinette ML, Bando JK, Song W, Ulland TK, Gilfillan S, Colonna M. IL-15 sustains IL-7R-independent ILC2 and ILC3 development. *Nat Commun*. 2017;8:14601. doi:10.1038/ncomms14601
141. Facchetti F, Blanzuoli L, Ungari M, Alebardi O, Vermi W. Lymph node pathology in primary combined immunodeficiency diseases. *Springer Semin Immunopathol*. Published online 1998. doi:10.1007/BF00792602
142. Stephan JL, Vlekova V, Deist F Le, et al. Severe combined immunodeficiency: A retrospective single-center study of clinical presentation and outcome in 117 patients. *J*

Pediatr. 1993;123(4):564-572. doi:10.1016/S0022-3476(05)80951-5

143. Vély F, Barlogis V, Vallentin B, et al. Evidence of innate lymphoid cell redundancy in humans. *Nat Immunol*. Published online 2016. doi:10.1038/ni.3553
144. Ahn YO, Blazar BR, Miller JS, Verneris MR. Lineage relationships of human interleukin-22-producing CD56+ RORgt1 innate lymphoid cells and conventional natural killer cells. *Blood*. Published online 2013. doi:10.1182/blood-2012-07-440099
145. Huntington ND. The unconventional expression of IL-15 and its role in NK cell homeostasis. *Immunol Cell Biol*. 2014;92(3):210-213. doi:10.1038/icb.2014.1
146. Kennedy MK, Glaccum M, Brown SN, et al. Reversible defects in natural killer and memory CD8 T cell lineages in interleukin 15-deficient mice. *J Exp Med*. Published online 2000. doi:10.1084/jem.191.5.771
147. Lodolce JP, Boone DL, Chai S, et al. IL-15 receptor maintains lymphoid homeostasis by supporting lymphocyte homing and proliferation. *Immunity*. Published online 1998. doi:10.1016/S1074-7613(00)80664-0
148. Gilmour KC, Fujii H, Cranston T, Graham Davies E, Kinnon C, Gaspar HB. Defective expression of the interleukin-2/interleukin-15 receptor β subunit leads to a natural killer cell-deficient form of severe combined immunodeficiency. *Blood*. Published online 2001. doi:10.1182/blood.V98.3.877
149. Delconte RB, Shi W, Sathe P, et al. The Helix-Loop-Helix Protein ID2 Governs NK Cell Fate by Tuning Their Sensitivity to Interleukin-15. *Immunity*. Published online 2016. doi:10.1016/j.immuni.2015.12.007
150. Mrózek E, Anderson P, Caligiuri MA. Role of interleukin-15 in the development of human CD56+ natural killer cells from CD34+ hematopoietic progenitor cells. *Blood*. 1996;87(7):2632-2640. doi:10.1182/blood.v87.7.2632.bloodjournal8772632
151. Lee JS, Cella M, Colonna M. AHR and the transcriptional regulation of type-17/22 ILC. *Front Immunol*. Published online 2012. doi:10.3389/fimmu.2012.00010
152. Chea S, Perchet T, Petit M, et al. Notch signaling in group 3 innate lymphoid cells modulates their plasticity. *Sci Signal*. 2016;9(426):ra45. doi:10.1126/scisignal.aaf2223
153. Klose CSN, Kiss E a, Schwierzeck V, et al. A T-bet gradient controls the fate and function of CCR6-RORγt+ innate lymphoid cells. *Nature*. 2013;494(7436):261-265. doi:10.1038/nature11813
154. Kyoizumi S, Kubo Y, Kajimura J, et al. Fate Decision Between Group 3 Innate Lymphoid and Conventional NK Cell Lineages by Notch Signaling in Human Circulating Hematopoietic Progenitors. *J Immunol*. Published online 2017. doi:10.4049/jimmunol.1601711
155. Yang Q, Monticelli LAA, Saenz SAA, et al. T cell factor 1 is required for group 2 innate lymphoid cell generation. *Immunity*. 2013;38(4):694-704.

doi:10.1016/j.immuni.2012.12.003

156. Wong SH, Walker JA, Jolin HE, et al. Transcription factor RORα is critical for nuocyte development. *Nat Immunol*. 2012;13(3):229-236. doi:10.1038/ni.2208
157. Yu H, Fehniger TA, Fuchshuber P, et al. Flt3 ligand promotes the generation of a distinct CD34+ human natural killer cell progenitor that responds to interleukin-15. *Blood*. Published online 1998. doi:10.1182/blood.v92.10.3647
158. Pike BL, Robinson WA. Human bone marrow colony growth in agar-gel. *J Cell Physiol*. 1970;76(1):77-84. doi:10.1002/jcp.1040760111
159. Moore KA, Lemischka IR. Stem cells and their niches. *Science (80-)*. Published online 2006. doi:10.1126/science.1110542
160. Cho SK, Webber TD, Carlyle JR, Nakano T, Lewis SM, Zuniga-Pflucker JC. Functional characterization of B lymphocytes generated in vitro from embryonic stem cells. *Proc Natl Acad Sci U S A*. Published online 1999. doi:10.1073/pnas.96.17.9797
161. Lagergren A, Månsson R, Zetterblad J, et al. The Cxcl12, Periostin, and Ccl9 genes are direct targets for early B-cell factor in OP-9 stroma cells. *J Biol Chem*. Published online 2007. doi:10.1074/jbc.M610263200
162. Nakano T, Kodama H, Honjo T. Generation of lymphohematopoietic cells from embryonic stem cells in culture. *Science (80-)*. 1994;265(5175):1098-1101. doi:10.1126/science.8066449
163. Schmitt TM, Zúñiga-Pflücker JC, Zuniga-Pflucker JC. Induction of T Cell Development from Hematopoietic Progenitor Cells by Delta-like-1 In Vitro. *Immunity*. 2002;17(6):749-756. doi:10.1016/S1074-7613(02)00474-0
164. Mohtashami M, Shah DK, Nakase H, Kianizad K, Petrie HT, Zúñiga-Pflücker JC. Direct Comparison of Dll1- and Dll4-Mediated Notch Activation Levels Shows Differential Lymphomyeloid Lineage Commitment Outcomes. *J Immunol*. Published online 2010. doi:10.4049/jimmunol.1000782
165. Benne C, Lelievre JD, Balbo M, Henry A, Sakano S, Levy Y. Notch increases T/NK potential of human hematopoietic progenitors and inhibits B cell differentiation at a pro-B stage. *Stem Cells*. 2009;27(7):1676-1685. doi:10.1002/stem.94
166. Rawlings DJ, Quan SG, Kato RM, Witte ON. Long-term culture system for selective growth of human B-cell progenitors. *Proc Natl Acad Sci U S A*. 1995;92(5):1570-1574. doi:10.1073/pnas.92.5.1570
167. La Motte-Mohs RN, Herer E, Zúñiga-Pflücker JC. Induction of T-cell development from human cord blood hematopoietic stem cells by Delta-like 1 in vitro. *Blood*. 2005;105(4):1431-1439. doi:10.1182/blood-2004-04-1293
168. Brauer PM, Singh J, Xhiku S, Zúñiga-Pflücker JC. T Cell Genesis: In Vitro Veritas Est? *Trends Immunol*. 2016;37(12):889-901. doi:10.1016/j.it.2016.09.008

169. Blom B, Spits H. Development of human lymphoid cells. *Annu Rev Immunol*. 2006;24:287-320. doi:10.1146/annurev.immunol.24.021605.090612
170. Yang Q, Li F, Harly C, et al. TCF-1 upregulation identifies early innate lymphoid progenitors in the bone marrow. *Nat Immunol*. 2015;16(10):1044-1050. doi:10.1038/ni.3248
171. Bal SM, Golebski K, Spits H. Plasticity of innate lymphoid cell subsets. *Nat Rev Immunol*. Published online 2020. doi:10.1038/s41577-020-0282-9
172. Kotecha N, Krutzik PO, Irish JM. Web-based analysis and publication of flow cytometry experiments. *Curr Protoc Cytom*. 2010;Chapter 10(1):Unit10.17. doi:10.1002/0471142956.cy1017s53
173. Kim D, Pertea G, Trapnell C, Pimentel H, Kelley R, Salzberg SL. TopHat2: Accurate alignment of transcriptomes in the presence of insertions, deletions and gene fusions. *Genome Biol*. 2013;14(4). doi:10.1186/gb-2013-14-4-r36
174. Langmead B, Salzberg SL. Fast gapped-read alignment with Bowtie 2. *Nat Methods*. 2012;9(4):357-359. doi:10.1038/nmeth.1923
175. Frankish A, Diekhans M, Ferreira AM, et al. GENCODE reference annotation for the human and mouse genomes. *Nucleic Acids Res*. 2019;47(D1):D766-D773. doi:10.1093/nar/gky955
176. Liao Y, Smyth GK, Shi W. FeatureCounts: An efficient general purpose program for assigning sequence reads to genomic features. *Bioinformatics*. 2014;30(7):923-930. doi:10.1093/bioinformatics/btt656
177. Love MI, Huber W, Anders S. Moderated estimation of fold change and dispersion for RNA-seq data with DESeq2. *Genome Biol*. 2014;15(12). doi:10.1186/s13059-014-0550-8
178. Bray NL, Pimentel H, Melsted P, Pachter L. Near-optimal probabilistic RNA-seq quantification. *Nat Biotechnol*. Published online 2016. doi:10.1038/nbt.3519
179. Melsted P, Sina Booeshaghi A, Gao F, et al. Modular and efficient pre-processing of single-cell RNA-seq. *bioRxiv*. Published online 2019. doi:10.1101/673285
180. Stuart T, Butler A, Hoffman P, et al. Comprehensive Integration of Single-Cell Data. *Cell*. Published online 2019. doi:10.1016/j.cell.2019.05.031
181. Lun ATL, McCarthy DJ, Marioni JC. A step-by-step workflow for low-level analysis of single-cell RNA-seq data with Bioconductor. *F1000Research*. 2016;5:2122. doi:10.12688/f1000research.9501.2
182. Zheng GXY, Terry JM, Belgrader P, et al. Massively parallel digital transcriptional profiling of single cells. *Nat Commun*. 2017;8. doi:10.1038/ncomms14049
183. Roelli P, bbimber, Flynn B, santiagorevale, Gui G. Hoohm/CITE-seq-Count: 1.4.2. Published online March 2019. doi:10.5281/ZENODO.2590196

184. Butler A, Hoffman P, Smibert P, Papalexi E, Satija R. Integrating single-cell transcriptomic data across different conditions, technologies, and species. *Nat Biotechnol*. 2018;36(5):411-420. doi:10.1038/nbt.4096
185. Rohart F, Gautier B, Singh A, Lê Cao KA. mixOmics: An R package for 'omics feature selection and multiple data integration. *PLoS Comput Biol*. 2017;13(11). doi:10.1371/journal.pcbi.1005752
186. Subramanian A, Tamayo P, Mootha VK, et al. Gene set enrichment analysis: a knowledge-based approach for interpreting genome-wide expression profiles. *Proc Natl Acad Sci U S A*. 2005;102(43):15545-15550. doi:10.1073/pnas.0506580102
187. Hernández DC, Juelke K, Müller NC, et al. An in vitro platform supports generation of human innate lymphoid cells from CD34+ hematopoietic progenitors that recapitulate ex vivo identity. *Immunity*. 2021;54(10):2417-2432.e5. doi:10.1016/j.immuni.2021.07.019
188. Galy A, Travis M, Cen D, Chen B. Human T, B, natural killer, and dendritic cells arise from a common bone marrow progenitor cell subset. *Immunity*. 1995;3(4):459-473. doi:10.1016/1074-7613(95)90175-2
189. Hordyjewska A, Popiołek Ł, Horecka A. Characteristics of hematopoietic stem cells of umbilical cord blood. *Cytotechnology*. 2015;67(3):387-396. doi:10.1007/s10616-014-9796-y
190. Vranjkovic A, Crawley AM, Gee K, Kumar A, Angel JB. IL-7 decreases IL-7 receptor α (CD127) expression and induces the shedding of CD127 by human CD8+ T cells. *Int Immunol*. 2007;19(12):1329-1339. doi:10.1093/intimm/dxm102
191. Bernink JH, Krabbendam L, Germar K, et al. Interleukin-12 and -23 Control Plasticity Of Cd127+ Group 1 And Group 3 Innate Lymphoid Cells In The Intestinal Lamina Propria. *Immunity*. 2015;43(1):146-160. doi:10.1016/j.immuni.2015.06.019
192. Amir ED, Davis KL, Tadmor MD, et al. viSNE enables visualization of high dimensional single-cell data and reveals phenotypic heterogeneity of leukemia. *Nat Biotechnol*. 2013;31(6):545-552. doi:10.1038/nbt.2594
193. Minter LM, Turley DM, Das P, et al. Inhibitors of gamma-secretase block in vivo and in vitro T helper type 1 polarization by preventing Notch upregulation of Tbx21. *Nat Immunol*. 2005;6(7):680-688. Accessed October 31, 2019. http://www.ncbi.nlm.nih.gov/pubmed/15991363
194. Maekawa Y, Tsukumo SI, Chiba S, et al. Delta1-Notch3 interactions bias the functional differentiation of activated CD4+ T cells. *Immunity*. Published online 2003. doi:10.1016/S1074-7613(03)00270-X
195. Cella M, Otero K, Colonna M. Expansion of human NK-22 cells with IL-7, IL-2, and IL-1beta reveals intrinsic functional plasticity. *Proc Natl Acad Sci U S A*.

2010;107(24):10961-10966. doi:10.1073/pnas.1005641107

196. Huang Y, Guo L, Qiu J, et al. IL-25-responsive, lineage-negative KLRG1(hi) cells are multipotential “inflammatory” type 2 innate lymphoid cells. *Nat Immunol*. 2015;16(2):161-169. doi:10.1038/ni.3078
197. Ohne Y, Silver JS, Thompson-Snipes L, et al. IL-1 is a critical regulator of group 2 innate lymphoid cell function and plasticity. *Nat Immunol*. 2016;17(6):646-655. doi:10.1038/ni.3447
198. Silver JS, Kearley J, Copenhaver AM, et al. Inflammatory triggers associated with exacerbations of COPD orchestrate plasticity of group 2 innate lymphoid cells in the lungs. *Nat Immunol*. 2016;17(6):626-635. doi:10.1038/ni.3443
199. Gao Y, Souza-Fonseca-Guimaraes F, Bald T, et al. Tumor immunoevasion by the conversion of effector NK cells into type 1 innate lymphoid cells. *Nat Immunol*. 2017;18(9):1004-1015. doi:10.1038/ni.3800
200. Hochdörfer T, Winkler C, Pardali K, Mjösberg J. Expression of c-Kit discriminates between two functionally distinct subsets of human type 2 innate lymphoid cells. *Eur J Immunol*. 2019;49(6):884-893. doi:10.1002/eji.201848006
201. Rothenberg E V. T cell lineage commitment: identity and renunciation. *J Immunol*. 2011;186(12):6649-6655. doi:10.4049/jimmunol.1003703
202. Phillips JH, Hori T, Nagler A, Bhat N, Spits H, Lanier LL. Ontogeny of human natural killer (NK) cells: fetal NK cells mediate cytolytic function and express cytoplasmic CD3 epsilon,delta proteins. *J Exp Med*. 1992;175(4):1055-1066. doi:10.1084/jem.175.4.1055
203. Robinette ML, Fuchs A, Cortez VS, et al. Transcriptional programs define molecular characteristics of innate lymphoid cell classes and subsets. *Nat Immunol*. 2015;16(3):306-317. doi:10.1038/ni.3094
204. Ettersperger J, Montcuquet N, Malamut G, et al. Interleukin-15-Dependent T-Cell-like Innate Intraepithelial Lymphocytes Develop in the Intestine and Transform into Lymphomas in Celiac Disease. *Immunity*. 2016;45(3):610-625. doi:10.1016/j.immuni.2016.07.018
205. De Smedt M, Taghon T, Van de Walle I, De Smet G, Leclercq G, Plum J. Notch signaling induces cytoplasmic CD3ϵ expression in human differentiating NK cells. *Blood*. 2007;110(7):2696-2703. doi:10.1182/blood-2007-03-082206
206. Shikhagaie MM, Björklund ÅK, Mjösberg J, et al. Neuropilin-1 Is Expressed on Lymphoid Tissue Residing LTi-like Group 3 Innate Lymphoid Cells and Associated with Ectopic Lymphoid Aggregates. *Cell Rep*. 2017;18(7):1761-1773. doi:10.1016/j.celrep.2017.01.063
207. Yu Y, Wang C, Clare S, et al. The transcription factor Bcl11b is specifically expressed in group 2 innate lymphoid cells and is essential for their development. *J Exp Med*.

2015;212(6):865-874. doi:10.1084/jem.20142318

208. Califano D, Cho JJ, Uddin MN, et al. Transcription Factor Bcl11b Controls Identity and Function of Mature Type 2 Innate Lymphoid Cells. *Immunity*. 2015;43(2):354-368. doi:10.1016/j.immuni.2015.07.005
209. Walker JA, Oliphant CJ, Englezakis A, et al. Bcl11b is essential for group 2 innate lymphoid cell development. *J Exp Med*. 2015;212(6):875-882. doi:10.1084/jem.20142224
210. Golebski K, Layhadi JA, Sahiner U, et al. Induction of IL-10-producing type 2 innate lymphoid cells by allergen immunotherapy is associated with clinical response. *Immunity*. 2021;54(2):291-307.e7. doi:10.1016/j.immuni.2020.12.013
211. Morita H, Kubo T, Rückert B, et al. Induction of human regulatory innate lymphoid cells from group 2 innate lymphoid cells by retinoic acid. *J Allergy Clin Immunol*. 2019;143(6):2190-2201.e9. doi:10.1016/j.jaci.2018.12.1018
212. Salimi M, Xue L, Jolin H, et al. Group 2 Innate Lymphoid Cells Express Functional NKp30 Receptor Inducing Type 2 Cytokine Production. *J Immunol*. 2016;196(1):45-54. doi:10.4049/jimmunol.1501102
213. Burgueño-Bucio E, Mier-Aguilar CA, Soldevila G. The multiple faces of CD5. *J Leukoc Biol*. 2019;105(5):891-904. doi:10.1002/JLB.MR0618-226R
214. Nagasawa M, Germar K, Blom B, Spits H. Human CD5+ Innate Lymphoid Cells Are Functionally Immature and Their Development from CD34+ Progenitor Cells Is Regulated by Id2. *Front Immunol*. 2017;8(August):1-12. doi:10.3389/fimmu.2017.01047
215. Haraguchi K, Suzuki T, Koyama N, et al. Notch Activation Induces the Generation of Functional NK Cells from Human Cord Blood CD34-Positive Cells Devoid of IL-15. *J Immunol*. Published online 2009. doi:10.4049/jimmunol.0803036
216. Stoeckius M, Hafemeister C, Stephenson W, et al. Simultaneous epitope and transcriptome measurement in single cells. *Nat Methods*. 2017;14(9):865-868. doi:10.1038/nmeth.4380
217. Zhu J, Paul WE. Peripheral CD4+ T-cell differentiation regulated by networks of cytokines and transcription factors. *Immunol Rev*. Published online 2010. doi:10.1111/j.1600-065X.2010.00951.x
218. Ferreira ACF, Szeto ACH, Heycock MWD, et al. RORα is a critical checkpoint for T cell and ILC2 commitment in the embryonic thymus. *Nat Immunol*. 2021;22(2):166-178. doi:10.1038/s41590-020-00833-w
219. Qian L, Bajana S, Georgescu C, et al. Suppression of ILC2 differentiation from committed T cell precursors by E protein transcription factors. *J Exp Med*. 2019;216(4):884-899. doi:10.1084/jem.20182100
220. Viant C, Rankin LC, Girard-Madoux MJH, et al. Transforming growth factor-β and Notch

ligands act as opposing environmental cues in regulating the plasticity of type 3 innate lymphoid cells. *Sci Signal*. 2016;9(426):ra46. doi:10.1126/scisignal.aaf2176

221. Sojka DK, Plougastel-Douglas B, Yang L, et al. Tissue-resident natural killer (NK) cells are cell lineages distinct from thymic and conventional splenic NK cells. *Elife*. 2014;2014(3):e01659. doi:10.7554/eLife.01659
222. Cortez VS, Ulland TK, Cervantes-Barragan L, et al. SMAD4 impedes the conversion of NK cells into ILC1-like cells by curtailing non-canonical TGF-β signaling. *Nat Immunol*. 2017;18(9):995-1003. doi:10.1038/ni.3809
223. Spits H, Bernink JH, Lanier L. NK cells and type 1 innate lymphoid cells: partners in host defense. *Nat Immunol*. 2016;17(7):758-764. doi:10.1038/ni.3482
224. Riggan L, Freud AG, Sullivan TEO, O'Sullivan TE. True Detective : Unraveling Group 1 Innate Lymphocyte Heterogeneity. *Trends Immunol*. 2019;40(10):1-13. doi:10.1016/j.it.2019.08.005
225. Zhang M, Wen B, Anton OM, et al. IL-15 enhanced antibody-dependent cellular cytotoxicity mediated by NK cells and macrophages. *Proc Natl Acad Sci U S A*. Published online 2018. doi:10.1073/pnas.1811615115
226. Wagner JA, Rosario M, Romee R, et al. CD56bright NK cells exhibit potent antitumor responses following IL-15 priming. *J Clin Invest*. Published online 2017. doi:10.1172/JCI90387

7 Abbreviations

In order of appearance.

Abbreviation	
ILCs	Innate lymphoid cells
NK	Natural killer
TCR	T cell receptor
BCR	B cell receptor
IL-	Interleukin
IFNγ	Interferon-γ
TF	Transcription factor
Eomes	Eomesodermin
T-bet	T-box expressed in T cells
GATA3	GATA binding protein 3
RORγt	RAR-related orphan receptor-γ
TNFα	Tumor necrosis factor α
NCR	Natural cytotoxicity receptor
MHC	Major histocompatibility complex
KIR	Killer-cell immunoglobulin-like receptor
ie	Intraepithelial
CNS	Central nervous system
CRTH2	Prostaglandin D_2 receptor
PDG2	Prostaglandin D_2
RORα	RAR Related Orphan Receptor α
HPGD	Hydroxyprostaglandin dehydrogenase-15
HPGDS	Hematopoietic prostaglandin D synthase
LTi	Lymphoid tissue inducer
LT	Lymphotoxin
PP	Peyer's patches
RANKL	Receptor activator of nuclear factor kappa-B ligand
GM-CSF	Granulocyte macrophage-colony stimulating factor
MELC	Multi-epitope ligand cartography
HSC	Hematopoietic stem cell
HPC	Hematopoietic progenitor cell
HSTC	Hematopoietic stem cell transplant
MPP	Multipotent progenitor cells

CMP	Common myeloid progenitor
CLP	Common lymphoid progenitor
ILCP	Innate lymphoid cell precursor
ID2	Inhibitor of DNA binding 2
MACS	Magnetic-activated cell sorting

8 Table of figures

Figure 16: CD161^{-} subset defined by T-cell associated transcriptome. Adapted from Hernández et al., Immunity, 2021. Sequencing data processed by Dr. Pawel Durek.

Figure 17: CD161^{+} ILC subsets display individual transcriptome profiles. Adapted from Hernández et al., Immunity, 2021. Sequencing data processed by Dr. Pawel Durek.

Figure 18: *In vitro* generated NKp44^{+} ILC3 showcase robust transcriptional, phenotypic, and functional ILC3 identifying profile. Adapted from Hernández et al., Immunity, 2021. Sequencing data processed by Dr. Pawel Durek.

Figure 19: *In vitro* generated NKp44^{+} ILC3 share transcriptional profile with *ex vivo* isolated tonsil ILC3. Adapted from Hernández et al., Immunity, 2021. Sequencing data processed by Dr. Pawel Durek.

Figure 20: *In vitro* generated ILC2 showcase robust transcriptional, phenotypic, and functional ILC2 identifying profile. Adapted from Hernández et al., Immunity, 2021. Sequencing data processed by Dr. Pawel Durek.

Figure 21: *In vitro* generated ILC2 share transcriptional profile with *ex vivo* isolated tonsil ILC2. Adapted from Hernández et al., Immunity, 2021. Sequencing data processed by Dr. Pawel Durek.

Figure 22: CD5^{+} ILC2 are generated *in vitro* and have comparable *GATA3* and *IL13* transcripts. Adapted from Hernández et al., Immunity, 2021. Sequencing data processed by Dr. Pawel Durek.

Figure 23: CD5^{+} ILC2 generated *in vitro* retain ILC2 transcriptomic and protein profile. Adapted from Hernández et al., Immunity, 2021. Sequencing data processed by Dr. Pawel Durek.

Figure 24: CD5 is transiently and selectively expressed in ILC2. Adapted from Hernández et al., Immunity, 2021

Figure 25: *In vitro* generated NK/ILC1 showcase robust transcriptional type 1 gene signature. Adapted from Hernández et al., Immunity, 2021. Sequencing data processed by Dr. Pawel Durek.

9 Eidesstattliche Erklärung

Hiermit erkläre ich an Eides statt, die vorliegende Dissertation selbstständig angefertigt und keine anderen als die angegeben Hilfsmittel verwendet zu haben.
Weiterhin erkläre ich hiermit, dass die Dissertation oder Teile davon nicht bereits bei einer anderen wissenschaftlichen Einrichtung eingereicht, angenommen oder abgelehnt wurden und auch kein anderwärtiger Doktorgrad erworben wurde.

Berlin, den 5. Februar 2022

Daniela Carolina Hernández Torres

Ergebnisse der vorliegenden Arbeit wurden veröffentlicht:

Hernández DC, Juelke K, Müller NC, Durek P, Ugursu B, Mashreghi MF, Rückert T, Romagnani C. An in vitro platform supports generation of human innate lymphoid cells from $CD34^+$ hematopoietic progenitors that recapitulate ex vivo identity. Immunity. 2021 Oct 12;54(10):2417-2432.e5. doi: 10.1016/j.immuni.2021.07.019. Epub 2021 Aug 27. PMID: 34453879.

In Kooperation erzeugte Daten sind in den jeweiligen Autorenbeitragen der Publikationen sowie im Abbildungsverzeichnis dieser Arbeit vermerkt.

10 Acknowledgements

A vast network of people contributed to the shaping of this work, and importantly, of my scientific growth, throughout my doctoral education. First and foremost a profound thank you to my supervisor, Chiara Romagnani, for being a steadfast source of expertise, mentorship, and inspiration throughout my doctorate, for guiding me gracefully through the scientific landscape, and for fostering curiosity-driven science.

My academic journey has been supported since the first day by the fantastic persons, scientific and otherwise, of the Deutsches Rheuma-Forschungszentrum (DRFZ). For providing a collaborative environment in which to grow as a researcher and for in-depth discussions from technicalities to conceptual questions, I have the sincere community of the DRFZ to thank. A grateful thank you to the lab managers and the flow cytometry facility, Toralf Kaiser and Jenny Kirsch, whose technical support eased the many hours put into this work. To the group of Mir-Farzin Mashreghi, in particular to Pawel Durek, for their instrumental sequencing expertise and support throughout the years, thank you.

I am indebted to my entire lab family, past and present, for their incredible companionship throughout this journey, for constantly pushing for scientific discourse and growth, and for their effortless way to keep spirits high through thick or thin. I could not have imagined a more supportive group of scientists, and most importantly, friends, to flourish in. To Tina, my symbiotic desk partner, for your infectious positivity, our unspoken agreement to keep as much sunshine in the lab as possible, regardless of screen visibility, and to our constant stream of ridiculous plans to balance out long work days. To Marina, for espresso martini getaways and for stimulating discussions on doctoral life and beyond. To Kerstin, for your endless patience in introducing me into ILC work, and for supporting this project since my Masters. To Timo, for your unwavering support and great listening skills, and for all the sequencing help in the last high pressure experiments. To Nils, my most trusted Steglitz partner, who made countless

hours of gut processing almost pleasant, and for always being up for a good discussion and a beer. To Christo, for do be making me cry-laugh, and for (unwillingly) keeping one of my posters safe for 4 years and counting. To Alex, for being the best Strong Independent Master's Student (SIMS), for teaching me how to teach, and for all our strange jokes together. To Marion, a literal national treasure, for your fierce optimism and single handed way to keep everything and everyone afloat.

I thank the IMPRS as well as the TRR241 and its graduate program, encompassed under the ZIBI graduate school, for providing not only the funding for my scientific education, but also structure and opportunities for self-improvement and collaboration, such as those I could undertake in Erlangen in the groups of Christoph Becker and Claudia Günther.

Estoy profundamente agradecida a mi familia, que ha soportado este largo proceso conmigo, con enorme comprensión y ánimo en los últimos años. No estaría aquí si no fuera por su apoyo y fe inquebrantables.

To Sebastian, who experienced all aspects of this journey with me, with unconditional and unequivocal support, I express my endless gratitude. Thank you for making every chapter of life an adventure better than the last.